Spatio-temporal coordination of Rho GTPase activity patterns in cell migration

PhD Dissertation

Department of Chemistry and Chemical biology
Technical University, Dortmund

International Max Planck Research School for Living Matter, Dortmund

Arya Sachan

April 2026

First examiner: Priv.-Doz. Dr. Leif Dehmelt

Second examiner: Prof. Dr. Jan G. Hengstler

The work presented in this thesis was performed in the group of Dr. Leif Dehmelt in the Department of Chemistry and Chemical Biology, TU Dortmund, Germany. I am also affiliated with the graduate program International Max Planck Research School for Living Matter (IMPRS-LM).

Publications

Results presented in this thesis contributed to the following publications:

Nanda, S*., Calderon, A*., Sachan, A.*, Duong, T. T. *, Koch, J., Xin, X., Solouk-Stahlberg, D., Wu, Y. W., Nalbant, P., & Dehmelt, L. (2023). Rho GTPase activity crosstalk mediated by Arhgef11 and Arhgef12 coordinates cell protrusion-retraction cycles. Nature Communications, 14(1). https://doi.org/10.1038/s41467-023-43875-y

Sachan, A.*, Gierse, C., Nanda, S., Xin, X., Wu, Y.W., & Dehmelt, L. (2025) Rnd3 regulates cell morphodynamics by spatial restriction of cell contraction signaling. bioRxiv. https://www.biorxiv.org/content/10.1101/2025.09.23.677979v1.full

*: first authors

Acknowledgements

Firstly, I would like to express my sincere gratitude to Leif for giving me the opportunity to pursue my PhD in his lab and for supporting my successful application for the DAAD doctoral scholarship by helping me develop the research proposal. I am deeply thankful for his continuous guidance and support throughout my PhD journey. Having a supervisor who values your ideas and encourages independent work not only builds confidence but also makes the challenging journey of a PhD both enjoyable and achievable. I truly appreciate the trust he placed in me when making important decisions, such as discontinuing projects that were not progressing well and allowing me to pursue directions I strongly believed in. This freedom enabled me to work efficiently and generate substantial results within a limited timeframe.

I would also like to thank Prof. Dr. Jan G. Hengstler for kindly taking on the responsibility of serving as the second examiner for my PhD thesis.

My sincere thanks also go to the members of my Thesis Advisory Committee (TAC), Prof. Dr. Perihan Nalbant and Prof. Dr. Stefan Westermann, for their valuable time, guidance, and constructive feedback throughout my PhD project.

A special thank you goes to the IMPRS coordinators, Christa and Lucia, who consistently supported me and helped me with many matters outside the lab. I would particularly like to acknowledge Christa, who helped me with everything from finding an apartment in Dortmund to picking me up from the train station on my first day and ensuring that my initial days in the city were comfortable by lending me essential items during my first month.

I would also like to thank my colleagues, especially Caro and Ricarda, who made my time in the lab both pleasant and comfortable. You both supported me scientifically and personally whenever I needed help, which made my PhD journey and life in Dortmund much easier. I have many wonderful memories with you both inside and outside the lab that I will always cherish. Thank you for making this challenging journey so enjoyable. I would also like to thank Suchet for helping me with my initial experiments, teaching me how to use TIRF microscopy, and always being available

whenever I needed help throughout my PhD. My thanks also go to Luisa and Lara for efficiently managing the lab and organizing everything so well, which greatly contributed to smooth and productive work in the lab.

I would also like to thank everyone from the Summerer lab for the wonderful moments we shared during lunch breaks and various celebrations. Especially now, when I am the only one in my lab, having you around makes it feel less lonely. I will truly miss our lunchtime conversations.

I am also grateful to the lab of Dr. Perihan Nalbant for the engaging discussions during our joint lab meetings and for the many enjoyable gatherings, including barbeques and Christmas parties.

Next, I would like to thank the friends I made during my PhD, Bhavana, Raveena, and Shanice. Thank you for making my time in Dortmund so enjoyable. I cherish all the trips, outings, and moments we shared together. This journey would have been much more difficult without your friendship, and I hope we will have many more trips together in the future.

Finally, my deepest gratitude goes to my parents, Rakesh and Rekha, my brother Harsh, and my cousins Yash and Vishu, who have always supported me through every high and low despite the distance between us. Talking to them has always been my greatest source of comfort during stressful times. Without their unwavering support, living so far away from my family and country and completing this doctoral journey would not have been possible.

Contents

Abbreviations

ADP	adenosine diphosphate
Arp2/3	actin related protein 2/3
ATP	adenosine triphosphate
BFP	blue fluorescent protein
Cdc42	cell division cycle 42
CFP	cyan fluorescent protein
delCMV	truncated CMV promoter
DH	Dbl homology domain
DHFR	dihydrofolate Reductase
DMEM	Dulbecco's modifies Eagle's medium
dNTPs	deoxyribonucleoside triphosphate
ECM	extracellular matrix
FAB	F-actin binding domain
FKBP	FK506-binding protein
FRET	fluorescence resonance energy transfer
GAP	GTPase activating protein
GBD	GTPase binding domain
GDI	guanosine nucleotide dissociation inhibitor
GDP	guanosine diphosphate
GEF	guanine nucleotide exchange factor
GFP	green fluorescent protein
GTP	guanosine triphosphate
LOV	light oxygen voltage

MLC	myosin light chain
MLCK	myosin Light Chain Kinase
MLCP	myosin Light Chain Phosphatase
PAKs	p21-activated kinases
PA-Rac1	photoactivable Rac1
PH	pleckstrin homology domain
Rac1	ras related C3 botulinum toxin substrate 1
RBD	ras binding domain
RFP	red fluorescent protein
RhoA	ras homolog family member A
RGS	Regulator of G protein Signalling
RNAi	RNA interference
ROCK	Rho-associated coiled-coil containing protein kinase
SEM	standard error of mean
siRNA	small interfering RNA
SLF'-TMP	Synthetic Ligand for FKBP – Trimethoprim
TIRF-M	total internal reflection fluorescence microscopy
TMP	Trimethoprim
WAVE	WASP-family Verprolin-homologous protein
YFP	Yellow fluorescent protein

Abstract

Changes in cell shape play a central role in the function of cells, for example during immune cell migration, or cancer metastasis. These changes are driven by highly dynamic local cell protrusions and cell retractions, which are controlled by local dynamic states of signal networks. Small GTPases of the Rho family, such as Rac1 and Rho, play key roles in controlling these dynamic signal network states: Cell protrusion is induced by Rac1, and cell contraction is induced by RhoA. The activation of both molecules is catalysed by guanine-nucleotide exchange factors (GEFs). Previous work suggested that mutual inhibition between Rac1 and RhoA could stabilize cell polarization during migration by segregating protrusion and retraction in different regions of the cell. However, recent studies found that Rac1 and RhoA do not mutually inhibit each other, but that Rac1 instead activates Rho. This crosstalk cannot stabilize protrusion and retraction in directional migration but instead could explain the generation of dynamic cycles of cell protrusion and retraction. Such dynamic cycles are typically observed in A431 epidermal carcinoma cells, which migrate in a less directional, more exploratory mode. These dynamic cycles and the activity crosstalk between Rac1 and RhoA were recently proposed to be mediated by the RhoA activating GEFs Arhgef11 and Arhgef12.

Here, I present a more detailed investigation into the underlying mechanisms that link Rac1 and Rho activity. Firstly, Arhgef11 and Arhgef12 were shown to be recruited to the plasma membrane by active Rac1 and thereby proposed to play a role in mediating the observed activity crosstalk between Rac1 and RhoA. Mutagenesis studies further revealed that the plasma membrane recruitment of Arhgef12 is mediated by its PH domain. In contrast, Arhgef11 is recruited to sites close to the plasma membrane downstream of Rac1-induced actin polymerization via its unique F-actin binding (FAB) motif. Thus, these results together reveal a molecular mechanism, by which Arhgef11 and Arhgef12 can mediate Rac1/Rho activity crosstalk to promote the coupling between cell protrusion and cell retraction.

However, this crosstalk cannot explain the highly localized activity patterns of the cell protrusion regulator Rac1 and of the cell retraction regulator RhoA, which are both selectively active at the cell periphery. This kind of activity pattern was previously

explained by the stabilization of the local signal network state via mutual inhibition between the most-studied, canonical Rho GTPases Rac1 and RhoA. However, as stated above, such a crosstalk was not confirmed experimentally. Therefore, it was hypothesized that another signal molecule might be linked to these Rho GTPases via mutual inhibition to generate the observed spatio-temporal activity patterns. Based on previous studies, the unconventional small Rho GTPase Rnd3 (also known as RhoE) was a promising candidate for this function. Indeed, mutual inhibition between RhoA and Rnd3 was confirmed in this study in A431 epidermal carcinoma cells by combining rapid optogenetic or chemical perturbations with measurements of the signaling network response. However, contrary to expectations based on this crosstalk, mutually exclusive patterns of Rho induced cell retraction and Rnd3 activity were not observed. Instead, Rnd3 was observed to be even slightly increased during cell retraction. Additionally, Rnd3 was surprisingly reduced during cell protrusion, suggesting that Rac1 might be able to inhibit Rnd3 as well. Indeed, rapid optogenetic perturbation of Rac1 activity confirmed this hypothesis. Interestingly, this newly identified inhibition of Rnd3 by Rac1 was much stronger compared to its inhibition by Rho. Further investigations into the underlying mechanism revealed that the inhibition of Rnd3 by Rac1 is mediated by Rac1 effectors of the p21-activated kinase (PAK) family. Functional investigations demonstrate that Rnd3 acts as a selective cell contraction inhibitor that suppresses ectopic, highly dynamic pulses of Rho activity throughout the entire cell attachment area and only allows local contraction and retraction at the cell edge. Moreover, in the absence of Rnd3, protrusion-retraction dynamics were strongly inhibited, and overexpression had the opposite effect. These results therefore show that Rac and not Rho functions as the major Rnd3 inhibitor, and that Rnd3 functions as a Rho inhibitor, which is locally released at the cell edge to promote morphodynamics in migrating cells.

Taken together, the coordinated crosstalk between Rac, Rnd3 and Rho can explain how protrusion-retraction cycles are generated near the edge of migrating cells and thereby offer deeper insights into the mechanism that controls this central cellular process in physiological and pathological conditions, such as cancer metastasis.

Zusammenfassung

Dynamische Veränderungen der Zellform sind zentral für zahlreiche physiologische und pathophysiologische Prozesse, wie der Chemotaxis von Immunzellen und Metastasierung von Krebszellen. Sie beruhen auf lokal koordinierten Zellvorstülpungen und Zellrückziehungen, die durch subzellulär organisierte Signalnetzwerke gesteuert werden. Eine zentrale Rolle spielen kleine GTPasen vom Rho-Typ. Während Rac1 Zellvorstülpungen stimuliert, fördert RhoA Zellkontraktion und Zellrückziehungen. Die Aktivierung beider GTPasen wird durch Guanin-Nukleotid-Austauschfaktoren (GEFs) vermittelt. Frühere Arbeiten legten nahe, dass Rac1 und RhoA sich gegenseitig hemmen und dadurch Vorstülpung und Rückzug räumlich trennen, was eine stabile Zellpolarisation während gerichteter Migration ermöglichen würde. Aktuellere Studien, die schnelle Aktivitätsstörungen mit Messungen der Netzwerkantwort kombinierten, zeigten jedoch, dass eine solche gegenseitige Hemmung nicht vorliegt. Stattdessen aktiviert Rac1 Rho. Diese Wechselwirkung eignet sich zwar nicht zur Stabilisierung von Vorstülpung und Rückzug in der gerichteten Migration, könnte jedoch dynamische Zyklen von Zellvorstülpung und Zellrückziehung erklären. Solche Zyklen treten typischerweise in A431-Epidermoidkarzinomzellen auf, die eine wenig gerichtete, explorative Migration zeigen. In diesen Zellen werden die RhoA-aktivierenden GEFs Arhgef11 und Arhgef12 der Lbc-Familie zu neu gebildeten Zellausläufern rekrutiert und könnten dort die beobachtete Aktivitätswechselwirkung zwischen Rac1 und Rho vermitteln.

In dieser Arbeit wurden die Mechanismen untersucht, die der Kopplung von Rac1- und Rho-Aktivität zugrunde liegen. Zunächst konnte gezeigt werden, dass Arhgef11 und Arhgef12 durch aktives Rac1 an die Plasmamembran rekrutiert werden und damit zur Vermittlung der beobachteten Aktivitätswechselwirkung zwischen Rac1 und RhoA beitragen. Mutagenese-Studien ergaben, dass die Rekrutierung von Arhgef12 über dessen PH-Domäne erfolgt. Arhgef11 wird dagegen über sein einzigartiges F-Aktin-Bindungsmotiv (FAB) infolge Rac1-induzierter Aktinpolymerisation in die Nähe der Plasmamembran rekrutiert. Diese Befunde identifizieren einen molekularen Mechanismus, durch den Arhgef11 und Arhgef12 die Wechselwirkung zwischen Rac1- und Rho-Aktivität vermitteln und so die Kopplung von Zellausstülpung und Zellrückzug fördern.

Diese Wechselwirkung kann jedoch nicht die lokalisierten Aktivitätsmuster des Zellauswuchsregulators Rac1 und des Zellrückzugsregulators RhoA erklären, welche selektiv an der Zellperipherie aktiv sind. Solche lokalisierten Aktivitätsmuster wurden bislang durch eine gegenseitige Hemmung zwischen Rac1 und RhoA erklärt, welche jedoch nicht bestätigt werden konnte. Daher wurde untersucht, ob ein weiteres Signalmolekül über gegenseitige Hemmung mit diesen Rho-GTPasen interagiert. Auf Grundlage früherer Arbeiten war die unkonventionelle kleine Rho-GTPase Rnd3 (RhoE) hierfür ein vielversprechender Kandidat. Die gegenseitige Hemmung zwischen RhoA und Rnd3 konnte in A431 Zellen durch schnelle optogenetische oder chemische Störungen bestätigt werden. Entgegen der Erwartung zeigten sich jedoch keine sich gegenseitig ausschließenden Muster von Rho-induzierter Zellretraktion und Rnd3-Aktivität. Vielmehr stieg Rnd3 während der Zellretraktion leicht an. Gleichzeitig war Rnd3 während der Zellausstülpung reduziert, was auf eine mögliche Hemmung von Rnd3 durch Rac1 hindeutete. Diese Hypothese wurde durch optogenetische Störungen der Rac1-Aktivität bestätigt. Dabei erwies sich die Hemmung von Rnd3 durch Rac1 als stärker als die durch Rho vermittelte Hemmung. Weitere Analysen zeigten, dass die Hemmung von Rnd3 durch Rac1 Effektoren der p21-aktivierten Kinasen (PAKs) Familie vermittelt wird. Funktionelle Analysen ergaben, dass Rnd3 als selektiver Inhibitor der Zellkontraktion wirkt, der ektopische, hochdynamische Rho-Aktivitätsimpulse im gesamten Zellhaftungsbereich unterdrückt und nur lokale Kontraktion am Zellrand zulässt, die zu Zellrückziehungen führt. In Abwesenheit von Rnd3 war die Dynamik von Zellvorstülpungen und Zellrückziehungen stark vermindert, während Überexpression den gegenteiligen Effekt hatte. Diese Ergebnisse zeigen, dass Rnd3 eine wichtige Funktion in der Zellmorphodynamik besitzt, dass Rac und nicht Rho der wichtigste Inhibitor von Rnd3 ist und dass Rnd3 als lokal am Zellrand freigesetzter Rho-Inhibitor die Morphodynamik migrierender Zellen fördert.

Zusammenfassend zeigt diese Arbeit, dass die koordinierte Wechselwirkung zwischen Rac, Rnd3 und Rho die Entstehung zyklischer Zellvorstülpungen und Zellrückziehungen in peripheren Bereichen migrierender Zellen erklären kann. Die gewonnenen Erkenntnisse liefern damit vertiefte Einblicke in Mechanismen, die den zentralen zellulären Prozess der Morphodynamik unter physiologischen und pathophysiologischen Bedingungen, etwa im Kontext der Krebsmetastasierung, steuern.

1. Introduction

1.1 Fundamental mechanisms underlying cell migration

Cell migration is very important for many physiological and pathophysiological processes. It plays a fundamental role in the development and homeostasis of multicellular organisms. The formation of tissues during embryogenesis, immune responses (such as immune cell chemotaxis) and wound healing all rely on cells moving in a highly coordinated manner in a particular direction. Disruption of this process can lead to several pathophysiological processes, including cancer metastasis. During migration, cells undergo dynamic and continuous shape changes to facilitate their movement. Cell migration is a complex process and it relies on the actin rich cell cortex near the plasma membrane. It mainly involves three different processes: Protrusion, in which the plasma membrane is pushed out in the front of the cell; Attachment, in which the cell connects to the extracellular matrix via specialized adhesions; and contraction, in which the trailing part of the cytoplasm is retracted (Lauffenburger & Horwitz, 1996). Cell protrusion is powered by a force that is generated at the cell front due to actin polymerization (Pollard & Borisy, 2003; Ridley et al., 2003). Subsequently, focal adhesions are generated at the front that link the cell to the substrate (Gardel et al., 2010; Parsons et al., 2010). Finally, the cell body moves in the direction of protrusion by coordinating the retraction at the rear end with adhesion disassembly (Webb et al., 2002). Thus, cell migration is tightly regulated both spatially and temporally, by coordinating actin polymerization, dynamic adhesion turnover, and myosin-mediated contraction (Figure 1).

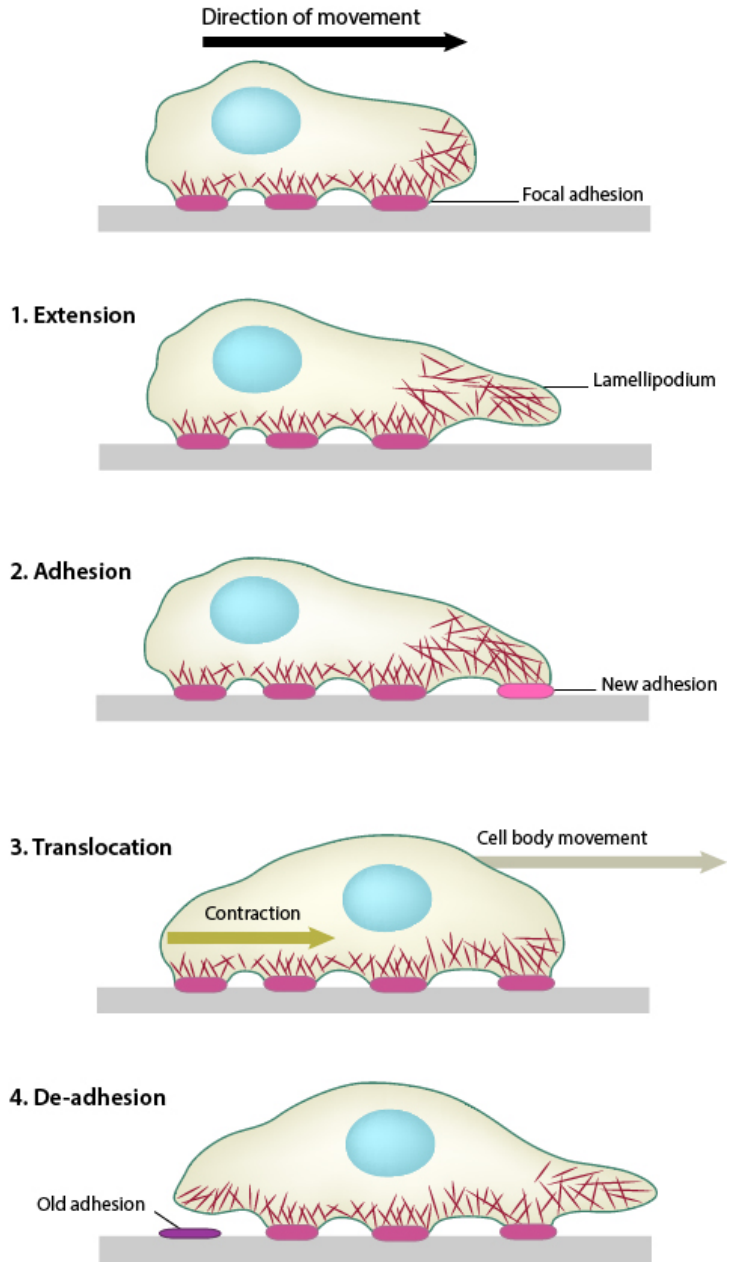

Figure 1. Schematic illustration of distinct steps of cell migration. 1. Extension of the cell by actin filament polymerization at the leading edge of the cell. **2.** Cell surface receptors in the newly generated protrusion attach to the substratum, forming new adhesions that link intracellular actin filaments with the extracellular matrix. **3.** Retrograde flow of actin and the contractile forces from stress fibres produce the required tension to move the cell forward. **4.** Finally, contractile network forces, together with actin filament and focal adhesion disassembly, drive the retraction of the trailing edge. Figure source: (Ladoux & Nicolas, 2012)

During protrusion, cells form Lamellipodia and filopodia-like structures in the front of the cell. Lamellipodia and filopodia are both actin-dependent cellular structures involved in cell migration, environment sensing and morphogenesis (Ridley, 2011). Although both are generated by dynamic rearrangements of the actin cytoskeleton, they differ in shape, their regulatory mechanism and some aspects of their biological function. Lamellipodia are highly dynamic, sheet-like protrusions of the plasma membrane that consists of a dense, branched network of actin filament generated by the Arp2/3 complex, activated downstream of small GTPases like Rac1 (Mattila & Lappalainen, 2008; Small et al., 2002) (Figure 2). Predominantly situated at the front of migrating cells, they play a central role in producing the protrusive forces necessary for forward movement. In contrast, filopodia are small finger-like structures consisting of bundles of 10-30 parallel, unbranched actin filaments with their barbed ends oriented toward the protrusion tip (Figure 2). They mainly serve as sensory structures, helping in exploring and navigating the extracellular environment during cell migration. Their assembly is primarily regulated by Cdc42 and formins, which drive the elongation of linear actin filaments (Faix & Rottner, 2006; Mattila & Lappalainen, 2008). The coordinated action of lamellipodia and filopodia facilitates cell migration by coupling lamellipodia-driven protrusive forces with filopodia-mediated environmental sensing and guidance. Such interplay is crucial for a range of biological processes dependent on cell migration, from development and wound healing to immune responses and cancer cell invasion.

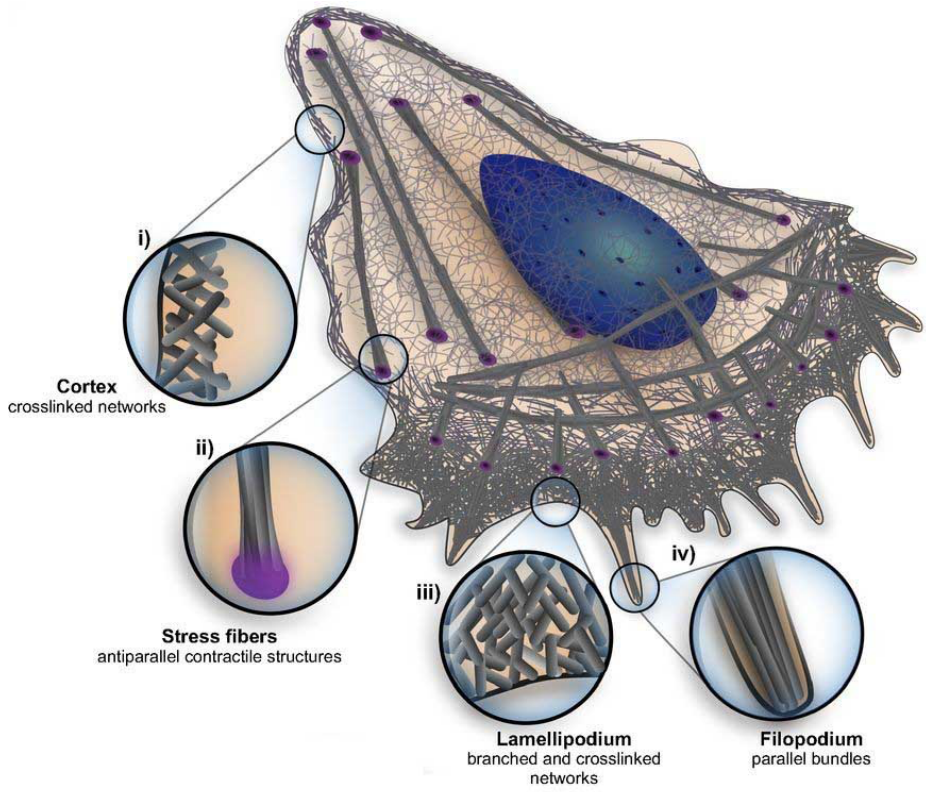

Figure 2. Schematic illustration of different types of actin structures in a typical migrating cell. Four actin-based structures are shown: actin cortex, stress fibres, lamellipodia and filopodia. The actin cortex is a thin network of actin filaments, myosin minifilaments and actin-binding proteins that are associated with the plasma membrane via adapter proteins. Stress fibres are bundles of anti-parallel actin filaments that are associated with myosin minifilaments, that generate contractile forces in non-muscle cells. Lamellipodia are wide, flat protrusions consisting of a branched and crosslinked network of actin. Filopodia are thin, finger like extensions comprising tight, parallel cross-linked bundles of actin filaments. Figure source: (Blanchoin et al., 2014)

In contrast, cell contraction is primarily driven by actomyosin structures that contain antiparallel actin filaments that interact with small bipolar filaments of non-muscle myosin II motor proteins. In this configuration, Myosin II motors generate contractile forces by sliding the anti-parallel actin filaments against each other in a process is powered by ATP hydrolysis (Figure 3) (Pollard & Cooper, 2009; Svitkina, 2018; Vicente-Manzanares et al., 2009). This sliding mechanism results in the shortening of actomyosin structures both in stress fibres and in the actin cortex. Cell contraction is locally regulated by several signalling pathways. In particular, the RhoA/ROCK

pathway plays a central role in non-muscle cells by regulating myosin II activity via phosphorylating myosin light chains (Vicente-Manzanares et al., 2009).

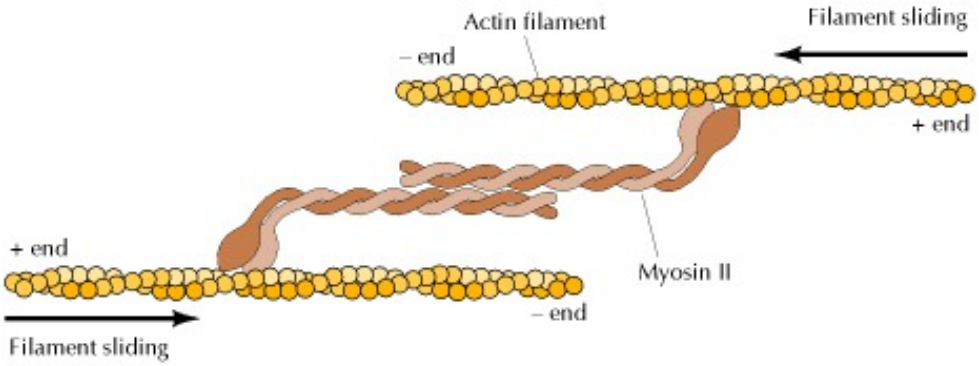

Figure 3. Schematic representation of actomyosin contraction in non-muscle cells. Bipolar myosin II filaments generate contractile forces by moving anti-parallel actin filaments past each other in opposite directions. Figure source: (Geoffrey M Cooper, 2000).

1.2 Cell type and cell state specific modes of cell migration

Cells can migrate using different modes that differ in their morphology and the spatio-temporal dynamics of protrusion and retraction signals. Classical classifications distinguish mesenchymal and ameboid migration modes (Friedl & Wolf, 2003; Sahai, 2005). Mesenchymal cell migration is characterized by an elongated cell shape and relies on strong adhesion. On the other hand, cells migrating via the ameboid mode are typically rounded or irregular and less dependent on adhesion. However, more recently a much broader spectrum of migration modes is recognized which extends these classifications (Paluch et al., 2016; Yamada & Sixt, 2019). Considering mesenchymal cell migration, some specific cell types, such as primary keratinocytes and highly polarized and migrate in a very persistent, directional manner with a stable leading edge accompanied by a retracting trailing edge (Cooper & Schliwa, 1986), even in the absence of spatial cues such as chemotactic gradients. In contrast, several cancer cells, like for example the epidermal carcinoma cell line A431 are less polarized

and generate transient protrusion-retraction cycles throughout the cell edge, and migrate in a more dynamic, exploratory manner (Figure 4) (Nalbant & Dehmelt, 2018).

These cycles of protrusion and retraction are generated by counteracting forces. The forward movement of a cell is induced by actin polymerization at its leading edge, while actomyosin contractility networks at the protrusion base act in opposition. The interplay and spatial distribution of these forces determines whether a cell persistently extends, retracts, or undergoes repeated cycles of extension and retraction within a local region (Lim et al., 2010). These processes are controlled by local dynamic states of signal networks. Rho family small GTPases play key roles in controlling these dynamic signal network states (Ridley, 2015).

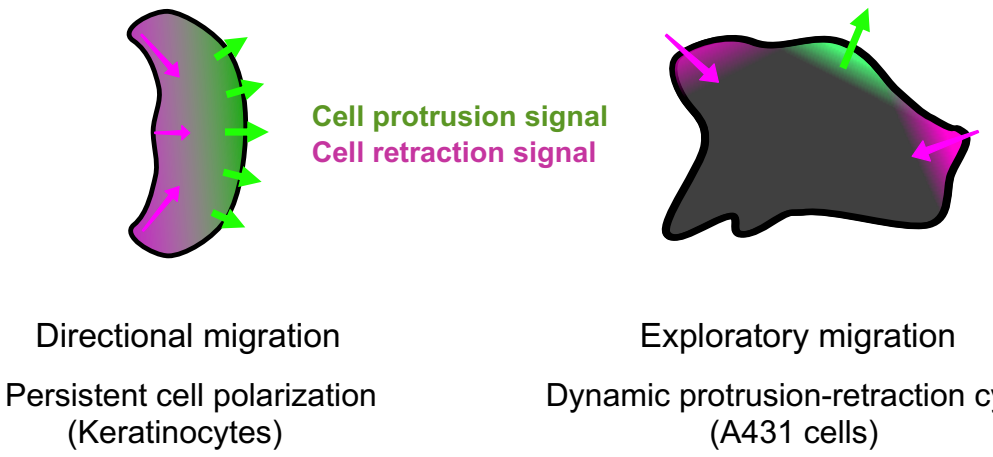

Figure 4. Schematic representation of cell protrusion and retraction signals in cells. Spatio-temporal organization of cell protrusion and retraction signals in primary, untransformed keratinocytes (left), which are characterized by strong and persistent cell polarization, leading to highly directional migration, or in A431 cancer cells (right), which generate short-lived, dynamic protrusion-retraction cycles that lead to a more stochastic, exploratory migration mode. Green represents cell protrusion and magenta represents cell retraction.

1.3 Rho-type small GTPases: Master regulators of cell migration

The Rho GTPases constitute a family of small signalling proteins of ~21 kDa, that belongs to the Ras superfamily. These molecules are considered to be molecular switches that can exist in an active and in an inactive state, determined by the bound nucleotide (Schmidt & Hall, 2002). They switch to their active, GTP-bound form by guanine nucleotide exchange factors (GEFs), which catalyse the exchange of GDP to GTP. Conversely, they switch to their inactive, GDP-bound form by GTPase activating proteins (GAPs), that stimulate the hydrolysis of GTP to GDP. In their active state, Rho GTPases are bound to plasma membrane where they can then interact with the GTPase-binding domain (GBD) of specific downstream effectors. In their inactive state, they are predominantly localized in the cytoplasm, where they are bound to RhoGDIs (Rho Guanine Nucleotide Dissociation Inhibitors), which stabilize the Rho GTPases in their inactive state (Garcia-Mata et al., 2011).

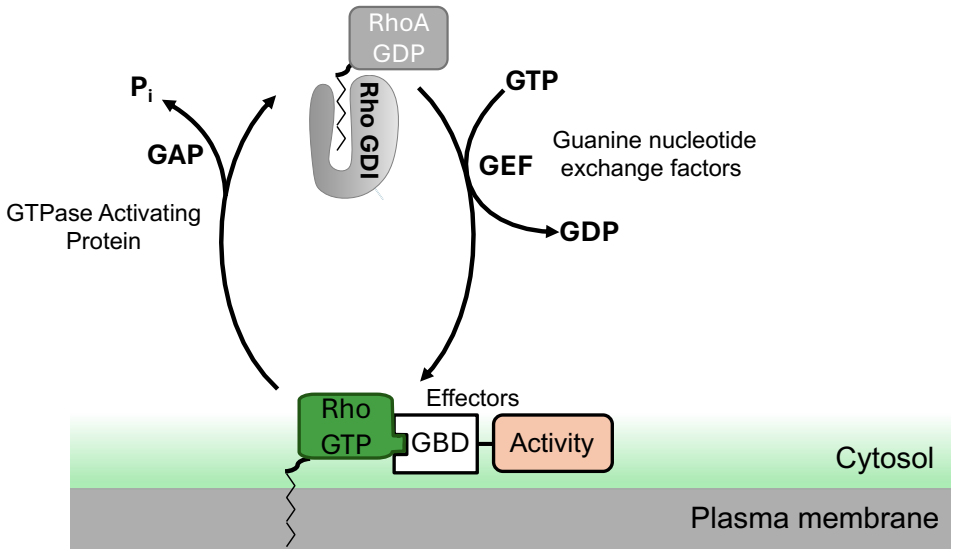

Figure 5. Schematic for the regulation of small GTPases of the Rho subfamily. Rho GTPases alternate between an active GTP form and an inactive GDP form, which is regulated by GDIs, GEFs, and GAPs. GDIs stabilize the inactive Rho GTPases in the cytosol. While GEFs activate the Rho GTPases by facilitating the exchange of GDP to GTP, GAPs stimulate the hydrolysis of GTP to GDP and switch the active Rho GTPase back to their inactive state. GTP: Guanosine triphosphate, GDP: Guanosine diphosphate, GEF: guanine nucleotide exchange factor, GAP: GTPase activating protein, GDI: Guanosine nucleotide dissociation inhibitor, GBD: GTPase-binding domain.

The Rho GTPase family members play an important role in regulating cytoskeletal organization and dynamics (Etienne-Manneville & Hall, 2002). In particular, cell protrusions are stimulated by the GTPase Rac1 by promoting actin polymerization and extension of the cell front (Ridley 2015), whereas another GTPase RhoA stimulates cell contraction by the activation of the motor protein Myosin II.

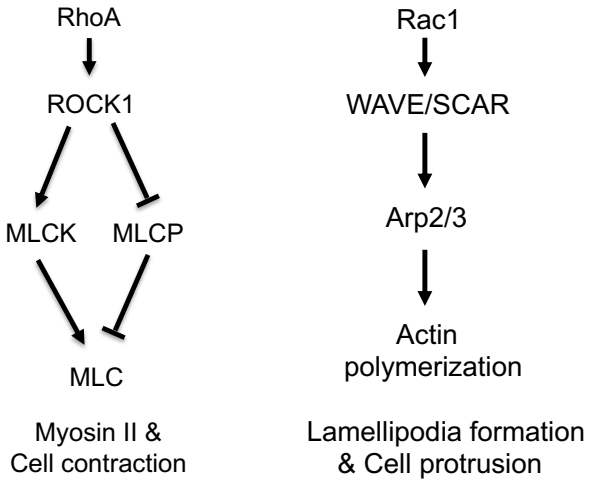

Figure 6. RhoA and Rac1 downstream signalling pathways. RhoA promotes cell contraction through activation of ROCK1, MLCK/MLCP and MLC signalling. In contrast, Rac1 stimulates cell protrusion via the WAVE/SCAR complex, Arp2/3 and actin polymerization.

Rac1 and RhoA perform these function by activating specific effectors. Rac1 activates its effector WAVE, which then activates the actin nucleator Arp2/3, leading to the formation of a dendritic actin network that pushes the cell's leading edge forward via lamellipodial cell protrusions (Eden et al., 2002; Miki et al., 1998; Pollard & Borisy, 2003). RhoA on the other hand activates its effector ROCK, which is a kinase that phosphorylates MLCK (Myosin light chain kinase) and MLCP (Myosin light chain phosphatase). This phosphorylation activates MLCK and inactivates MLCP. MLCK can activate myosin by phosphorylation of the Myosin light chain (MLC), while MLCP can inactivate myosin by dephosphorylation of MLC. Taken together, ROCK1 thereby acts via two distinct signals to stimulate myosin activity, either by activating the myosin activator MLCK or by inactivating the myosin inhibitor MLCP. Activation of Myosin leads to the formation of actomyosin structures, in particular stress fibres and the cortical actomyosin network, to generate contractile forces.

The biochemical processes that control the activity state of the Rho GTPases and their most prominent cellular functions are relatively well understood. However, how these GTPases are regulated in space and time in living cells is still unclear and is currently under active investigation.

1.4 Measuring the activity state of Rho GTPases

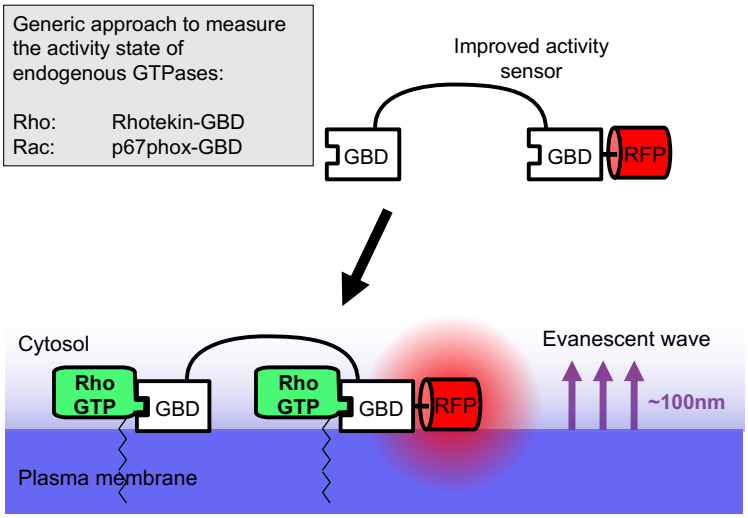

Figure 7. Strategy for measuring Rho GTPase activity at the plasma membrane via translocation sensors. Translocation of a GTPase binding domain (GBD)-based fluorescent reporter construct to the plasma membrane is measured via total internal reflection fluorescence microscopy (TIRF-M). These GBDs selectively bind to the active, GTP-bound form of small Rho GTPases localized at the plasma membrane. The use of tandem GBD repeats in the sensor construct enhances the sensitivity of the sensors. To measure the activity of Rho and Rac, the specific effector proteins Rhotekin, and $p67^{phox}$ were used, respectively. RFP: red fluorescent protein.

In this study, a translocation sensor-based method was used to measure the activity of small Rho GTPases in cells (Benink & Bement, 2005; Nanda et al., 2023)[1]. This translocation sensor consists of a GTPase binding domain (GBD) derived from a specific Rho GTPase effector, which was fused to a fluorophore. These sensors simply

[1] Nanda S. Investigation of signal networks that control dynamic cell shape changes (Doctoral dissertation), TU Dortmund, 2023

translocate from the cytosol to the plasma membrane as they specifically bind to the GTP bound, active form of Rho GTPases that is localized at the plasma membrane, and not to the GDP bound inactive GTPases that are localized in the cytosol bound to Rho GDIs. Thus, such sensors enable direct measurement of the endogenous Rho GTPase activity in living cells. This is in contrast to typical FRET-based methods, which are based on complex reporter constructs that measure the ratio of upstream GEF/GAP activities and were shown to be prone to artifacts (de Seze et al., 2023). The GBDs of Rhotekin and p67phox were specifically used to measure the activity of Rho and Rac GTPases, respectively. To increase the affinity of these GBDs to active Rho and Rac, double and triple tandem domain constructs of these GBDs were employed in this study to measure their activity (Nanda et al., 2023)[1]. TIRF (Total internal reflection fluorescence) microscopy was then used to monitor the translocation of these sensors from the cytoplasm to the plasma membrane to measure the local amount of active, endogenous Rho GTPases. TIRF microscopy is particularly well-suited for this purpose, as it allows the selective excitation of only those fluorescent signals that originate from proteins within a range of ~100nm from the plasma membrane, and thus can be used to sensitively detect cytosol to plasma membrane translocation events.

1.5 Methods for rapid perturbation of signal networks

1.5.1 Direct optogenetic control of Rac1 activity

One of the most effective methods for perturbing Rac1 is the use of a specifically designed photoactivable Rac1 (PA-Rac1) construct (Wu et al., 2009). In this construct, constitutively active Rac1 Q61L is fused to the C-terminal of the light sensitive light-oxygen-voltage 2 (LOV2) domain, which sterically prevents the effector binding site of the Rac1, such that it can no longer bind to its effectors in the dark state. The LOV2 domain consists of a coiled-coil helix structure that undergoes a conformational change upon illumination with 445 nm light. This conformational change exposes

[1] Nanda S. Investigation of signal networks that control dynamic cell shape changes (Doctoral dissertation), TU Dortmund, 2023

Rac1's effector binding site, thereby enabling interaction with its downstream effectors and downstream signaling pathways. This rapid perturbation can be easily combined with a readout of the signal network response. For example, the translocation of a Rho GTPase activity sensor from the cytosol to the plasma membrane (Section 1.4) or of any other protein of interest (POI) fused to a fluorescent protein can be measured via TIRF microscopy (Nanda et al., 2023)1.

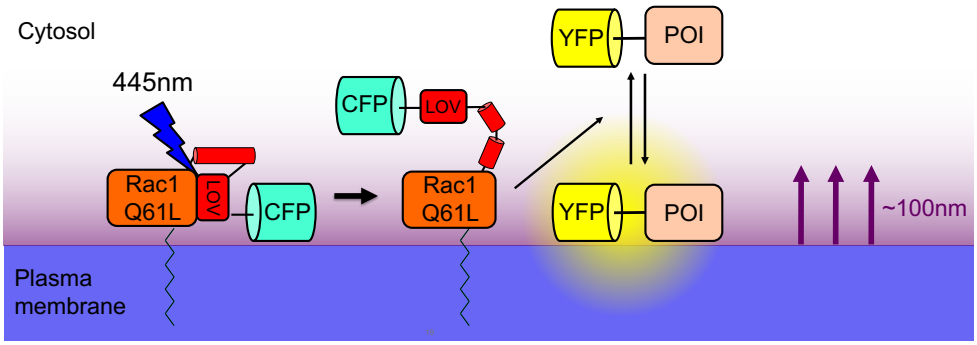

Figure 8. Signal crosstalk measurements by combining perturbations with simultaneous monitoring of the cellular response. Schematic representation of rapid optogenetic Rac1 perturbation via PA-Rac1 (Photoactivable Rac1), which can be combined with network response measurements based on an arbitrary protein of interest (POI) in living cells. The PA-Rac1 construct consists of a constitutively active Rac1 fused with LOV domain which is activated upon illumination with 445nm laser light. Translocation of a POI is measured via a fused fluorescent protein, such as YFP, using TIRF microscopy. LOV: Light oxygen voltage, POI: Protein of interest, CFP: Cyan fluorescent protein, YFP: Yellow fluorescent protein.

1.5.2 The generic LOVTRAP perturbation strategy for rapid perturbation of signal network components

In this thesis, the previously established LOVTRAP system (Wang et al., 2016) was used to introduce the perturbation of a protein of interest (POI) based on its effective cytosolic concentration (Figure 9). Using this system, the concentration of the POI can be manipulated in the cytosol by releasing it from the surface of mitochondria via

a light-controlled mechanism. For this, the POI is fused to the Zdk1 (Zdark1) domain, which binds to the LOV domain localized at the outer mitochondrial membrane in the dark. Upon illumination with 445nm light, this POI-Zdk1 complex dissociates from the LOV domain and is released into the cytosol, allowing it to freely interact with other molecules. Again, this rapid perturbation can be easily combined with a readout of signal network response, analogous to PA-Rac1 based perturbations described above (Section 1.5.1).

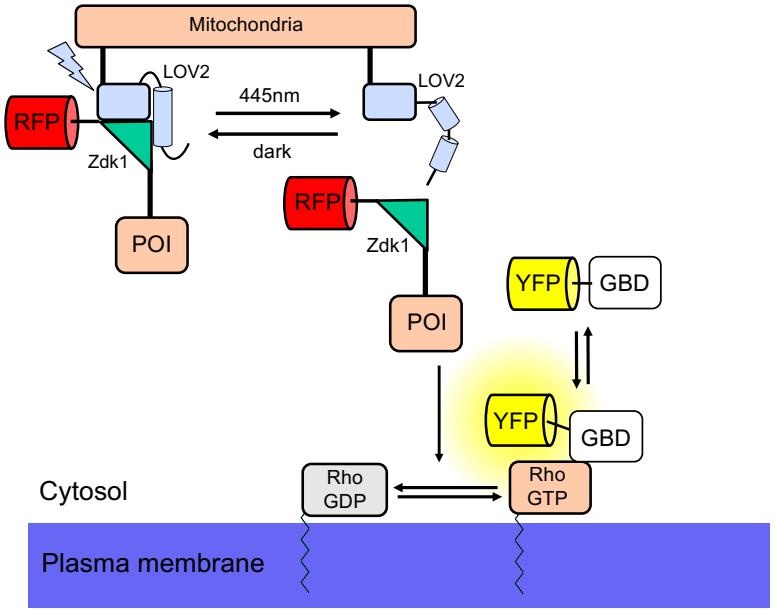

Figure 9. Rapid optogenetic perturbations of signal networks via the LOVTRAP system. Schematic representation of the LOVTRAP system, which is a generic method to introduce perturbations based on changing the effective cytosolic levels of the protein of interest (POI). Analogous to Figure 8, this can be combined with network response measurements, for instance by measuring the activity of Rho type GTPase via a translocation sensor. For optogenetic perturbation, the protein of interest (POI) is fused to Zdk1, and the LOV domain is localized to the outer mitochondrial membrane in the dark. Upon illumination with 445nm light, the LOV domain unfolds, releasing the POI into the cytosol and increasing its effective concentration. Rho GTPase activity is investigated by measuring the translocation of a YFP tagged GBD that specifically binds to the active Rho GTPase. LOV2: Light oxygen voltage 2, Zdk1: Zdark1, POI: Protein of interest, GBD: GTPase binding domain, RFP: Red fluorescent protein, YFP: Yellow fluorescent protein.

1.5.3 Chemical dimerizer induced rapid perturbation of signal network components

The third method employed in this thesis for rapid perturbation of Rho GTPases is chemically induced dimerization (Liu et al., 2014). In this method, a protein of interest (POI) is targeted to the plasma membrane and combined with readouts of the system response. Specifically, the POI is fused to a pair of tandem FKBP domains, together with a plasma membrane anchor linked to two tandem DHFR domains. Heterodimerization of these fusion proteins can be induced by adding the small molecule dimerizer SLF'-TMP, and this process can be reversed by adding the dimerization competitor TMP.

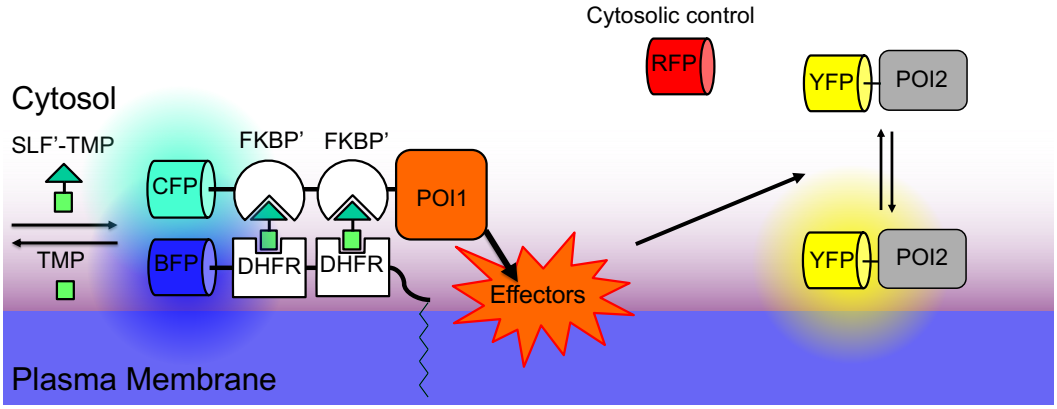

Figure 10. Rapid perturbation of signal networks via chemically induced dimerization. Schematic representation of the rapid and reversible signal network perturbation by enforcing the plasma membrane recruitment of protein of interest 1 (POI1) via chemically induced dimerization, combined with readout via plasma membrane translocation of a protein of interest 2 (POI2) that acts downstream of effectors of POI1. Dimerization of FKBP and DHFR is induced by adding small molecule dimerizer SLF-TMP, and translocation of POI1 and POI2 are measured via fused fluorescent proteins CFP and YFP using TIRF. An additional fluorescent protein (RFP) is used as a negative control readout. The competitor TMP is used to reverse this process. FKBP: FK506 binding protein, DHFR: dihydrofolate reductase, SLF'-TMP: Synthetic ligand of FKBP-Trimethoprim, TMP: Trimethoprim, CFP: Cyan fluorescent protein, BFP: Blue fluorescent protein, RFP: Red fluorescent protein, YFP: Yellow fluorescent protein.

Chapter 1: Crosstalk between Rac1 and RhoA mediated by Arhgef11/12.

2. Introduction

2.1 Crosstalk between the protrusion regulator Rac and the retraction regulator Rho

Previous studies suggested that Rac1 and RhoA mutually inhibit each other, which was thought to segregate protrusion and retraction in different regions of cell, leading to a stable cell polarization during directional migration (Figure 4) (Guilluy et al., 2011). However, cells undergoing mesenchymal migration exhibit highly dynamic protrusion-retraction cycles (Nalbant & Dehmelt, 2018), which are not easily explainable by Rac1-RhoA mutual antagonism. Recent studies of Rho GTPase crosstalk, that used rapid perturbations via chemically induced dimerization, found several functional interactions between Rho GTPase activity dynamics (Nanda et al., 2023)[1]. In agreement with previous studies that proposed mutual inhibition between Rac and Rho, rapid activation of RhoA was indeed found to inhibit Rac1. However, surprisingly, rapid activation of Rac1 was found to activate RhoA which is not compatible with the mutual inhibition theory (Nanda et al., 2023)[1]. While the activation of RhoA by Rac1 cannot explain stable spatial segregation between protrusion and retraction in directional migration, this mechanism together with inhibition of Rac1 by RhoA, could stimulate oscillatory dynamics and explain rapid cycling between protrusion and retraction in less directional and more exploratory cell migration. This crosstalk between Rac and Rho could link cell protrusion and retraction in space and time, and therefore could play an important role in dynamic cell protrusion-retraction cycles, which in turn play a central role in cell migration (Nanda et al., 2023)[1]. Potential molecules that can link Rac and Rho activity in cells and can possibly mediate this

[1] Nanda S. Investigation of signal networks that control dynamic cell shape changes (Doctoral dissertation), TU Dortmund, 2023

crosstalk, are Rho activating GEFs that can also act as effectors of active Rac (Dada et al., 2018).

2.2 Role of RhoGEFs in Rac/Rho activity crosstalk

Most RhoGEFs are members of the Dbl family, which are defined by the presence of a DH (Dbl Homology) and a PH (pleckstrin homology) tandem domain (Schmidt & Hall, 2002). The DH domain of these GEFs stimulates the nucleotide exchange on the target small GTPase. Specifically, the Lbc type GEFs are known to be activators of RhoA (Medina et al., 2013). The PH domain on the other hand primarily guides the localization of the GEF in cells. PH domains are best known for their interactions with phospholipids which is thought to mediate targeting to cell membranes. However, not all PH domains bind to phospholipids (Scheffzek & Welti, 2012). In particular, the PH domain of the Lbc type GEF, GEF-H1 was shown to be unable to bind phospholipids due to steric hindrance in the canonical binding pocket (Jiang et al., 2016). However, interestingly, the PH domains of all Lbc type GEFs were shown to specifically bind to the active form of RhoA (Medina et al., 2013). Based on these studies, a positive feedback mechanism was proposed, in which Lbc GEFs are recruited by active RhoA to the plasma membrane to amplify Rho activity. Recent studies also showed that the PH domain of some Lbc GEFs can also bind to active Rac1 (Dada et al., 2018). This makes the Lbc type GEFs interesting candidates for mediating the Rac/Rho activity crosstalk.

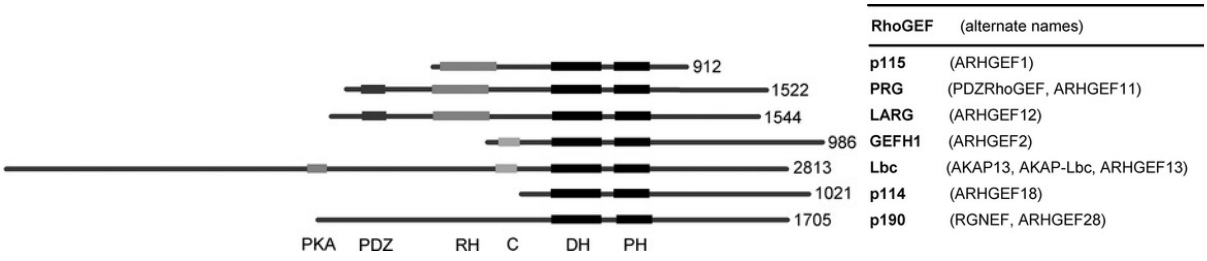

Figure 11. Schematic representation of the domain structure of Lbc-type RhoGEFs. PKA: Binding site for protein kinase A, PDZ: Domain present in PSD-95, Dlg, and ZO-1/2, RH: RGS homology domain, regulator of G protein signalling, C: C1 homology domain, DH: Dbl homology domain, PH: Pleckstrin homology domain. Figure from (Medina et al., 2013).

Figure 11 shows the names and domain structures of all the seven human Lbc type GEFs. More recent data showed that out of these seven RhoA activating Lbc type GEFs, Arhgef11 and Arhgef12 are particularly recruited to nascent cell protrusions where they could play a role in mediating the observed activity crosstalk between the cell protrusion regulator Rac1 and the cell contraction regulator RhoA (Nanda et al., 2023)[1]. Furthermore, increasing Arhgef11 or Arhgef12 expression levels lead to a corresponding increase in the dynamics of protrusion-retraction cycles. Conversely, RNA-interference based depletion of Arhgef11 or Arhgef12 lead to the opposite effect. These changes in the dynamics of cellular protrusion and retraction were also associated with corresponding changes in migration directionality. Together, these results show that Arhgef11 and Arhgef12 are regulators that mediate Rac/Rho activity crosstalk to promote the coupling between cell protrusion and cell retraction, and to promote a less directional, and more exploratory cell migration mode (Nanda et al., 2023)[1]. These observations raised the question, how Arhgef11 and Arhgef12 are mediating this crosstalk.

[1] Nanda S. *Investigation of signal networks that control dynamic cell shape changes* (Doctoral dissertation), TU Dortmund, 2023

3. Objective

Previous work that investigated the crosstalk between two major Rho-type small GTPases, Rac and Rho found the surprising result that Rho is activated by Rac. Two Lbc-type GEFs, Arhgef11 and Arhgef12 were candidates for possible mediators of this crosstalk. The main objective of this section of my thesis was to investigate the mechanism behind the activation of Rho by Rac via Arhgef11 and Arhgef12 and to identify which domains of these proteins are involved in this crosstalk.

4. Results

4.1 Proposed mechanism for Rac1/RhoA activity crosstalk via Arhgef11/12

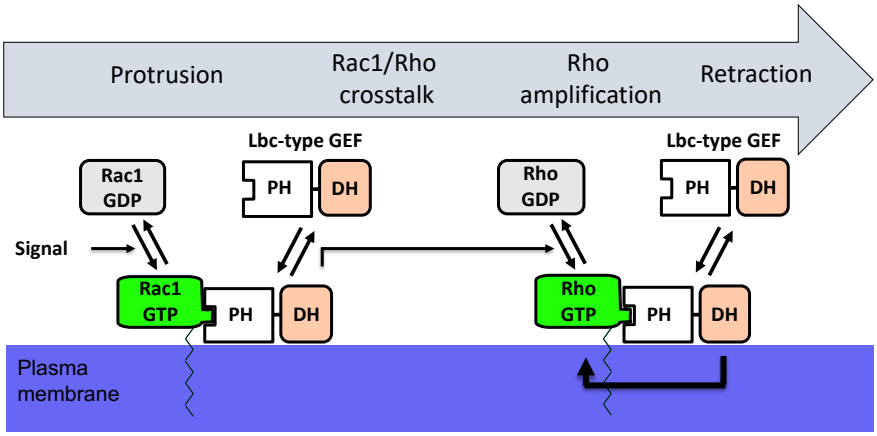

Figure 12. Schematic illustration of a proposed mechanism in which Lbc-type GEFs mediate the crosstalk between Rac1 and Rho activity. The Lbc-type GEFs can get recruited to the plasma membrane by interacting with active Rac1 via their PH domains. Once the GEF is localized at the plasma membrane its DH domain gets in close proximity of other, inactive Rho molecules, which can be activated by its GEF activity. Together, this process can mediate the crosstalk between Rac1/Rho. The Lbc-type GEFs can also bind to active Rho via their PH domains and can thereby also amplify Rho activity via positive feedback.

To investigate the molecular mechanism, by which Arhgef11 and Arhgef12 mediate Rac1/Rho activity crosstalk to couple cell protrusion and cell retraction, the following hypothesis was proposed: 1) Protrusions, which are generated spontaneously or via an external signal are associated with increased Rac1 activity at the plasma membrane. 2) Based on previous biochemical work, active Rac1 might be able to recruit Arhgef11/12 to the plasma membrane, for example via its PH domain. 3) Arhgef11/12 then activate Rho via their DH domain and thereby mediate Rac1/Rho activity crosstalk. 4) Arhgef11, Arhgef12 or another RhoGEF can then further increase Rho activity, for example via positive feedback, which could also be mediated by the

PH domain. 5) Increased Rho activity stimulates contractile forces that lead to local cell retraction (Figure 12).

Several aspects of this mechanism are already very well established, in particular the ability of Arhgef11 and Arhgef12 to activate Rho via their DH domains (Fukuhara et al., 1999, 2000), and the recruitment of these GEFs by active Rho via their PH domain to amplify Rho activity (Medina et al., 2013). While some biochemical evidence for an interaction of active Rac1 with the PH domain of Arhgef11 and Arhgef12 exists (Dada et al., 2018), it is less clear, if this interaction also occurs in cells. Previous studies only directly investigated this interaction in U2OS cells (Nanda et al., 2023)[1] which is a cell type that does not migrate efficiently and does not generate dynamic protrusion-retraction cycles. These studies were therefore not suitable to address the question, how Arhgef11 and Arhgef12 can stimulate these cycles.

To address this lack in our knowledge, I employed A431 cells, which are highly migratory, and which spontaneously generate highly dynamic protrusion-retraction cycles. Using this cell system, I performed optogenetic experiments for investigating if Arhgef11 or Arhgef12 are recruited to the plasma membrane by active Rac1 (Figure 13).

[1] Nanda S. *Investigation of signal networks that control dynamic cell shape changes* (Doctoral dissertation), TU Dortmund, 2023

4.2 Recruitment of Arhgef11 and Arhgef12 by active Rac1

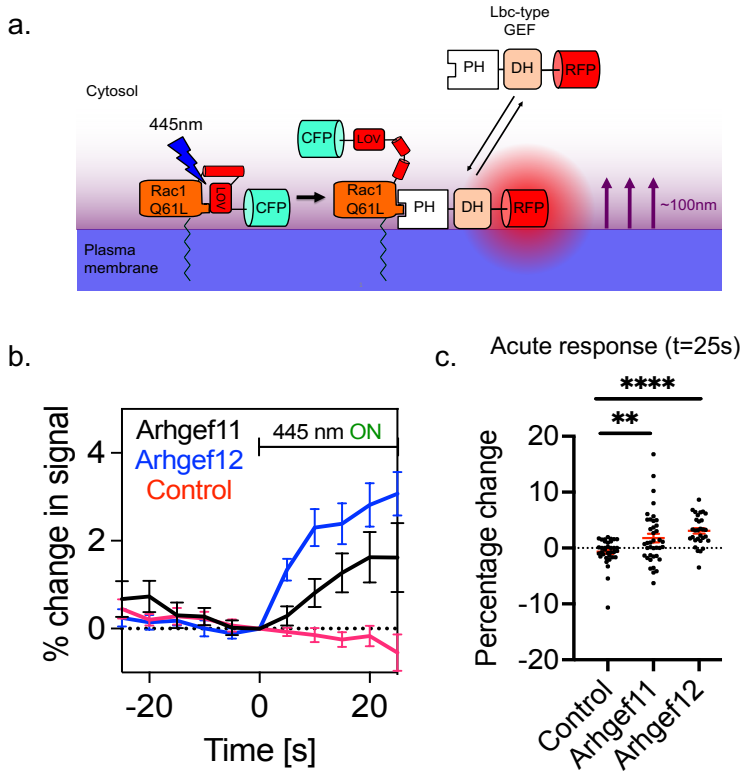

Figure 13. Direct measurement of the Arhgef11/12 plasma membrane recruitment response to rapid Rac1 activation in A431 cells. a Schematic illustration of the optogenetic method used to investigate the recruitment of Lbc-family GEFs by active Rac1. **b,c.** Measurement of the recruitment of Lbc-type GEF and control construct following rapid Rac activation at t=0s. b: Recruitment kinetics; c: Comparison of recruitment at the timepoint of maximal recruitment of Arhgef11 and Arhgef12 by active Rac1 (t=25s). Error bars represent standard error of the mean. **: p<0.01; ****: p<0.0001; One-way ANOVA with Dunnett's post-test; n=3 independent experiments with >35 cells per condition. Adapted from Nanda et al., (2023).

In these experiments, a light-controlled PA-Rac1 construct (Wu et al., 2009) was used, which is based on the constitutively active Q61L mutant of Rac1. Here I directly investigated, if this light-triggered activation can stimulate the recruitment of Arhgef11 or Arhgef12 as potential Rac1 effectors. These GEFs were labelled with fluorescent proteins, and their plasma membrane translocation was measured using TIRF

microscopy. As shown in Figure 13b-c, acute optogenetic activation of Rac1 induces rapid recruitment of both Arhgef11 and Arhgef12 to the plasma membrane.

These results show that both Arhgef11 and Arhgef12 can be recruited by active Rac to the plasma membrane, which is a critical step in the hypothetical mechanism which was proposed above (Figure 12).

4.3 Mechanism of Rac1/RhoA crosstalk by Arhgef11 and Arhgef12

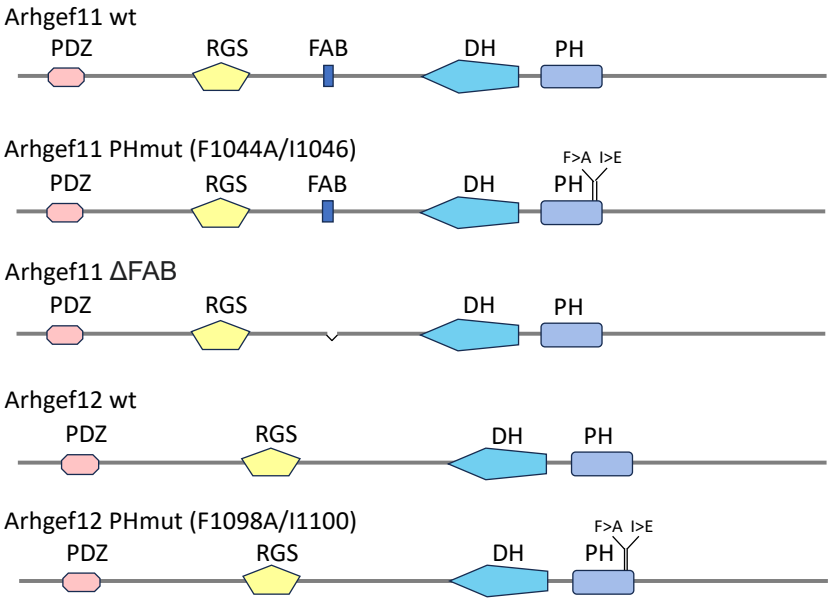

Figure 14. Domain structure of WT and mutated Arhgef11 and Arhgef12. PDZ: Domain present in PSD-95, Dlg, and ZO-1/2, RGS: Regulator of G protein signalling domain, FAB: F-actin binding motif, DH: Dbl homology domain, PH: Pleckstrin homology domain. Adapted from Nanda et al., (2023).

Next, I investigated which domains of Arhgef11 and Arhgef12 are involved in their Rac1-activity dependent plasma membrane recruitment. Based on previous reports that the PH domain of some Lbc type GEFs can bind active Rac1 (Dada et al., 2018), I first tested the hypothesis, that the PH domain of Arhgef11/12 plays a role in mediating this Rac1/Rho activity crosstalk.

To test this hypothesis, I introduced point mutations into the PH domain of Arhgef11 and Arhgef12 that are known to interfere with its interaction with active Rho family GTPases (Medina et al., 2013; Dada et al., 2018). In particular, I introduced the point mutations F1044A and I1046E in Arhgef11 and the point mutations F1098A and I1100E in Arhgef12 (Figure 14) (Medina et al., 2013). Using these mutated Arhgef11 and Arhgef12 constructs, I investigated whether these mutants are still recruited to the plasma membrane by active Rac1 using the same experimental strategy as shown in Figure 13a.

4.3.1 Recruitment of PH mutant Arhgef11 and Arhgef12 by active Rac1

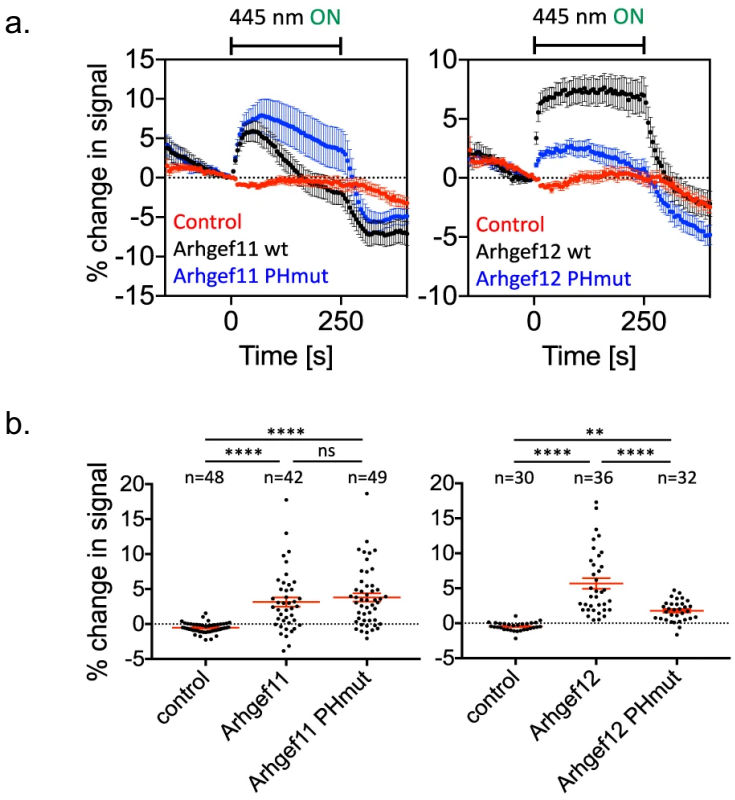

Figure 15. Role of the PH domain for Rac1-dependent Lbc-GEF plasma membrane recruitment. a,b. Analysis of plasma membrane recruitment of full length and mutant Lbc-type GEFs in A431 cells after optogenetic activation of Rac1. **a**. Analysis of recruitment kinetics. **b**. Quantitative analysis of recruitment at 25s after photoactivation (early response). Error bars represent standard error of the mean. **: p<0.01; ****: p<0.0001; ns: not significant;

One-way ANOVA with Tukey's post-test; at least 3 independent experiments with >29 cells per condition. Adapted from Nanda et al., (2023).

As shown in Figure 15, I found that the PH domain of Arhgef12 must remain intact to enable effective plasma membrane recruitment, demonstrating the functional importance of this domain. However, corresponding mutations in the PH domain of Arhgef11 did not affect its recruitment to the plasma membrane, which suggests that another domain of this molecule might be critical for its recruitment.

A possible alternative mechanism might involve the F-actin binding motif of Arhgef11 (Figure 13) (Banerjee & Wedegaertner, 2004). As Rac1 is known to stimulate actin polymerization, Arhgef11 could also be recruited to the cell cortex near the plasma membrane by this F-actin binding motif.

Interestingly, the recruitment patterns of Arhgef11 and Arhgef12 were different between central and peripheral areas of cell attachment. Especially in the case of Arhgef11, it was observed that it is initially recruited more strongly to the central cell attachment area, followed by a strong enrichment at the periphery (Figure 16a). Therefore, it was hypothesized that these complex spatio-temporal dynamics may result from the interaction of Arhgef11 with F-actin, which is likely to increase particularly strongly in the cell periphery at a later time after Rac1 activation, when actin-rich lamellipodial protrusions are formed. To investigate this idea, I deleted the F-actin binding domain from Arhgef11 (Figure 14) and then measured the recruitment of this mutated Arhgef11 construct by active Rac1.

4.3.2 Recruitment of F-actin binding domain mutant Arhgef11 by active Rac1

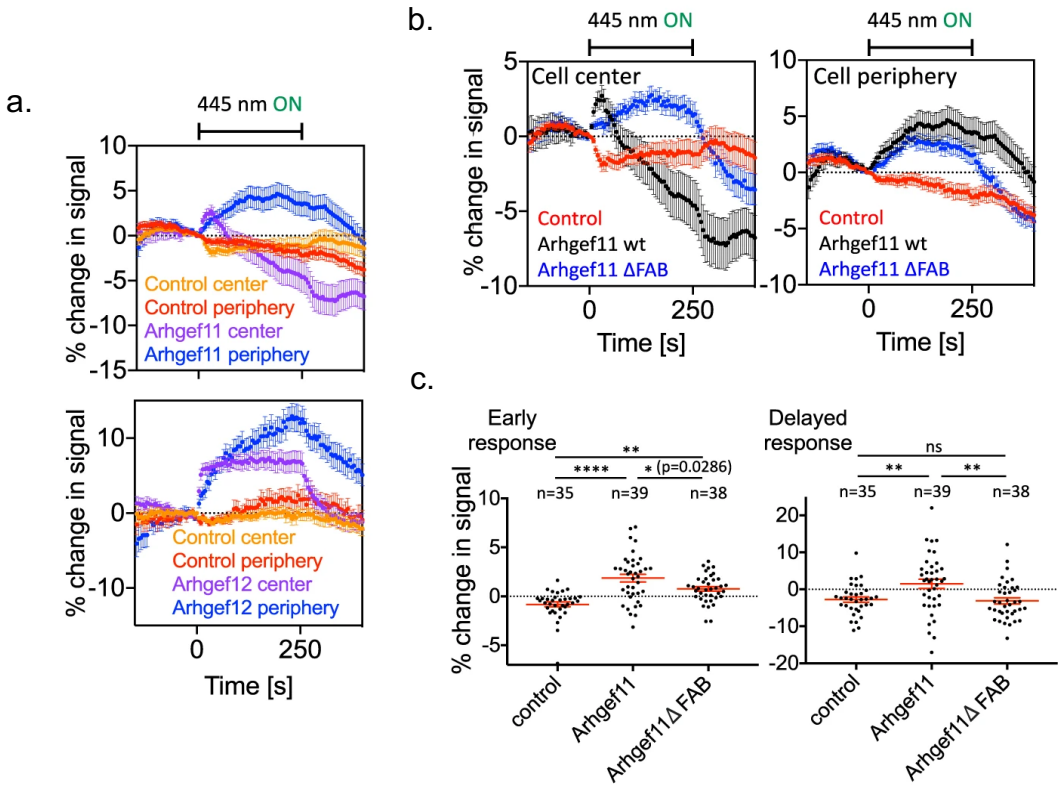

Figure 16. Role of F-actin binding domain in Rac1 induced plasma membrane recruitment of Arhgef11. a-c. Measurement of plasma membrane localization of full length and mutant Lbc-family GEF by active Rac1 in A431 cells co-expressing PA-Rac1. **a,b.** Measurement of plasma membrane recruitment kinetics of Arhgef11 and Arhgef12 in peripheral vs central areas of cell attachment. **c.** Recruitment of full length and mutant Arhgef11 along with the control construct was quantified at both 25 s (early response) or 1 min (late response) after photoactivation. Error bars represent standard error of the mean. *: p<0.05; **: p<0.01; ****: p<0.0001; ns: not significant; One-way ANOVA with Tukey's post-test; at least 3 independent experiments with >35 cells per condition. Adapted from Nanda et al., (2023).

As expected, removal of the F-actin binding motif of Arhgef11 significantly reduced the early response in the central region of the cell as well as delayed response at the peripheral regions (Figure 16b,c). These results indicate that Arhgef12 is primarily recruited to the plasma membrane through direct binding of its PH domain to active

Rac1, while recruitment of Arhgef11 to the cell cortex is mediated as a result of its binding to F-actin, which is upregulated downstream of Rac1 activation.

However, since these mutations did not fully inhibit plasma membrane recruitment of Arhgef11 and Arhgef12, additional factors such as Arhgef11/12 heterodimerization (Chikumi et al., 2004) or interactions with other proteins like Gα12/13 (Fukuhara et al., 1999, 2000) may also contribute to its recruitment.

5. Discussion

In this part of the thesis, I investigated the mechanism how Lbc-type GEFs, Arhgef11 and Arhgef12 mediate the crosstalk by which the protrusion regulator Rac activates the retraction regulator Rho (Nanda et al., 2023)[1]. Detailed investigations into this process revealed that both Arhgef11 and Arhgef12 mediate this crosstalk using different domains. In the case of Arhgef12, the PH domain interacts with active Rac1, which in turn, through its DH domain, activates Rho and thereby can mediate Rac-dependent Rho activation. In contrast, for Arhgef11, the PH domain does not appear to participate in this process, as mutating the PH domain of this molecule did not alter its recruitment by active Rac1. Instead, Arhgef11 has an additional F-actin binding (FAB) domain which was found to play a key role in mediating this crosstalk. Active Rac is known to stimulate cell protrusion by stimulating directional polymerization of actin at the front of the cell (Nobes & Hall, 1995). The F-actin binding domain of Arhgef11 binds to this newly polymerized actin in the cell cortex near the plasma membrane which is downstream of Rac1 (Banerjee & Wedegaertner, 2004). Then, similar to Arhgef12, Arhgef11 also activates Rho via its free DH domain to mediate Rac-dependent Rho activation.

I also observed that the recruitment pattern of Arhgef11 and Arhgef12 by active Rac1 differs between cell periphery and cell center. For Arhgef12, the recruitment was similar at both the cell periphery and the cell center. In contrast, Arhgef11 exhibited a notable difference between its recruitment at the cell center and periphery. At the cell center, Arhgef11 was recruited rapidly within seconds after Rac1 activation but subsequently declined despite continued Rac1 activity, suggesting the presence of a negative feedback mechanism that inhibits its central recruitment. In contrast, at the cell periphery, recruitment of Arhgef11 reached its maximum after a delay, probably due to the time required for newly polymerized actin to form following Rac1 activation. This newly polymerized actin could then recruit Arhgef11 via its F-actin binding domain. This additional domain in Arhgef11 accounts for the observed differences in recruitment patterns compared to Arhgef12, which lacks an F-actin binding domain.

[1] Contribution from this thesis

It was also observed that, even with mutation of the PH domain in Arhgef12 and removal of the F-actin binding (FAB) domain in Arhgef11, the recruitment of Arhgef11 and Arhgef12 by active Rac1 was not completely abolished. This suggests that additional domains in these proteins contribute to their recruitment process.

Besides the DH and PH domains, Arhgef11 and Arhgef12 also contain RGS and PDZ domains, which may play a role in this mechanism. The RGS domain is related to regulators of G protein signalling, as it specifically interacts with the heterotrimeric Gα12/13 subunits (Fukuhara et al., 1999, 2000). Consequently, if Rac can activate this pathway in A431 cells. Arhgef11 and Arhgef12 can be recruited to the plasma membrane via their RGS domain to heterotrimeric G proteins and subsequently activate Rho. The PDZ domains of Arhgef11 and Arhgef12, on the other hand, are known to interact with Plexin-B1, a transmembrane receptor (Aurandt et al., 2002; Driessens et al., 2002; Hirotani et al., 2002). This receptor can also interact with active Rac1 via the CRIB motif in its cytoplasmic domain (Driessens et al., 2001; Vikis et al., 2000). Thus, active Rac1 may recruit Arhgef11 and Arhgef12 indirectly by binding to Plexin-B, which in turn interacts with their PDZ domains.

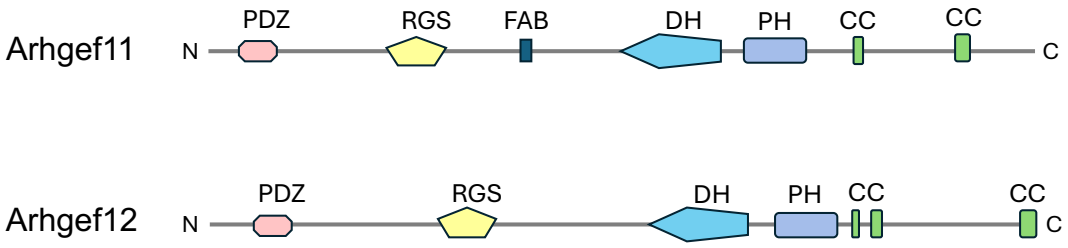

Figure 17. Domain structure of Arhgef11 and Arhgef12. PDZ: Domain present in PSD-95, Dlg, and ZO-1/2, RGS: Regulator of G protein signalling domain, FAB: F-actin binding motif, DH: Dbl homology domain, PH: Pleckstrin homology domain, CC: Coiled-coil domain.

In addition, Arhgef11 and Arhgef12 also contain a predicted C-terminal coiled-coil domain (Figure 17) that enables them to heterodimerize with each other (Chikumi et al., 2004) and thus allows them to be recruited together at the plasma membrane

downstream of active Rac1. Consequently, mutating only one of these molecules might not completely abolish the recruitment of the complex by active Rac1.

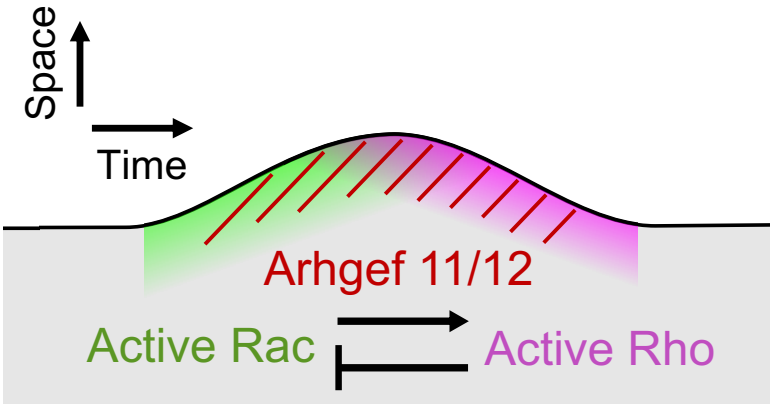

Figure 18. Schematic representation of the spatio-temporal activities linking cell protrusion and cell retraction, along with the signalling molecules mediating this process. Rac is predominantly active at cell protrusions while Rho activity is enriched at cell retractions. Active Rac promotes Rho activation via Arhgef11/12 while active Rho inhibits Rac activity. Adapted from Nanda et al., (2023).

Finally, in this section of the thesis, a mechanism was proposed by which Arhgef11 and Arhgef12 link the signalling molecules that regulate cell protrusion (Rac) and cell retraction (Rho) (Figure 18). By coordinating Rac and Rho activity, Arhgef11/12 apparently drive cell retraction after protrusion, enabling spontaneous changes in migration directionality. Thus, our findings uncover a mechanism by which crosstalk between the key morphogenetic regulators Rac and Rho integrates local protrusion-retraction dynamics to promote exploratory cell migration.

Chapter 2: Rnd3 regulates cell morpho-dynamics by spatial restriction of cell contraction signalling.

6. Introduction

6.1 Generation of spatio-temporal activity patterns by mutual signal inhibition

Mutual inhibition is a classic motif that can stabilize local cell states (Dehmelt & Bastiaens, 2010). For example, polarity signaling via Par proteins is thought to involve mutual inhibition, leading to bistability, resulting in the stabilization of mutually exclusive anterior and posterior regions of early C. elegans embryos (Lang & Munro, 2017). Results presented in Chapter I contributed to the idea, that Rac and Rho activities are not mutually inhibitory as it was previously thought in the field (Guilluy et al., 2011), but that instead Rac1 can activate Rho. Nevertheless, Rac and Rho activity was highly localized to the cell periphery during protrusion and retraction respectively, and the activities of both the Rho GTPase were mainly absent from more central cell regions. This raised the question, how this specific localization of Rac and Rho is achieved. It was therefore hypothesized that a different pair of mutual inhibitory proteins might be responsible to generate the observed Rac1 and Rho activity patterns.

Based on the literature, the unconventional Rho GTPase Rnd3 is a promising candidate, as it was already known to interact mutually inhibitory with the retraction regulator RhoA (Aoki et al., 2016).

6.2 The atypical Rho type GTPase Rnd3

Rnd3, also referred to as RhoE, belongs to the Rho family of GTPases. It is a part of the Rnd subclass of the Rho family small GTPases comprising Rnd1, Rnd2, Rnd3/RhoE. Rnd GTPases are distinct from the conventional Rho-type GTPases as they lack intrinsic GTPase activity i.e. they are unable to switch from the GTP bound active state to the GDP bound inactive state (Wennerberg et al., 2003). Interestingly, other regulatory mechanisms exist that control the activity state of these molecules. These include in particular phosphorylation and interactions with 14-3-3 proteins (Madigan et al., 2009).

Active Rnd3 is unphosphorylated and primarily localized to the plasma membrane, where it binds to its effectors to transmit downstream signals. In contrast, phosphorylated Rnd3 interacts with 14-3-3 proteins, which promotes the translocation from the plasma membrane to the cytosol (Riou et al., 2013) to inhibit its activity (Figure 19 right). The most well-established function of Rnd3 is its ability to inhibit RhoA (Riento & Ridley, 2006; Wennerberg et al., 2003). As summarized in 1.3, Rho stimulates cell contraction by activating its effectors, in particular via its effector kinase ROCK. Thus, by inhibiting RhoA, Rnd3 can also inhibit its downstream signalling via ROCK and myosin and thereby inhibit cell contraction.

6.3 Mutual inhibition between Rnd3 and Rho

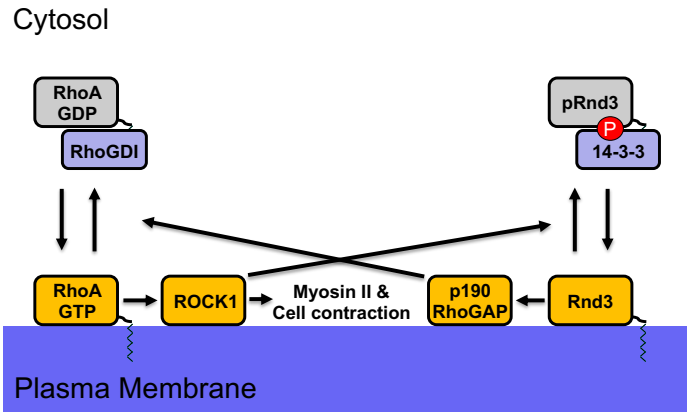

Figure 19. Schematic representation of the mechanism of mutual inhibition between Rho and Rnd3. Rho activates ROCK1, which in turn phosphorylates Rnd3 (pRnd3), leading to its extraction from the plasma membrane to the cytosol, thereby inhibiting Rnd3 downstream activity. In its unphosphorylated state, Rnd3 activates p190RhoGAP, which in turn inhibits Rho, leading to its extraction from the plasma membrane via RhoGDI. This simplified scheme does not show the activation of RhoA by RhoGEFs and the activation of Rnd3 by phosphatases.

Several lines of investigations suggest that Rnd3 and RhoA can mutually inhibit each other's activity. Mechanistically, it was shown that Rnd3 can inhibit RhoA by activating the Rho inhibitor p190RhoGAP (Wennerberg et al., 2003) (Figure 19, right). p190RhoGAP is a GTPase activating protein (GAP) which stimulates the hydrolysis of GTP to GDP in Rho and thereby converts Rho from its GTP-bound active state to its GDP-bound inactive state (Arthur & Burridge, 2001; Bidaud-Meynard et al., 2019). GDP-bound Rho is then extracted from the plasma membrane to the cytosol by the solubilization factor RhoGDI (Figure 19, left). Conversely, Rho is also able to inhibit Rnd3. This inhibitory action is mediated by the Rho effector kinase ROCK1, which phosphorylates Rnd3 at multiple sites (Komander et al., 2008), resulting in binding of 14-3-3 and translocation of the Rnd3/14-3-3 complex from the plasma membrane to the cytosol (Riou et al., 2013) as described above (Figure 19, right).

7. Objective

In our previous studies, highly localized activity patterns of the small GTPase Rac and Rho were observed at the cell edge during migration. A typical network motif that can explain these activity patterns is mutual inhibition between two signal molecules. Here, I hypothesize that the mutual inhibition between Rho and Rnd3 might be linked to the exclusive activity of Rho at the cell edge during migration. A similar mechanism might also exist to restrict Rac1 activity at the cell edge. The main objective of this section of my thesis is to characterize crosstalk between Rnd3 and Rho/Rac activity, and to investigate their activity patterns in migrating cells and how Rnd3 affects cellular morphology and morphodynamics.

8. Results

8.1 Rho is inhibited by Rnd3 perturbations induced via the LOVTRAP system

A rapid, light-based perturbation method combined with the readout of the response signal was used to investigate Rnd3/Rho crosstalk. Specifically, the LOVTRAP system that was previously developed (Wang et al., 2016) was used to introduce a rapid perturbation of Rnd3 (Figure 20a). This system enables light-controlled and reversible regulation of the concentration of a protein of interest in the cytosol by controlling its release from the mitochondrial surface. Here, I fused Rnd3 with the Zdk1 (Zdark1) domain. Cells also express the light-sensitive LOV domain on the membrane surface of mitochondria. The Rnd3- Zdk1 fusion protein binds tightly to the dark state of the LOV domain and is thereby targeted to the outer mitochondrial membrane. Upon exposure to 445nm light, the Zdk1-Rnd3 complex dissociates and is released in the cytosol, allowing it to freely interact with other cellular signaling molecules.

The rapid manipulation of Rnd3 activity was paired with measurements of Rho activity at the plasma membrane using a translocation sensor derived from the Rhotekin GTPase-binding domain (GBD) (Benink & Bement, 2005). This sensor selectively associates with the active, GTP-bound Rho, which is mainly found at the plasma membrane (Symons & Settleman, 2000), and it does not bind the inactive, GDP-bound Rho that is largely found in the cytoplasm where it is solubilized by RhoGDIs (Be & Mccormick, 1993; Garcia-Mata et al., 2011). In particular, I used a modified version of the sensor that is expressed downstream of the delCMV promoter at very low levels (Watanabe & Mitchison, 2002) and contains two tandem GBD domains to increase its affinity for active Rho (previously described in (Nanda et al., 2023)[1]). TIRF microscopy was then applied to measure the translocation of the sensor from the cytoplasm to the plasma membrane, providing a readout of the local levels of active endogenous Rho.

[1] Nanda S. Investigation of signal networks that control dynamic cell shape changes (Doctoral dissertation), TU Dortmund, 2023

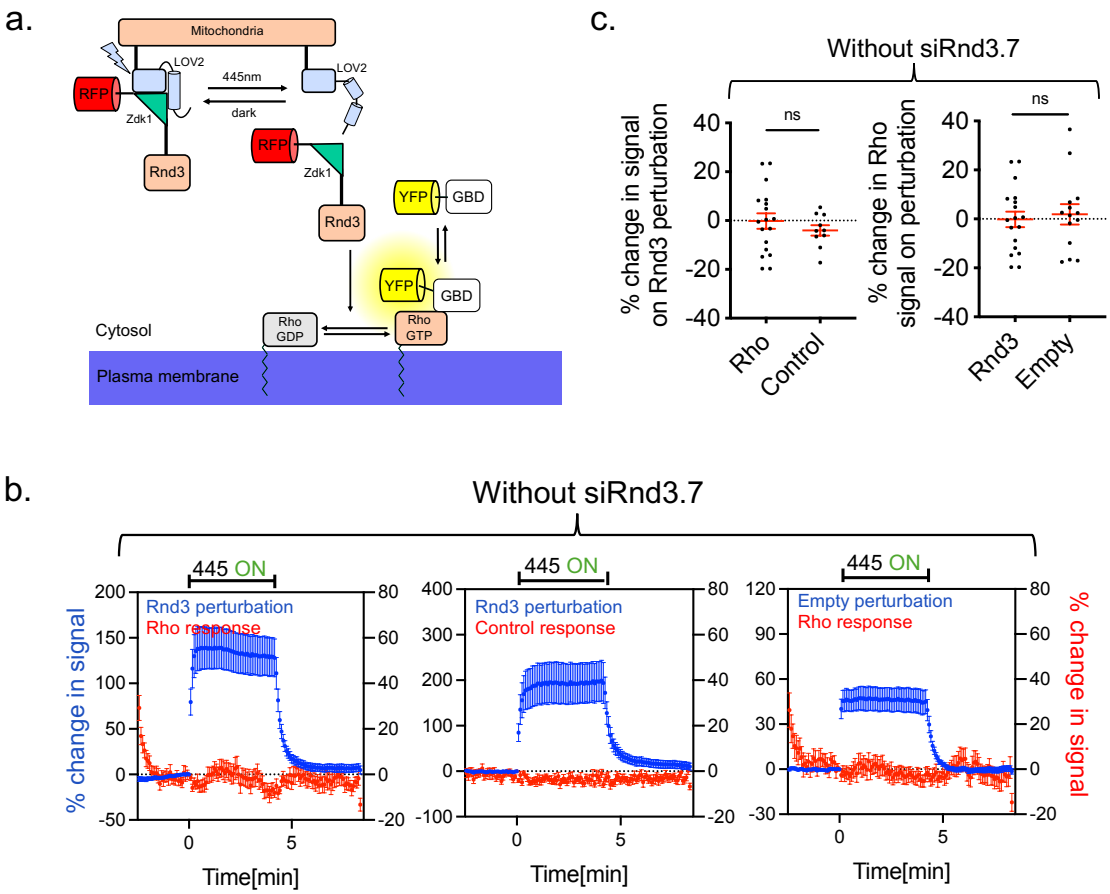

Figure 20. Direct measurement of the Rho activity response to rapid Rnd3 perturbations in A431 cells in the presence of endogenous Rnd3. a Schematic illustration for rapid and reversible light-based Rnd3 perturbation using the LOVTRAP system in combination with Rho activity sensor readout. **b.** Analysis of Rnd3 perturbation together with the recruitment kinetics of the Rho activity sensor over the whole cell attachment region. **c.** Quantification of the Rho and control sensor response 1 min following perturbation. *n* = 3 independent experiments with ≥10 cells per condition. ns: not significant; two-sided t-test. Error bars represent standard error of the mean. Adapted from Sachan et al., (2025).

In initial experiments, no change in the Rho activity signal was observed even after releasing a significant amount of Rnd3 into the cytosol via the LOVTRAP system (Figure 20b,c). This was unexpected, as Rnd3 is well-established as an inhibitor of Rho activity. A potential explanation for this lack of response could be due to high endogenous levels of the Rnd3 which may already be saturating, such that releasing more Rnd3 into the cytosol was not able to cause a noticeable effect.

Therefore, this experiment was then combined with Rnd3 knockdown using RNA interference to reduce the level of endogenous Rnd3.

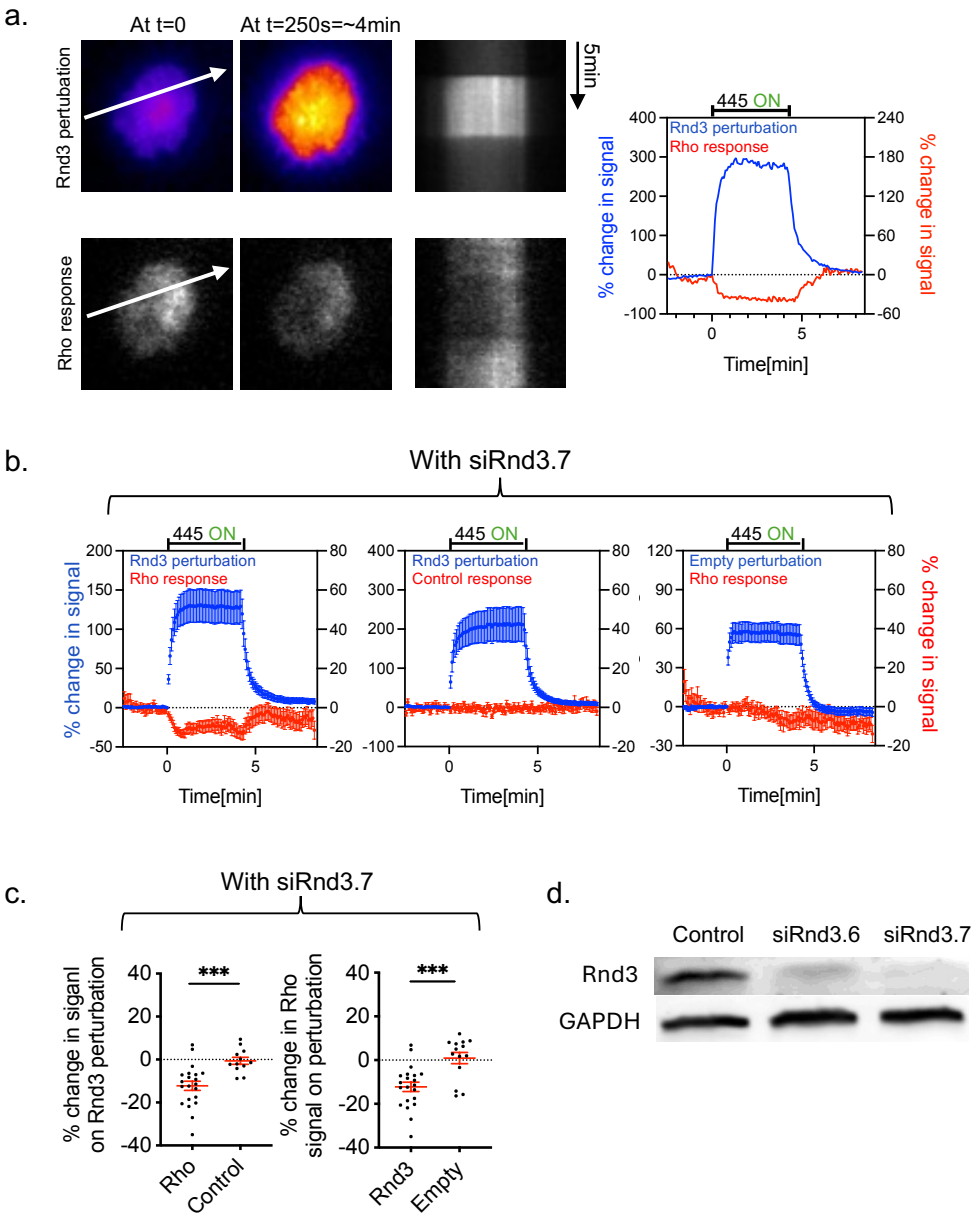

Figure 21. Direct measurement of the Rho activity response to rapid Rnd3 perturbations following knockdown of endogenous Rnd3. a. Representative TIRF microscopy images and corresponding kymographs from the region indicated by the white arrow in the cells for Rnd3 perturbation and Rho activity response along with the intensity profile measured across the entire cell adhesion area. **b.** Quantitative analysis of Rnd3 perturbation and the Rho activity recruitment in the whole area of cell adhesion. **c.** Quantification of the sensor response 1 min after perturbation. **d.** Representative western blot image confirming the knockdown of Rnd3.

n = 3 independent experiments with >11 cells per condition. ***$P < 0.001$; two-sided t-test. Error bars represent standard error of the mean. Adapted from Sachan et al., (2025).

First, an efficient knockdown of Rnd3 was established using two independent siRNAs and their efficiency was validated by western blot analysis (Figure 21d). These experiments showed that Rnd3 levels were successfully reduced by 72.05 ± 1.5% with siRnd3.6 and by 92.5 ± 3% with siRnd3.7. After knockdown of endogenous Rnd3 with siRnd3.7, a rapid increase in Rnd3-Zdk1 signal in the cytosol via the LOVTRAP system led to a rapid and significant inhibition of the Rho activity signal (Figure 21a-c). These findings suggest that Rnd3 negatively regulate Rho activity in our cell system, similar to previous observations in other systems.

8.2 Rnd3 is inhibited by RhoA perturbations induced via chemically induced dimerization

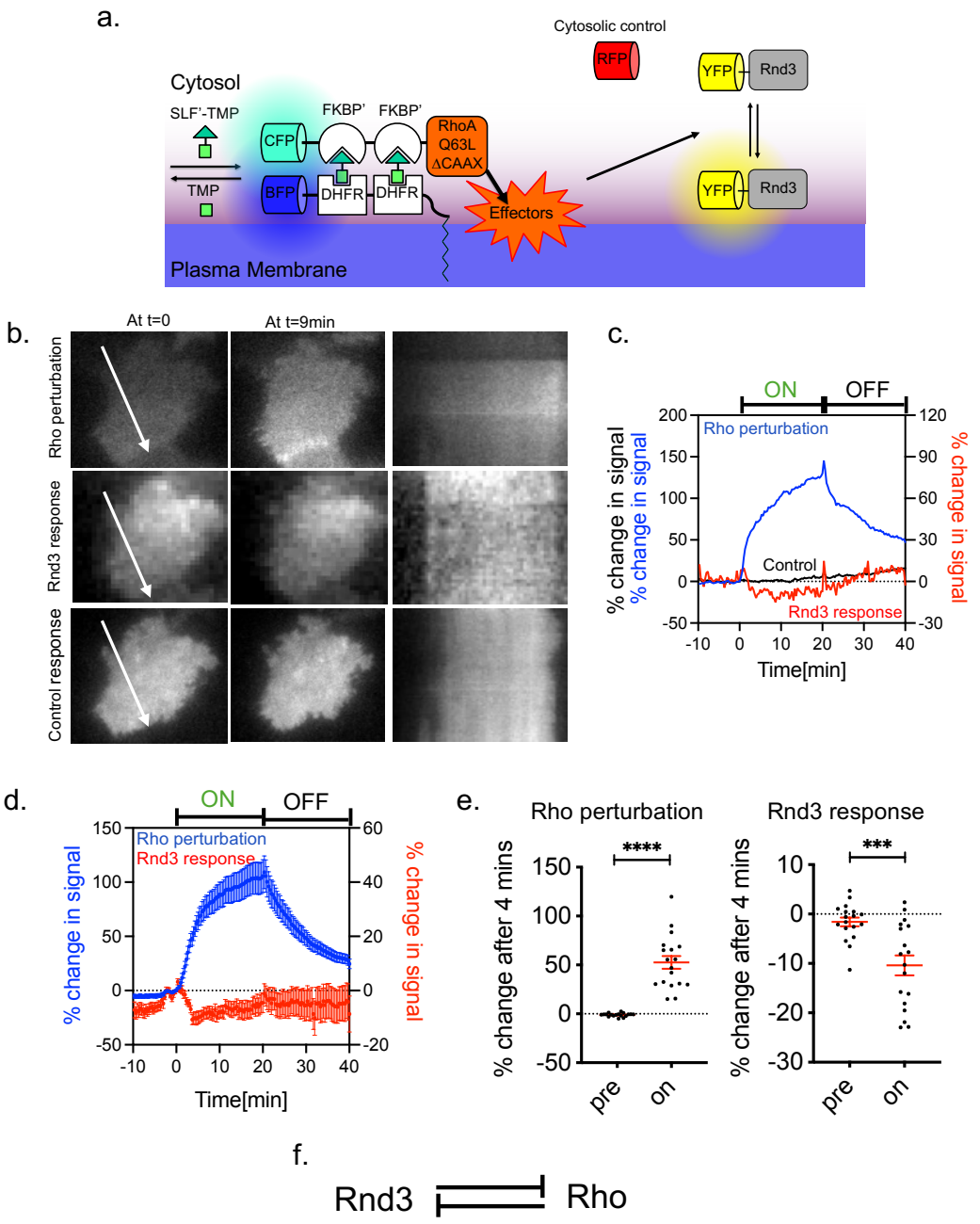

Figure 22. Direct measurement of the Rnd3 response to rapid Rho perturbations in A431 cells. a. Schematic illustration of rapid, reversible RhoA activity perturbation via chemically induced dimerization combined with a Rnd3 activity response readout. **b.** Representative TIRF microscopy images and associated kymographs (marked by the white arrow) of cells expressing Rho perturbation, Rnd3, or control sensor. For Rnd3 analysis, raw pixel intensities

were binned by averaging 4×4 pixels for kymographs and 8×8 pixels for images to enhance the signal-to-noise ratio. All the other measurements were performed using the original raw pixel intensities without any downscaling. **c.** Quantitative analysis of Rho perturbation together with the raw, uncorrected responses of the Rnd3 and control sensor measured across the entire cell adhesion area of the example cell depicted in b. **d.** Mean Rho perturbation and normalized Rnd3 sensor responses calculated from multiple cells. **e.** Analysis of Rho perturbation and normalized Rnd3 sensor response before (pre) and 4 mins after dimerizer addition (on). $n = 3$ independent experiments with 19 cells. **f.** Schematic model illustrating the proposed crosstalk between Rnd3 and Rho activity in A431 cells.$^{****}P < 0.0001$; $^{***}P < 0.001$; two-sided t-test. Error bars represent standard error of the mean. Adapted from Sachan et al., (2025).

Next, I investigated the effect of Rho on Rnd3. For this, a chemical dimerizer based method was used to target active Rho to the plasma membrane, and this was combined with a Rnd3 activity readout. For the perturbation, a constitutively active RhoA mutant was fused to two FKBP domains in tandem, while a plasma membrane anchor was linked to two tandem DHFR domains. The dimerization between these fusion proteins was then induced by adding the small molecule dimerizer SLF'-TMP (Figure 22a). This method was already established in a previous study where they showed that plasma membrane recruitment of active Rho successfully induced the expected phenotype of cell contraction (Nanda et al., 2023)[1]. Additionally, the perturbation of Rho via this method can also be reversed by adding dimerization competitor TMP to the cells. Addition of TMP also reversed the phenotype of cell contraction induced by activation of Rho (Nanda et al., 2023)[1].

For measuring the change in Rnd3 activity on Rho perturbation, I simply measured the association of a weakly expressed fluorescent fusion protein (delCMV-mCitrine-Rnd3) with the plasma membrane using TIRF microscopy. This is possible, because Rnd3 is an unconventional Rho-type GTPase, which is considered to be constitutively active as it exists in the GTP-bound state at all times (Foster et al., 1996). For Rnd3, its translocation from the cytosol to the plasma membrane or vice-versa is the main mechanism for turning the Rnd3 activity on or off respectively (see also Figure 18,

[1] Nanda S. Investigation of signal networks that control dynamic cell shape changes (Doctoral dissertation), TU Dortmund, 2023

right). Thus, measuring the plasma membrane association or dissociation dynamics of Rnd3 protein is sufficient to evaluate its local activity state in this critical cell compartment.

Using this method, rapid perturbation of RhoA lead to a significant inhibition of Rnd3 already at very early timepoints (Figure 22e). Thus, I was able to show that Rho can indeed inhibit Rnd3 in the A431 cell system (Figure 22b-e) (Riou et al., 2013). However, at later timepoints, Rnd3 inhibition became less pronounced despite the sustained presence of active RhoA, indicating potential adaptive mechanisms. (Figure 22d).

Overall, these findings confirm the mutual inhibition between Rnd3 and Rho (Figure 22f). However, Rho-mediated inhibition of Rnd3 was relatively modest and observed only for a brief period.

8.3 Rnd3 is depleted from the leading edge of migrating cells

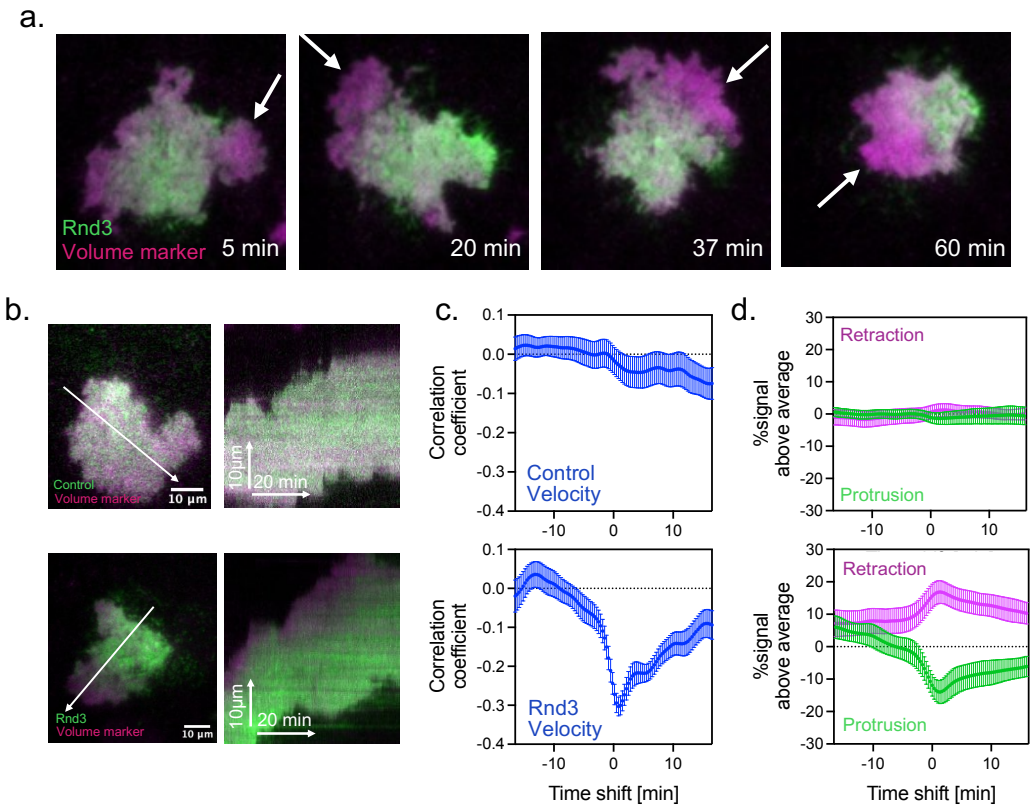

Figure 23. Rnd3 dynamics in migrating A431 cells. a. Sequential TIRF microscopy images of a A431 cell during migration co-expressing Rnd3 together with a cell volume marker. Newly generated protrusive regions are indicated by white arrows. **b.** Representative TIRF images showing either the Rnd3 sensor or the control sensor, co-expressed with the volume marker (left), along with the corresponding kymographs (right) derived from the regions indicated by white arrows. **c.** Cross-correlation analysis of Rnd3 and control sensor signals with cell edge velocity as a function of the temporal offset between the two measurements. **d.** Enrichment of the Rnd3 or control activity sensor signals in protruding (>0.075 µm/min) and retracting (<−0.075 µm/min) cell edge regions. Edge velocities were determined using a cell volume marker, and enrichment values were normalized relative to the mean enrichment of the volume marker signal. Error bars represent standard error of the mean. Adapted from Sachan et al., (2025).

The experiments above confirmed the mutual inhibition between Rho and Rnd3, which makes them potential candidates for generating mutually exclusive activity patterns during cell migration. The spatial-temporal activity pattern of Rho in migrating cells was

already known from our previous study (Nanda et al., 2023)[1]. Therefore, I investigated the spatio-temporal activity pattern of Rnd3 in protrusions and retractions during cell migration. For this, again a very simple low expressing Rnd3 construct (delCMV-mCitrine-Rnd3) was used and its translocation between the cytosol and the plasma membrane was measured using TIRF microscopy.

As Rho activity was known to be associated with cell retraction, a mutual inhibition between Rho and Rnd3 was expected to lead to a depletion of Rnd3 in cell retractions. However, surprisingly, these experiments suggested that Rnd3 is depleted in cell protrusions (Figure 23a). To quantify, how the Rnd3 protein signal changes with protrusion and retraction of the cell edge, an analysis protocol was implemented, which was previously established in the lab (Nanda et al., 2023)[1], and which is derived from a revised version of the ADAPT ImageJ plugin (Barry et al., 2015).

These analyses showed that Rnd3 activity has a negative correlation with cell edge velocity, with an average temporal delay of approximately 50s (Figure 23c). Furthermore, as the cross-correlation function cannot differentiate between signal reduction during protrusion and signal increase during retraction, Rnd3 signal enrichment was quantified in protrusive and retractive regions relative to the entire area of cell attachment via an analysis protocol that was previously established in the lab (Nanda et al., 2023)[1].

These experiments clearly confirmed that Rnd3 was not reduced during retraction contrary to what was expected, but rather enriched during retraction by up to ~ 10% with maximal enrichment occurring with a delay of ~ 80s after maximal cell retraction (Figure 23d). Moreover, Rnd3 activity was significantly reduced (~ 20%) in protruding regions, with a delay of about 80s relative to peak protrusion (Figure 23d).

These results suggest that Rnd3 is not only exclusively associated with cell retraction signals which are typically associated with Rho activity, as proposed earlier, but somehow also linked to cell protrusion signals which are associated with Rac activity. To investigate, whether there is a direct link between Rnd3 and cell protrusion signals,

[1] Nanda S. Investigation of signal networks that control dynamic cell shape changes (Doctoral dissertation), TU Dortmund, 2023

the crosstalk between Rac and Rnd3 was investigated by measuring Rnd3 responses to rapid Rac1 perturbations.

8.4 Crosstalk between Rac and Rnd3

8.4.1 Rnd3 is inhibited by Rac perturbations induced via chemically induced dimerization

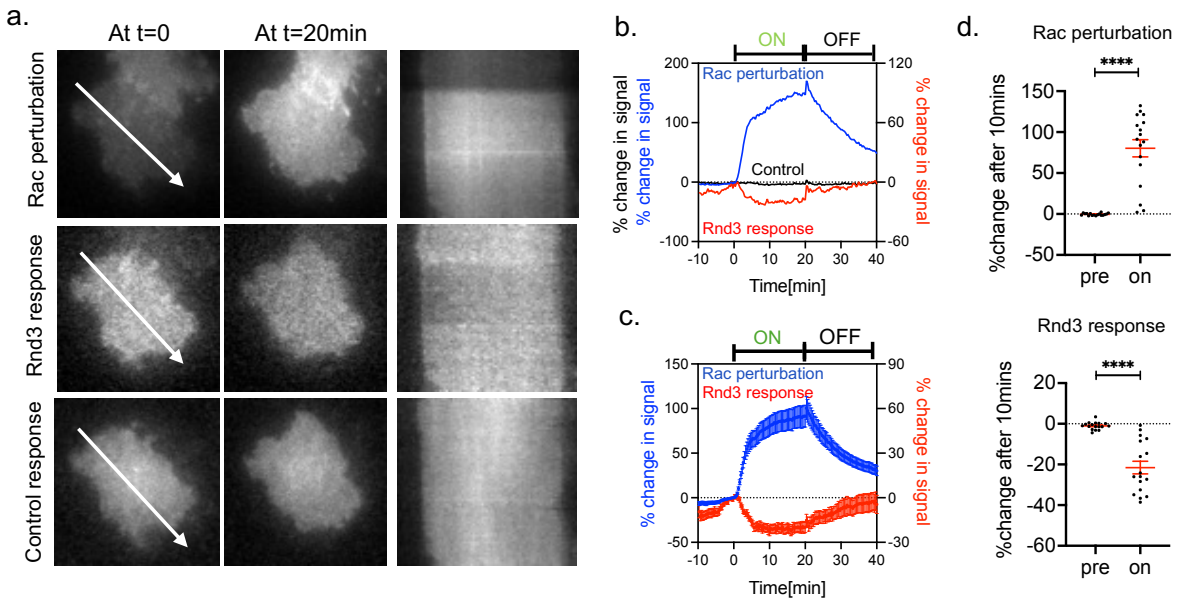

Figure 24. Direct measurement of the Rnd3 response to rapid Rac1 perturbations via chemically induced dimerization. a. Representative TIRF microscopy images and corresponding kymographs from the regions indicated by white arrows in cells expressing Rho perturbation together with the Rnd3 sensor and control sensor constructs. **b.** Quantitative analysis of Rac perturbation along with the raw, uncorrected responses of Rnd3 and control sensor in the whole cell adhesion area of the example cell depicted in a. **c.** Mean Rac perturbation and normalized Rnd3 sensor response calculated from multiple cells. **d.** Quantification of Rac perturbation and normalized Rnd3 sensor response before (pre) and 10 min after adding dimerizer (on). $n = 3$ independent experiments with 17 cells. ****$P < 0.0001$; two-sided t-test. Error bars represent standard error of the mean. Adapted from Sachan et al., (2025).

To investigate the crosstalk between Rac and Rnd3, I introduced rapid perturbations of Rac1 activity via chemically induced dimerization analogous to the experiments in 8.2 (Figure 22a). Here, the small molecule dimerizer SLF-TMP was used to initiate the plasma membrane recruitment of a constitutively active Rac1 mutant followed by addition of its competitor TMP to reverse the perturbation. Similar to Rho, the plasma membrane recruitment of active Rac was also previously shown to successfully induce the expected phenotype of cell protrusion which was also reversed by the addition of TMP (Nanda et al., 2023)[1]. As shown in Figure 24c-d, chemical dimerizer induced Rac1 perturbation leads to a significant inhibition of Rnd3 by ~20%. The inhibition of Rnd3 starts rapidly within seconds and reaches its maximum after about 5-10 minutes.

Given the observed depletion of Rnd3 during cell protrusions and its inhibition by active Rac was unexpected, an additional method was used to verify these results.

[1] Nanda S. Investigation of signal networks that control dynamic cell shape changes (Doctoral dissertation), TU Dortmund, 2023

8.4.2 Rnd3 is inhibited by rapid, optogenetic Rac1 activity perturbations

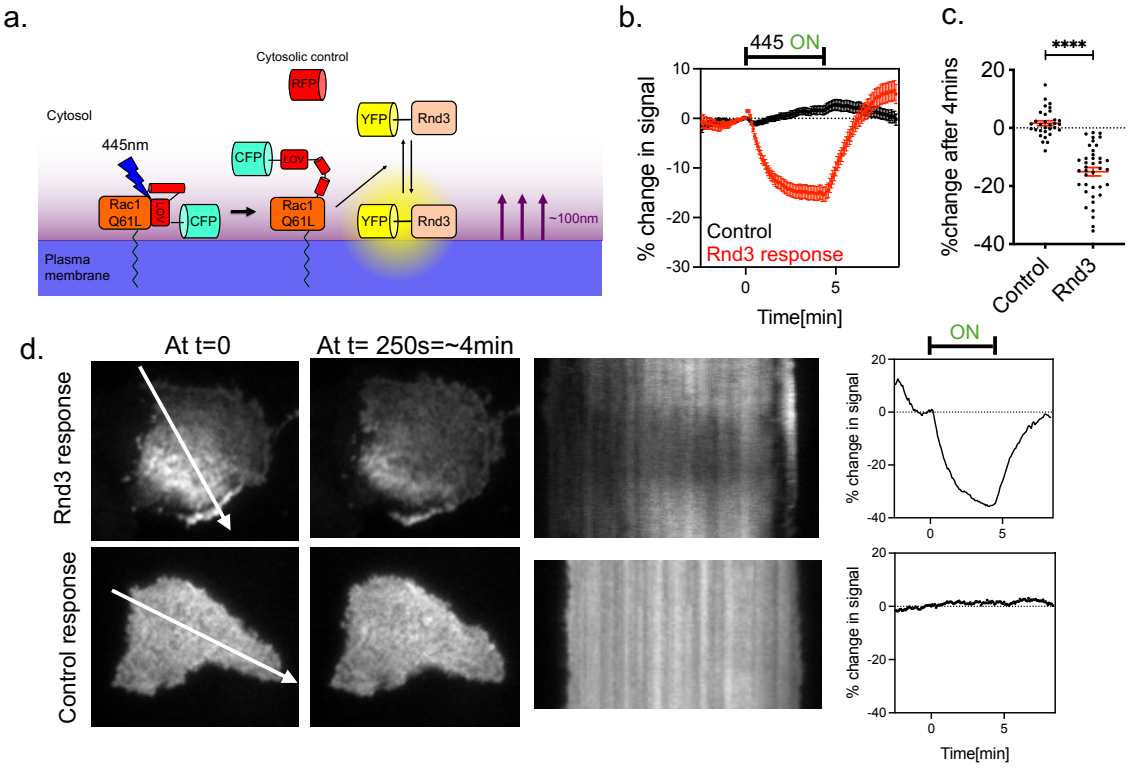

Figure 25. Direct measurement of the Rnd3 response to rapid Rac1 perturbations using photoactivatable Rac. a. Schematic diagram of the optogenetic approach used to analyse changes in Rnd3 recruitment in response to Rac1 activation. **b**. Quantitative analysis of the responses of the Rnd3 and control sensor following Rac perturbation in the whole cell adhesion area. **c.** Measurement of the Rnd3 and control sensor activity 4 min after photoactivation (on). **d.** Representative TIRF microscopy images and corresponding kymographs from the regions indicated by the white arrows in cells expressing PA-Rac1 together with either the Rnd3 or control sensor (left and middle panels). The right panels show the recruitment of Rnd3 or control sensor following Rac perturbation in the whole cell adhesion area of the same representative cells. n = 3 independent experiments with >31 cells per condition. ****P < 0.0001; two-sided t-test. Error bars represent standard error of the mean. Adapted from Sachan et al., (2025).

Here, I used a photoactivable Rac1 construct (PA-Rac1) (Wu et al., 2009), based on the constitutively active Q61L mutant of Rac1. This construct consists of Rac1Q61L fused to the LOV2 domain, which, prevents Rac1 from binding its effectors in the dark state. Illumination with 445nm light, triggers a conformational shift in the LOV2 domain, releasing its inhibition of Rac1 effector binding, such that the constitutively active Rac1 can freely interact with its downstream targets (Figure 25a). This rapid Rac1 perturbation was combined with the real-time monitoring of Rnd3 activity response. These experiments confirmed my previous observation that active Rac1 rapidly and significantly inhibits Rnd3 (Figure 25b,c). These results establish direct and rapid activity crosstalk, in which Rac1 inhibits Rnd3. Furthermore, this crosstalk is also consistent with the signal enrichment analysis, which indicates that Rnd3 is significantly depleted at the cell edge during protrusion in migrating cells (Figure 23d).

Interestingly, the strength of the Rnd3 inhibition triggered by Rac perturbation is more than twice compared to the Rnd3 inhibition triggered by Rho perturbation (Figure 22d,e and Figure 24c,d). Moreover, unlike Rho-mediated inhibition, which may involve adaptive feedback mechanisms that limit its effectiveness over time, Rac-mediated suppression of Rnd3 persists over an extended timeframe and is fully reversible, indicating that it does not involve long-term cellular adaptation or irreversible signalling changes. This suggests that Rac inhibits Rnd3 through a direct and non-adaptive pathway.

8.5 Rac is not strongly affected by rapid Rnd3 perturbations

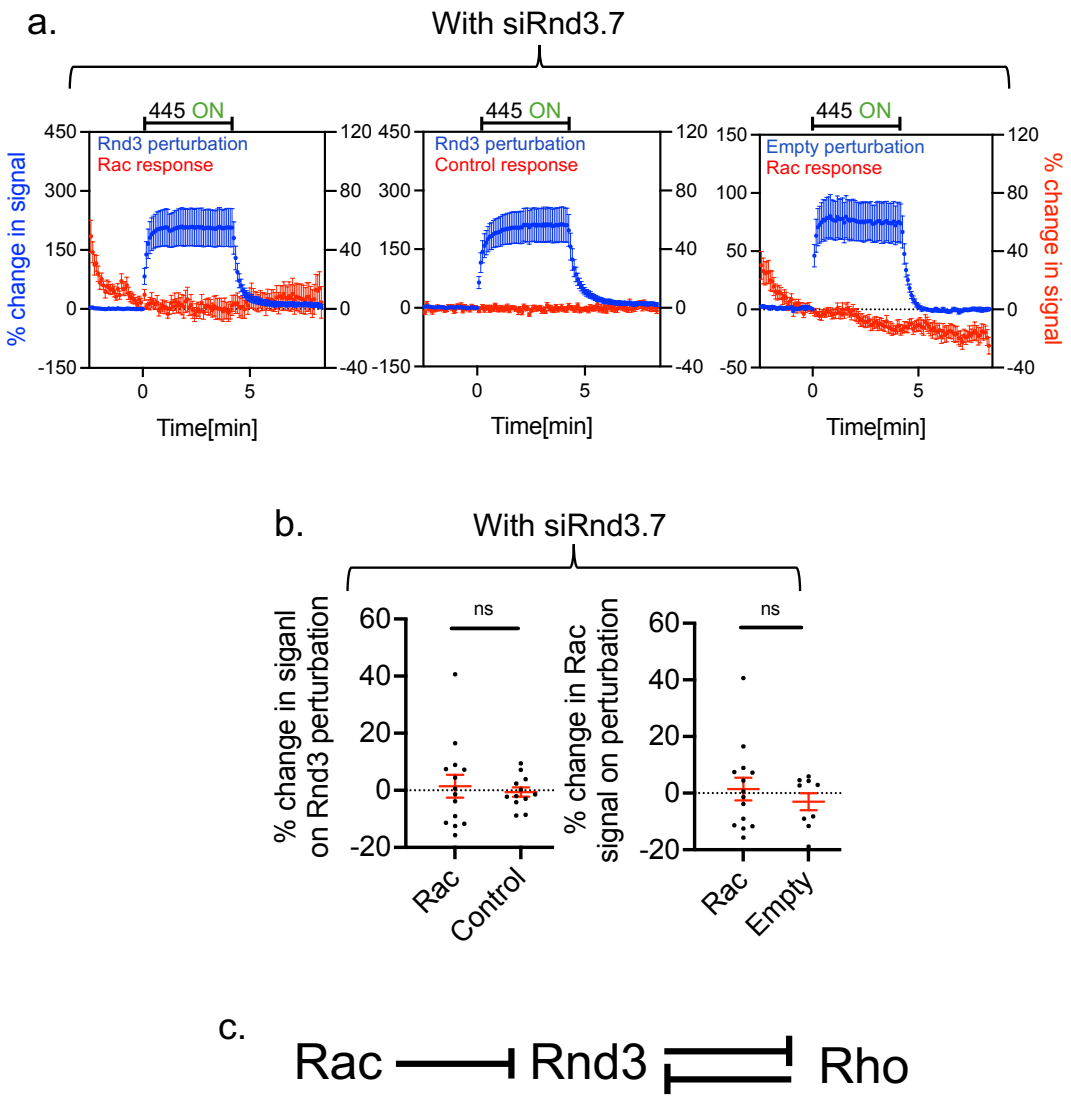

Figure 26. Direct measurement of the Rac1 response to rapid Rnd3 perturbations using the LOVTRAP method following endogenous Rnd3 knockdown. a. Quantitative analysis of the Rnd3 perturbation and recruitment dynamics of the Rac activity sensor across the whole cell adhesion area, including measurements obtained with a control sensor or an empty perturbation construct. **b.** Measurement of the sensor response 1 min following perturbation. *n* = 3 independent experiments with ≥9 cells per condition. **c.** Suggested model describing the interactions between Rac, Rnd3, and Rho signalling within cells. ns: not significant; two-sided t-test. Error bars represent standard error of the mean. Adapted from Sachan et al., (2025).

Next, I examined the effect of Rnd3 perturbation on Rac activity employing the same LOVTRAP system described above (Figure 20a). However, perturbation of Rnd3 didn't had any significant effect on Rac activity as shown in Figure 26a,b.

These findings collectively suggest that the crosstalk between Rac and Rnd3 is only unidirectional, such that Rac inhibits Rnd3 but Rnd3 has no effect on Rac activity.

8.6 Rac inhibits Rnd3 via a kinase-dependent mechanism

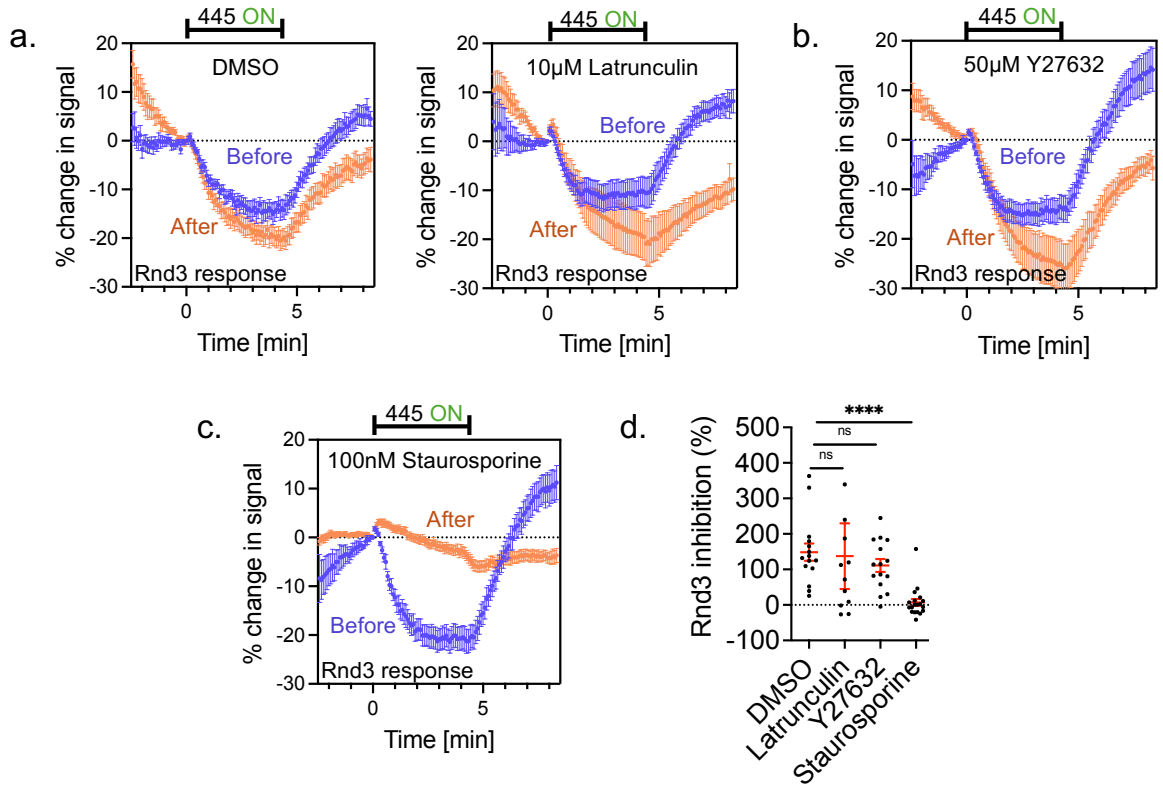

Figure 27. Rac1 inhibits Rnd3 via a kinase-dependent mechanism. Quantification of Rnd3 sensor recruitment during Rac activation before and 10 minutes after addition of the given small molecule inhibitors: **a.** DMSO or 10μM Latrunculin**. b.** 50μM Y27632 (ROCK inhibitor) **c.** 100nM Staurosporine (pan kinase inhibitor). **d.** Quantitative assessment of the impact of small molecule inhibitors on Rnd3 inhibition, evaluated 90s after the initiation of Rac1 photoactivation. The data is presented as the percentage of Rnd3 recruitment following inhibitor treatment relative to the recruitment measured prior to compound addition. All

experiments were conducted in a paired manner, with baseline measurements acquired before inhibitor treatment, followed by a 10-minute incubation period and subsequent analysis of the same set of cells. $n = 3$ independent experiments with >13 cells per condition. ****$P < 0.0001$; ns: not significant; two-sided t-test. Error bars represent standard error of the mean. Adapted from Sachan et al., (2025).

Next, I studied the underlying mechanism of inhibition of Rnd3 by Rac1. First, I investigated whether this process of inhibition of Rnd3 by Rac1 is actin dependent as Rac is best known for promoting actin polymerization to drive cell protrusion. For this, I used Latrunculin which has been shown to inhibit actin polymerization and measured the Rac/Rnd3 crosstalk before and after adding 10μM of the compound in a paired experiment. As can be seen in Figure 27a, the addition of latrunculin did not reverse the Rac1-mediated inhibition of Rnd3, indicating that this crosstalk is independent of actin.

Next, the effect of the ROCK inhibitor (Y27632) was investigated on the crosstalk between Rac and Rnd3. ROCK was a potential candidate for mediating this crosstalk, as previous work from the Dehmelt lab demonstrated that Rac could activate Rho, and it is well established that Rho inhibits Rnd3 via ROCK (Nanda et al., 2023; Riou et al., 2013)[1]. Therefore, to test whether this crosstalk between Rac and Rnd3 acts via this pathway, Rac/Rnd3 crosstalk was measured before and after adding 50μM of the ROCK inhibitor again in a paired experiment. However, the addition of ROCK inhibitor also didn't reverse the process of Rnd3 inhibition by Rac1 (Figure 27b), showing that the crosstalk between Rac and Rnd3 does not act via a ROCK-dependent mechanism.

The search was then broadened by using staurosporine, a highly effective but unspecific serine/threonine/tyrosine kinase inhibitor, to investigate whether the process of Rac1-stimulated Rnd3 inhibition is dependent on any kinase. After adding 100nM staurosporine, a complete reversal of the inhibition of Rnd3 by Rac1 was observed by almost 100% (Figure 27c-d), showing that Rac1 inhibits Rnd3 via a kinase-dependent mechanism.

[1] Nanda S. Investigation of signal networks that control dynamic cell shape changes (Doctoral dissertation), TU Dortmund, 2023

8.7 Rac inhibits Rnd3 via its effector kinase PAK (p21-activated kinases)

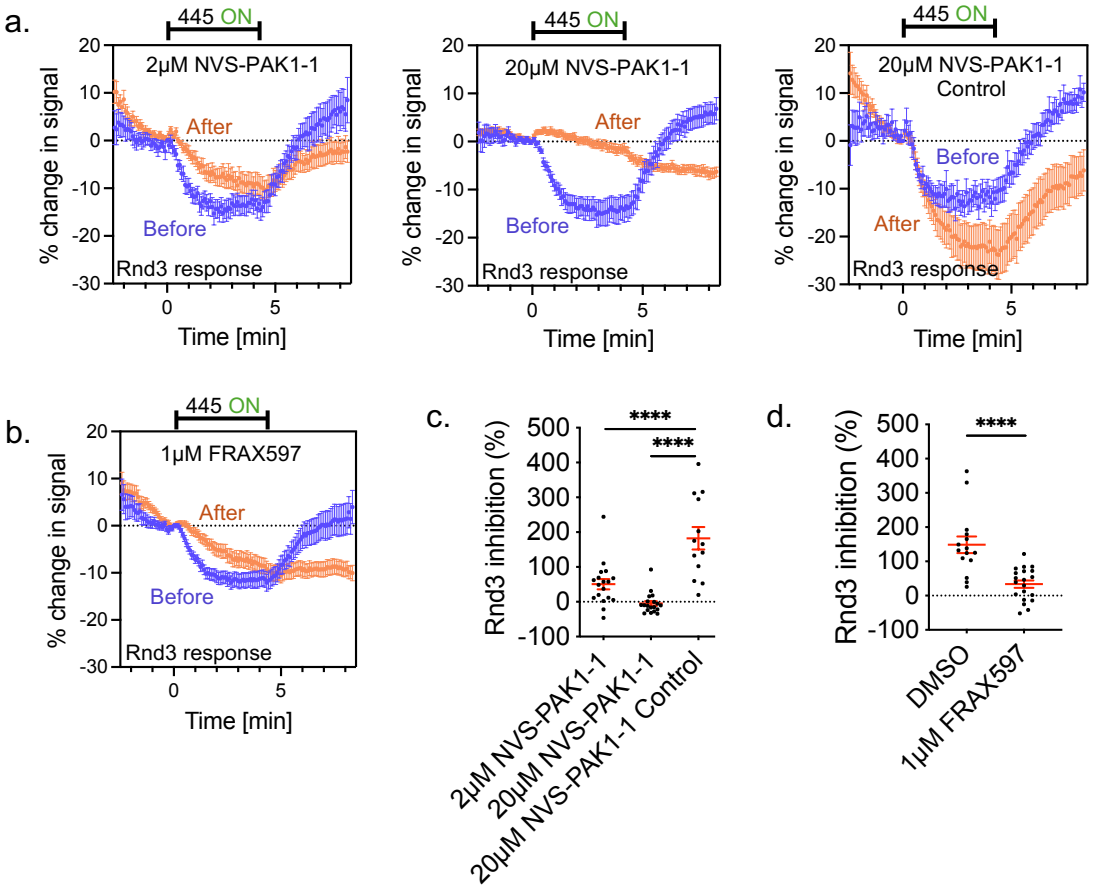

Figure 28. Rac1 inhibits Rnd3 through its downstream effector kinase PAK. Rnd3 sensor recruitment during Rac activation was measured before and 10 minutes after addition of the following Group I PAK inhibitors: **a.** 2μM NVS-PAK1-1, 20μM NVS-PAK1-1 and 20μM NVS-PAK1-1 Control or **b.** 1μM FRAX597. **c,d.** Quantitative analysis of the effect of Group I PAK inhibitors on Rnd3 inhibition, evaluated 90s after the initiation of Rac1 activation. Results are presented as the percentage of Rnd3 recruitment after inhibitor treatment relative to the corresponding recruitment measured prior to the treatment. All experiments were performed in a paired manner, with baseline measurements acquired before inhibitor treatment, followed by a 10-minute incubation period and subsequent analysis of the same set of cells. $n = 3$ independent experiments with >13 cells per condition. ****$P < 0.0001$; two-sided **c.** One-way ANOVA **d.** t-test. Error bars represent standard error of the mean. Adapted from Sachan et al., (2025).

To further identify the kinase responsible for mediating this crosstalk between Rac and Rnd3, the role of very common downstream effectors of Rac, the p21-activated kinases (PAK) was investigated (Cotteret & Chernoff, 2002; Knaus & Bokoch, 1998). For this, two different group I PAK inhibitors, NVS-PAK1-1 and FRAX597 were used and the effect of these inhibitors was measured on the crosstalk between Rac and Rnd3. Both FRAX597 and NVS-PAK1-1 were able to significantly reverse the Rnd3 inhibition by Rac1 (Figure 28a-d). 1μM FRAX597 lead to a reversal of ~70% (Figure 28d), and 2μM NVS-PAK1-1 to a reversal of ~50% (Figure 28c). At higher concentrations (20μM), NVS-PAK1-1 addition resulted in an almost complete reversal (~100%) of Rnd3 inhibition, whereas a structurally similar control compound, had no effect at the same concentration (Figure 28a). These findings suggest that pharmacological inhibition of Group I PAK kinases disrupts the crosstalk between Rac and Rnd3, indicating that this subgroup of kinases is responsible for mediating the crosstalk between Rac and Rnd3 activity.

8.8 Rnd3 regulates cell morphology and cell morpho-dynamics

Previous studies have associated Rnd3 only with retraction signaling, therefore suggested a very simple role of Rnd3 as a Rho activity antagonist. However, these new results showed that Rnd3 is not only associated with retraction signals but is also associated with protrusion signals. This unexpected observation suggests that Rnd3 may contribute to the spatiotemporal coordination of protrusion and retraction signals and could therefore play an important role in regulating cell morphodynamics, rather than acting solely as a simple inhibitor of Rho activity. Therefore, the effect of Rnd3 knockdown on cell morphology and cell morphodynamics was investigated.

8.8.1 Role of Rnd3 in controlling cell morphology

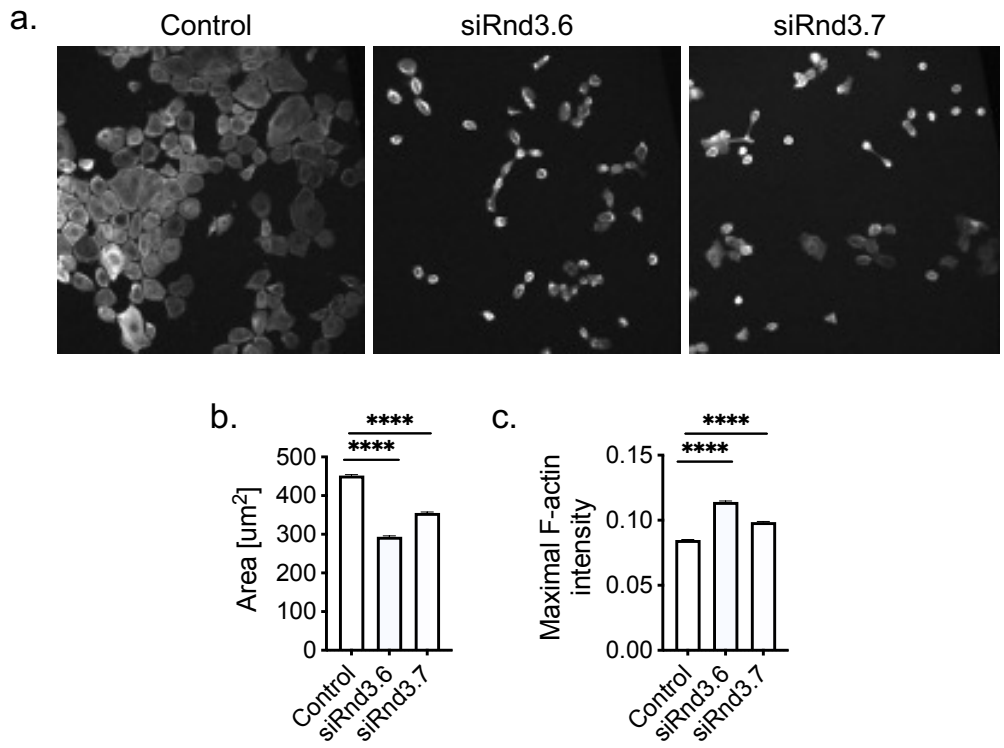

Figure 29. Rnd3 is a key regulator of cell morphology. a. Representative images of F-actin in control and Rnd3 knockdown cells, stained using phalloidin. **b-c.** Effect of Rnd3 knockdown on the cell adhesion area (b) and F-actin intensity (c) quantified using Cell Profiler. n = 3 independent experiments with >11,420 cells per condition. ****P < 0.0001; two-sided One-way ANOVA. Error bars represent standard error of the mean. Adapted from Sachan et al., (2025).

The effect of Rnd3 knockdown on cell morphology was evaluated by measuring the maximal F-actin intensity of cells. Loss of Rnd3 was expected to increase Rho activity, resulting in enhanced contractility and a smaller, more rounder cell morphology. In addition, cells were also expected to display highly concentrated F-actin structures as a result of assembly of F-actin rich contractile structures. Indeed, loss of endogenous Rnd3 strongly reduced cell adhesion area and significantly increased the maximal F-actin intensity in cells (Figure 29b-c). These findings confirm the well-established inhibitory effect of Rnd3 on Rho and its downstream effect on cell contraction/retraction in our system.

8.8.2 Role of Rnd3 in controlling cell morphodynamics

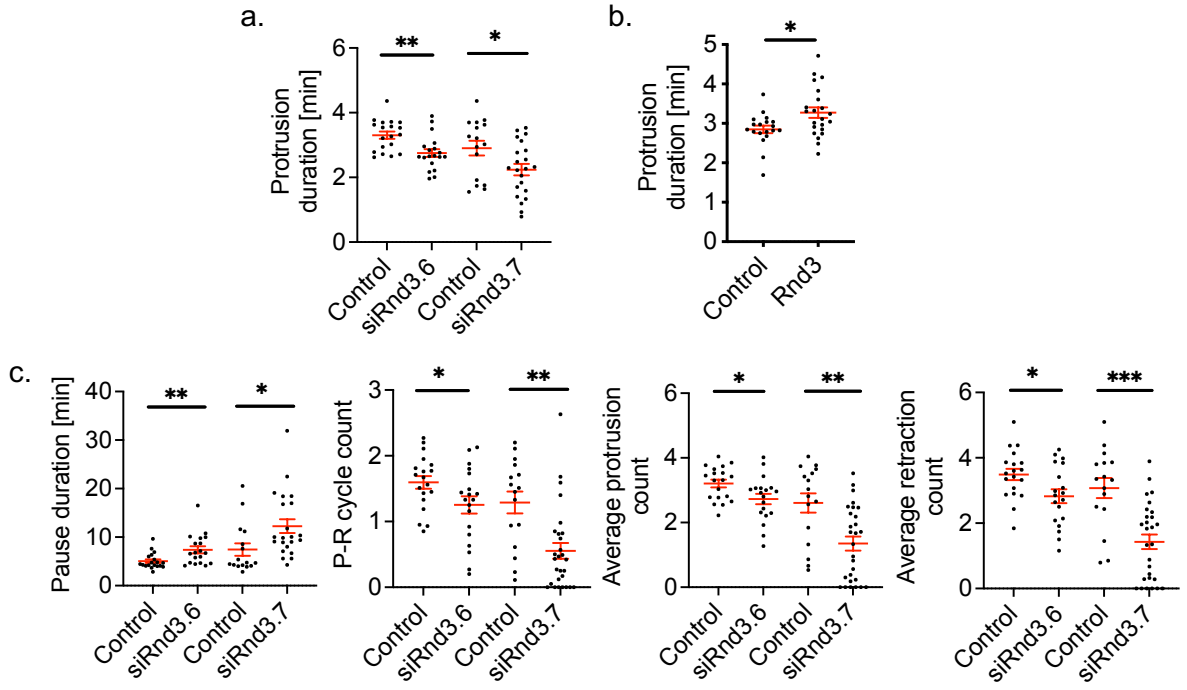

Figure 30. Rnd3 is an important regulator of cellular morphodynamics. Quantitative analysis of protrusion-retraction dynamics using measurements of cell edge velocity with Rnd3 knockdown (**a,c)**, $n = 3$ independent experiment with >16 cells per condition, or with Rnd3 overexpression (**b**), $n = 3$ independent experiments with >19 cells per condition. **a,b.** Quantification of protrusion duration **c.** Quantification of protrusion-retraction count and duration of pause phases. ***$P < 0.001$; **$P < 0.01$, *$P < 0.05$; two-sided t-test. Error bars represent standard error of the mean. Adapted from Sachan et al., (2025).

As it was well-known that Rnd3 functions as an inhibitor of Rho and cell contraction/retraction signals, it was expected that Rnd3 depletion would lead to less controlled, global cell contraction/retraction. Increased global cell contraction would be expected to interfere with cell protrusions, for example, reducing their extent or lifetime. On the other hand, overexpression of Rnd3 is expected to result in less retraction and might lead to prolonged protrusions duration. Indeed, Rnd3 knockdown reduces protrusion duration (Figure 30a), and its overexpression significantly increased the duration of protrusion events (Figure 30b).

In general, Rnd3 depletion led to a reduction in several additional morphodynamic parameters, suggesting that cells exhibit lower overall activity in the absence of Rnd3. (Figure 30c).

8.9 Rnd3 constrains retraction signals in cells

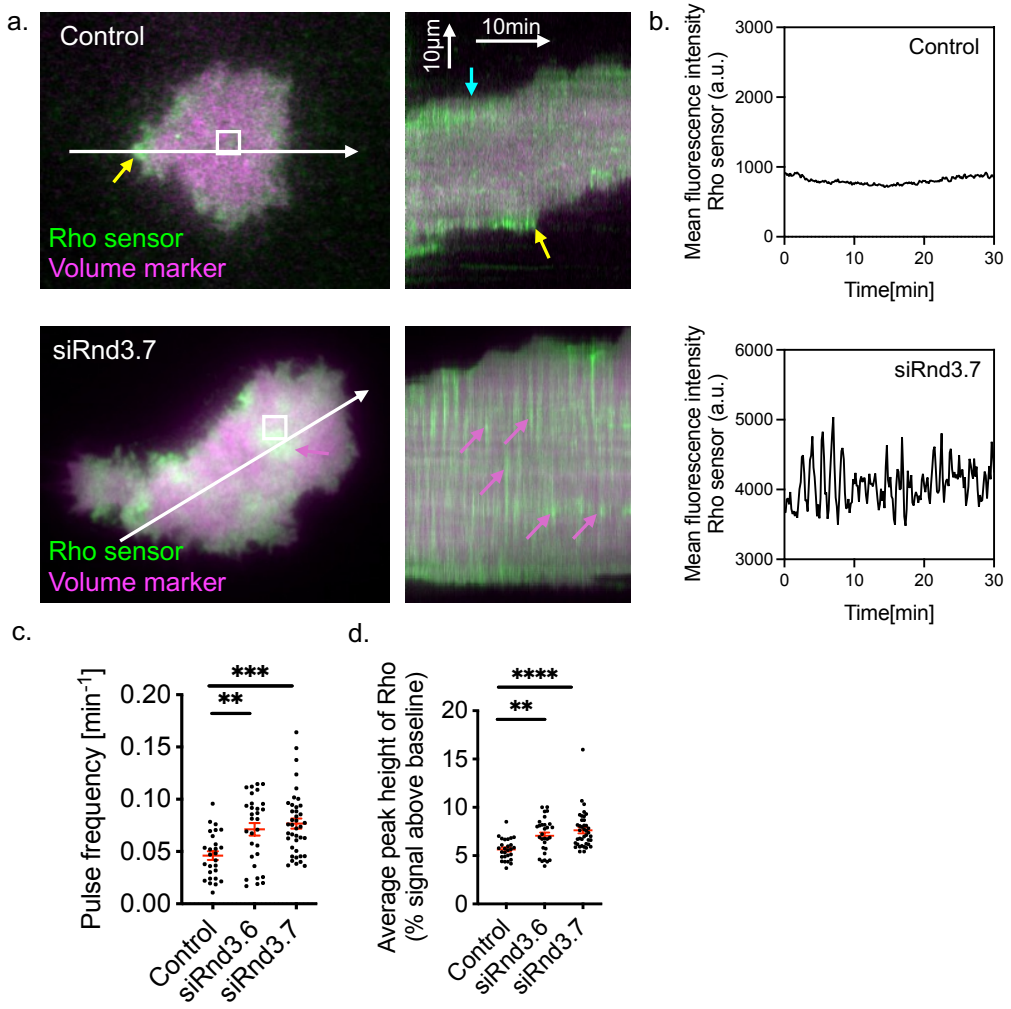

Figure 31. Rnd3 constrains retraction signals to the cell edge. a. Representative TIRF microscopy images (left), and the associated kymographs (right) from the regions indicated by the white arrows in control and Rnd3 knockdown cells co-expressing the Rho activity sensor together with a cell volume marker. **b.** Mean fluorescence intensity of the Rho sensor measured in the region marked by the white box in the cells displayed on the left. **c-d.** Analysis of the dynamics of Rho activity pulses in control versus Rnd3 knockdown cells **c.** frequency **d.** average peak height. n = 3 independent experiments with >26 cells per condition.

.****P < 0.0001; ***P < 0.001; **P < 0.01; two-sided One-way ANOVA. Error bars represent standard error of the mean. Adapted from Sachan et al., (2025).

The A431 cells which were used for this study exhibit high motility. Rather than forming a stable protrusive front and a defined contractile rear for directional migration, these cells display highly dynamic and repetitive protrusion–retraction cycles, resulting in a more exploratory and random mode of migration (Nanda et al., 2023)[1]. During these cycles, localized Rac1 activity closely correlates with membrane protrusion, which is rapidly followed by localized Rho activity associated with retraction within the same region of the leading edge (Nanda et al., 2023)[1].

These previous studies suggest a hierarchy between Rac1 and Rho, in which an initial signal, for example from growth factor receptors or from Ras-related small GTPases like Rap1 (Arthur et al., 2004; Lambert et al., 2002; Lüttig et al., 2025.), can activate Rac1, which then activates Rho. In contrast, spontaneous Rho activity was usually not observed in the absence of active Rac1, although mechanisms exist, by which Rho can get activated by growth factor signals (Jaffe & Hall, 2005) and by which it can amplify its own activity via a positive feedback loop (Graessl et al., 2017; Kamps et al., 2020). Indeed, in other cell systems, such as U2OS cells and mouse embryonic stem cells, this positive feedback amplification can result in the spontaneous pulses of Rho activity in the whole cell adhesion area (Graessl et al., 2017; Kamps et al., 2020).

In A431 cells, the inhibitory action of Rnd3 on Rho activity can play a role in suppressing such spontaneous Rho activity pulses. Furthermore, Rnd3 might even be able to spatially restrict contractile signals to the cell periphery. Rnd3 could do this by inhibiting Rho in the whole cell attachment and only allowing Rho activity transiently after being inhibited downstream of active Rac near the cell edge in areas where a protrusion was recently generated. Thus, to investigate this potential role of Rnd3, the effect of loss of Rnd3 on Rho activity dynamics was investigated in A431 cells.

[1] Nanda S. Investigation of signal networks that control dynamic cell shape changes (Doctoral dissertation), TU Dortmund, 2023

As shown in Figure 31a, Rho activity signals were mainly localized at the cell periphery of control cells, where they were associated with cell retraction (yellow arrows) or pausing events (cyan arrows). Furthermore, Rho activity is nearly absent from the central cell attachment areas of control A431 cells. However, loss of Rnd3 led to a pronounced shift in the Rho activity patterns towards the central cell adhesion area, where highly dynamic Rho activity pulses were observed (magenta arrows) (Figure 31a). Analysis of these Rho activity dynamics reveals that the frequency as well as the average peak height of pulses are highly increased following loss of endogenous Rnd3 (Figure 31c-d). Collectively, these results support the hypothesis that Rnd3 functions as a global Rho inhibitor, which is able to spatially restrict Rho activity to occur only close to the cell edge during migration.

9. Discussion

Classical models of cell migration suggested mutually inhibitory crosstalk between the protrusion-stimulating cell front signal Rac and the retraction-stimulating cell back signal Rho (Figure 32a, Top) (Guilluy et al., 2011). This type of crosstalk mechanism can generate a stable front and a stable back in migrating cells by enforcing mutually exclusive activity patterns of Rac and Rho, thereby driving directional migration. However, recent studies were not compatible with mutual inhibition between Rac1 and Rho in several cell lines, including the Neuro-2a, NIH 3T3, Hela, U2OS and A431 cell lines (Nanda et al., 2023). Furthermore, these studies did not confirm mutually exclusive activity patterns between protrusion regulator Rac and retraction regulator Rho activity in A431 cells (Nanda et al., 2023). In contrast, a significant spatial gap was observed between the Rac and Rho activities in migrating A431 cells (Figure 32a, Bottom) (Nanda et al., 2023)[1]. Here, I proposed that this activity pattern of Rac and Rho could be because of another molecule which also might be a part of this signal network. Such a signaling molecule would be expected to function as a mutual inhibitor of Rho, Rac or both. Based on the literature, it was proposed that the unconventional Rho GTPase, Rnd3 could have at least some of these properties, as it is known to be mutually inhibitory to Rho in DLD1 cells (Aoki et al., 2016). Here, this mutual inhibition between Rho and Rnd3 was confirmed in A431 cells (Figure 32b, Top). This mutual inhibition was expected to lead to mutually exclusive patterns of Rnd3 and Rho-associated cell retraction in migrating A431 cells. However, surprisingly, this was not observed. In contrast, Rnd3 was specifically reduced during cell protrusion. This reduction of Rnd3 during protrusion was due to the inhibition of Rnd3 by the protrusion regulator Rac1 via its p21 activated effector kinases (PAKs). Functional investigations of Rnd3 revealed that it acts as a key regulator of cell morphology and morphodynamics. Detailed analysis of the effect of Rnd3 depletion revealed that Rnd3 is critical to spatially restrict Rho activity only at the periphery of migrating cells. When Rnd3 is absent, this tight spatio-temporal regulation of Rho activity is lost (Figure 32b, Bottom).

[1] Nanda S. Investigation of signal networks that control dynamic cell shape changes (Doctoral dissertation), TU Dortmund, 2023

Specifically, ectopic, spontaneous highly dynamic pulses of Rho activity are generated throughout the whole area of cell attachment in the absence of Rnd3. Earlier studies have reported that such activity pulses are produced by combining a fast positive feedback loop, where Rho and its Lbc-GEF family activators mutually amplify each other, and a slower negative feedback loop, where the Lbc-GEF activity is suppressed via a myosin-dependent mechanism (Figure 32b) (Graessl et al., 2017; Kamps et al., 2020; Kowalczyk et al., 2022; Lee et al., 2010). Results in this thesis suggest that the endogenous levels of Rnd3 are sufficient to effectively suppress Rho activity pulses in migrating A431 cells under normal conditions (Figure 32b, Bottom). In contrast, under control conditions, the less migratory U2OS osteosarcoma cells exhibit Rho activity pulses across the whole cell adhesion area (Graessl et al., 2017), suggesting that Rnd3 is less abundant, less active, or regulated differently in these cells.

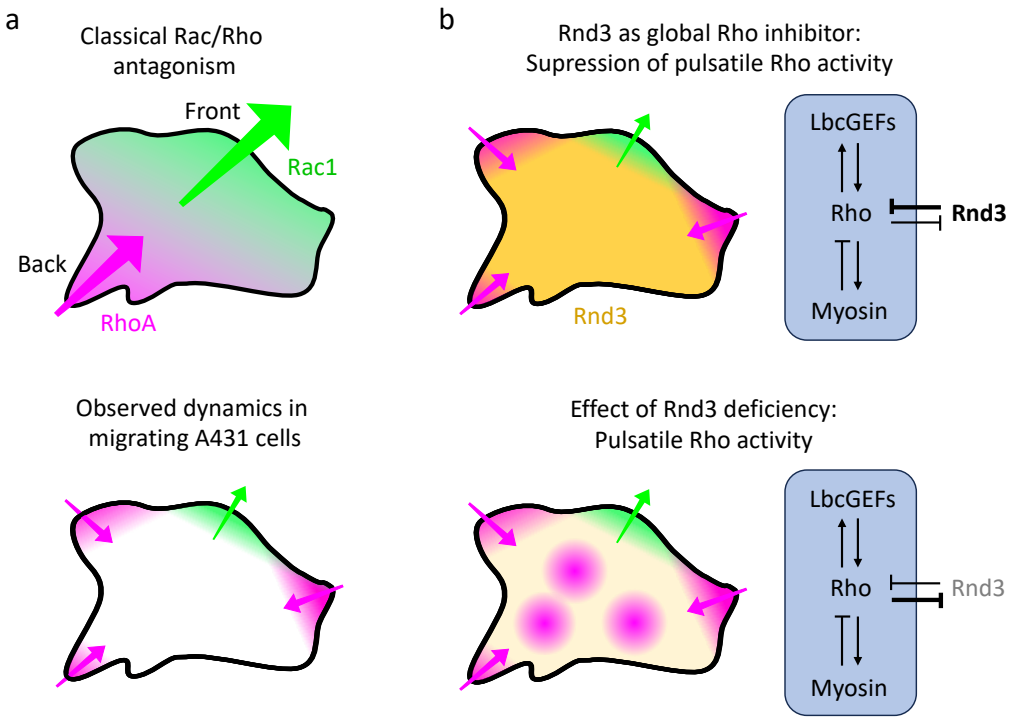

Figure 32. Predicted mechanism of spatio-temporal regulation of the retraction regulator Rho by Rnd3. a. Top: Classical model of mutual inhibition, in which Rac and Rho activity patterns during migration are mutually exclusive and partially overlap in central areas of the plasma membrane. Bottom: In A431 cells, distinct and non-overlapping activity patterns of Rac and Rho are both detected in peripheral regions of the cell. Central, white regions lack

signals from either Rac or Rho. **b.** Top: Activity pattern of Rnd3 in A431 cells indicates that Rnd3 is functioning as a global inhibitor of Rho which is selectively downregulated by Rac1 activity. Bottom: Absence or reduction of Rnd3 leads to spontaneous pulses of Rho activity in the whole cell adhesion area. These dynamics of Rho activity pulses can be generated by the combination of a fast positive and slow negative feedback mechanisms (blue box) (Graessl et al., 2017). These dynamics can be suppressed by the inhibitory action of high levels of Rnd3 on Rho. Adapted from Sachan et al., (2025).

Taken together, this model for the role of Rnd3 in regulating spatio-temporal Rho and Rac activity patterns (Figure 33) is proposed: This thesis surprisingly revealed that Rac can inhibit Rnd3 locally at the leading edge of the cell and can thereby release the inhibition of Rnd3 on Rho activity. Thus, Rac1 can indirectly activate Rho by suppressing its inhibitor, Rnd3 (Figure 33a). Rac1-mediated Rho activation was earlier reported in a previous study (Nanda et al., 2023)[1] and revealed that this crosstalk between Rac1/Rho is mediated by the activation of two Lbc-type GEFs, Arhgef11 (PDZ-RhoGEF) and Arhgef12 (LARG) by active Rac1 (Chapter I of this thesis). Upon sufficient activation, Rho reinforces its own activity through Lbc-GEFs, which then inhibit Rac activity (Guilluy et al., 2011; Kuo et al., 2011; Nanda et al., 2023; Ohta et al., 2006; Sanz-Moreno et al., 2008; Vicente-Manzanares et al., 2011)[1], and promote myosin-driven cell retraction (Figure 33b). Collectively, these processes result in highly dynamic protrusion-retraction cycles.

[1] Nanda S. Investigation of signal networks that control dynamic cell shape changes (Doctoral dissertation), TU Dortmund, 2023

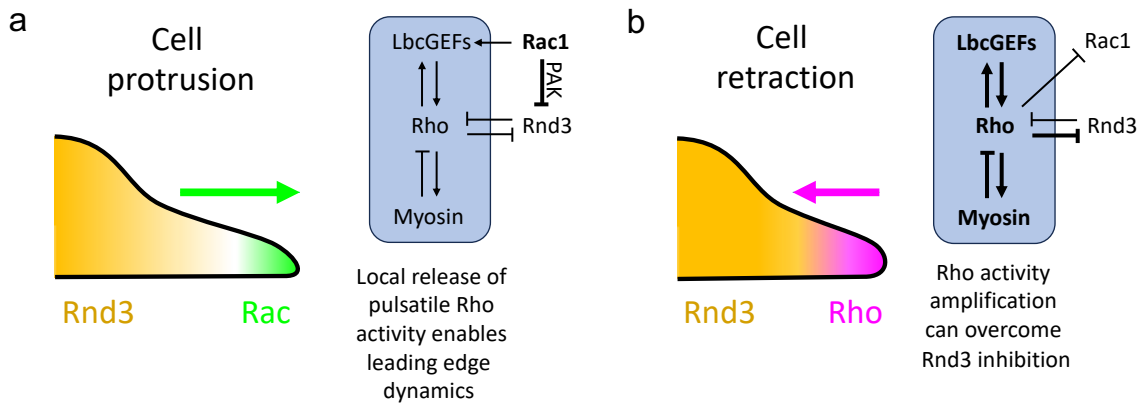

Figure 33. Proposed model for the spatial and temporal activity patterns of Rac, Rho and Rnd3 in cells during cell protrusion and retraction. a. During protrusion, local Rac1 activity inhibits Rnd3 thereby releases the inhibition of Rho by Rnd3. This can activate Rho at the leading edge, which can further be stimulated by activation of Lbc-type GEFs (Arhgef11 and Arhgef12) by Rac (Nanda et al., 2023)[1,1]. **b.** Rho, once active, can promote its own amplification via Lbc-type GEFs (ARHGEF2 and Arhgef12) (Graessl et al., 2017) by which they can overcome its inhibition by Rnd3. During retraction, active Rho inhibits Rac (Nanda et al., 2023)[1], while delayed myosin-mediated negative feedback of Rho resets the system, preparing the cell for the next protrusion-retraction cycle (Graessl et al., 2017). Adapted from Sachan et al., (2025).

Surprisingly, no reduction in Rnd3 activity was observed during retraction. This indicates that Rho is able overcome the inhibitory influence of Rnd3 during cell retraction. There are two possible ways how this observation can be explained. First, the amplification of Rho activity via the positive feedback mechanism might be much stronger than the inhibitory effect of Rnd3. Second, Rnd3 might somehow not be able to inhibit Rho even though it is present at the plasma membrane. One possibility might be that its ability of recruit inhibitory RhoGAPs might be reduced specifically during cell retraction (Wennerberg et al., 2003).

The mechanism proposed here proposes that Rac1 acts upstream to determine where Rho activity dynamics are present. This raises the question of how Rac1 activity is restricted to the cell leading edge. Mutual inhibition between Rac1 and Rnd3 is not

[1] Contribution from this thesis

supported by this thesis, as rapid Rnd3 perturbations did not have a detectable effect on Rac1 activity. Therefore, additional mechanisms must be present to suppress aberrant Rac1 activity. One possible explanation is the proposed positive feedback mechanism between Rac1 activity and membrane curvature, which supports the idea that efficient Rac1 activation requires the high curvature which is present at the leading edge of cells (Galic et al., 2014). Thus, local amplification of Rac1 activity by cell curvature signals could serve as a key initiating factor and could restrict maximal Rac1 activity at the leading edge, subsequently activating local Rho activity that is otherwise spatially restricted by Rnd3.

Taken together, in this part of the thesis, a novel inhibitory crosstalk has been described that couples Rac1, a protrusion regulator, with Rnd3, a contraction inhibitor. This novel link suggests a mechanism, where Rnd3 behaves as a global inhibitor, which spatially restricts the activity of the cell contraction/retraction regulator Rho to the cell edge during migration.

10. Materials

10.1 Devices and Equipment

Cell Culture dishes (35/60/100mm)	Sarstedt
8-well LabTek® chambers No. 1.0	Thermofischer Scientific
35-mm MatTek petri dishes No 1.5	MatTek Corporation
Centrifuge 5415R	Eppendorf
Centrifuge 5810R	Eppendorf
Research Plus Pipettes	Eppendorf
Serological pipettes	Sarstedt
SafeSeal microfuge tubes (2ml, 1.5 ml, 0.5ml, 0.1ml)	Sarstedt
Falcon tubes	Sarstedt
Agarose gel electrophoresis system	Bio-rad
CellXpert Cell Culture Incubator	Eppendorf
Microwave	Sharp
Nanodrop 2000 Spectrophotometer	Thermofischer Scientific

NALGENE™ Cryo 1°C freezing chamber	Thermofisher Scientific
NUAIRE™ class II biological safety cabinet	Integra Biosciences
Purelab flex 2, Water purification system	Elga
Parafilm®	Bemis
CFX 384™ Real-Time System	Bio-Rad
Thermocycler, Mastercycler personal	Eppendorf
Thermomixer compact	Eppendorf
Thermocycler, SimpliAmp	Thermofisher Scientific
UVP GelSolo, M-20V Geldokumentationssystem	analytikjena
Vacusafe comfort vacuum pump	IBS Integra Bioscience
Water bath	Köttermann
“Vortex Genie 2” touch mixer	Scientific Industries
BioRad Power Pac 300	Bio-Rad Laboratories, Inc.
Centrifuge tubes (15ml/50ml)	Sarstedt
Odyssey Infrared Imager Clx	Li-Cor® Biosciences
Immobilon-FL PVDF	Millipore, Merck KGaA

SDS – Polyacryl Amide gel electrophoresis system	Bio-rad
Mr. Frosty Cryo 1°C freezing chamber	Thermo Scientific
Thermocycler, Mastercycler 5341	Eppendorf
4-15% Mini-protean® TGX™ precast gels	Bio-Rad
Cryopure Tubes	Sarstedt
Cell scrapper	Sarstedt
Digital Dry Block Heater	PMC
Mixer 5432	Eppendorf
6-well cell culture plate	Sarstedt

10.2 Chemicals

2-mercaptoethanol	Sigma Aldrich
Agarose	Roth
EtBr (1% in ddH_20)	Gerbu
Ampicillin/ Carbenicillin	Roth

Kanamycin	Roth
DMEM (w/o phenol red)	PAN Biotech
DMEM (w phenol red)	PAN Biotech
Lipofectamin™ 3000	Invitrogen
Lipofectamin™ RNAiMax	Invitrogen
Fibronectin	Sigma Aldrich
DPBS	PAN Biotech
FBS	PAN Biotech, Sigma-Aldrich
Glycerol	Sigma Aldrich
Isopropanol	Roth
L-Glutamine	PAN Biotech
1 kb (+) / 100 bp DNA ladder	New England Biolabs
DAPI/ HOECHST 33342	Sigma Aldrich
dATP/dTTP/dCTP/dGTP/dNTP-Mix	New England Biolabs/ Novagen
DMSO anhydrous	Thermofisher
Ethanol	Roth

IRDye® 680RD Goat anti-Mouse secondary antibody	LICOR
IRDye® 800CW Goat anti-Rabbit secondary antibody	LICOR
$MgCl_2$	New England Biolabs/ Novagen
NAD	New England Biolabs
OptiMEM	Gibco
Purple Loading Dye	New England Biolabs
Rhodamin Phalloidin	Invitrogen
Restriction enzyme buffers	New England Biolabs
Tris-HCl	Sigma Aldrich
PEG-8000	Promega
ON-TARGET plus siRNAs	Dharmacon™, Horizon Discovery
Trypsin	PAN Biotech
Penicillin/Streptomycin Mix	PAN Biotech
DTT	Fluka Analytical
SLF-TMP	Yaowen-Wu lab

TMP	Yaowen-Wu lab
Q5 High Fidelity Polymerase Buffer	New England Biolabs
Q5 High GC Enhancer	New England Biolabs
Nuclease-free Water	Ambion
LB-Agar (Lennox)	Roth
LB-Medium (Lennox)	Roth
Formaldehyde solution 35%	Roth
10x Buffer T4 DNA Ligase with 10 mM ATP	New England Biolabs
Intercept Blocking Buffer	LICOR
Protease inhibitor cocktail tablets	Roche
10X TBS	Bio-Rad
4x Laemmli Sample Buffer	Bio-Rad
Tris	Roche
Glycine	Roche
Methanol	Sigma-Aldrich
Cell lysis buffer (10X)	Cell Signaling Technology

Precision Plus Protein Dual Color Standard	Bio-Rad
Rnd3 primary antibody	Sigma-Aldrich, 05-723
GAPDH antibody	Cell Signalling Technology
SDS	Gerbu
Triton X-100	Serva

10.3 Kits and enzymes

Miniprep/ Maxiprep Kit	Qiagen
PCR Purification Kit	Qiagen
Gel Extraction Kit	Qiagen
Pierce™ Bradford Plus Protein Assay Kit	Thermo scientific
Q5 High-Fidelity DNA Polymerase	New England Biolabs
Phusion DNA polymerase	New England Biolabs
Taq DNA ligase	New England Biolabs
T4 DNA ligase	New England Biolabs
T5 Exonuclease	New England Biolabs

Restriction enzymes and buffers	New England Biolabs
Taq DNA Polymerase	New England Biolabs

10.4 Media and buffers

A431 Culture Medium	DMEM, 10%FBS, 1% L-Glutamine
Imaging Medium	DMEM (w/o Phenol Red), 10 % FBS
5X Isothermal Buffer	25 % PEG-8000, 500 mM Tris-HCl (pH 7.5), 50 mM DTT, 50 mM $MgCl_2$, 5 mM NAD, 1 mM each of dATP, dTTP, dCTP and dGTP, H_2O
Gibson Master mix	100 µL 5x Isothermal Buffer, 2 µL (1 U/µL) T5 Exonuclease, 6.25 µL (2 U/µL) Phusion DNA Polymerase, 50 µL (40 U/µL) Taq DNA Ligase, 375 µL nuclease free H_2O
1X TAE Buffer	40 mM Tris-Acetate, 1 mM EDTA, pH 8.3
LB Medium	5 g/L Yeast-Extract, 10 g/L Tryptone (pH 7.4), 10 g/L NaCl, ddH_2O; Antibiotics: Kanamycin (50 µg/mL)
LB Agar Plates	LB Medium, 1.5 % Agar; Antibiotics: Kanamycin (50 mg/L) or Carbenicillin (100 mg/L)
SOC Medium	2 % Bactotryptone, 0.5 % Yeast-Extract, 20 mM Glucose, 10 mM NaCl, 10 mM $MgCl_2$, 2.5 mM KCl

10.5 Bacterial strains

Top 10 F– mcrA Δ(mrr-hsdRMS-mcrBC) Φ80lacZΔ M15 Δ lacX74 recA1 araD139 Δ(ara-leu) 7697 galU galK rpsL (StrR) endA1 nupG Λ-	Chemical Competent	Invitrogen
Top 10 F– mcrA Δ(mrr-hsdRMS-mcrBC) Φ80lacZΔ M15 Δ lacX74 recA1 araD139 Δ(ara-leu) 7697 galU galK rpsL (StrR) endA1 nupG Λ-	Electrocompetent	Invitrogen

10.6 Cellline

A431 (AtCC-Nr: CRL-1555, Epidermoid carcinoma, Homo sapiens)

11. Methods

11.1 Cell culture

A431 cells (CRL-1555, ATCC) were cultured using standard cell culture conditions at 37 °C in a humidified atmosphere containing 5% CO_2, in DMEM supplemented with 10% fetal bovine serum (FBS; PAN Biotech or Sigma-Aldrich Chemie GmbH/Merck) and 2 mM L-glutamine (PAN Biotech). For imaging, cells were seeded onto either glass-bottom dishes (MatTek) or LabTek chambered slides (Thermo Fisher Scientific). Prior to seeding, glass surfaces were coated using 10 µg/ml fibronectin diluted in Opti-MEM. For this, glass surfaces were incubated by fibronectin either for 45 min at room temperature for LabTek slides, or overnight at 4 °C for MatTek dishes. For cell migration experiments, cells were initially plated in 35 mm culture dishes and were replated on the day of imaging on fibronectin-coated MatTek dishes. Transient transfection of plasmid DNA was carried out using Lipofectamine™ 3000 (Invitrogen, Thermo Fisher Scientific).

11.2 Plasmid constructs

The construct TagBFP-2xeDHFR-CAAX, designed to recruit target proteins to the plasma membrane through a chemically induced dimerization approach, as previously reported by Liu et al. (2014). Similarly, the plasmids mTurquoise2-NES-2xFKBP'-RacQ61LΔCAAX and mTurquoise2-NES-2xFKBP'-RhoAQ63LΔCAAX, which enable plasma membrane localization of Rac and Rho upon chemical induction, together with the control constructs delCMV-mCherry and delCMV-mCitrine, were reported by Nanda et al. (2023)[1].

To construct CMV-mCitrine-Rnd3, the fluorescent protein in CMV-EGFP-Rnd3 (a plasmid kindly provided by Channing Der; Addgene #23229, http://n2t.net/addgene:23229; RRID:Addgene_23229) was excised

[1] Nanda S. Investigation of signal networks that control dynamic cell shape changes (Doctoral dissertation), TU Dortmund, 2023

using BspEI and AgeI-HF, and the resulting backbone was assembled via Gibson Assembly with an insert amplified from delCMV-mCitrine-RBD (Graessl et al., 2017). The amplification was performed using primers 5′-CGTCAGATCCGCTAGCGCTACCGGTCGCCACCATGGTGAGCAAG-3′ and 5′-TTCATGTCGACGGATCTGAGTCCACTTCCAGAACCGGAACCTCCGGACTTGTACAGCTCG-3′. The delCMV-mCitrine-Rnd3 construct was produced by substituting the promoter via ligation-based subcloning, using AseI and NheI-HF, with CMV-mCitrine-Rnd3 and delCMV-mCitrine as templates.

The PA-Rac plasmid (mCerulean-PA-Rac1Q61L) and pTriEx-mCherry-ZdkI were generously provided by Klaus Hahn (University of North Carolina) and have been previously characterized (Wu et al., 2009; Wang et al., 2016). The construct pTriEx-NTOM20-CCL-moxBFP-CCL-LOV2 was described by Kamps et al. (2020).

To generate the Rho activity biosensor (delCMV-mCitrine-2xRBD), the original fluorophore in delCMV-mCherry-2xRBD (Nanda et al., 2023)[1] was replaced via ligation-based subcloning using delCMV-mCitrine as the donor and the restriction enzymes BsrgI and AgeI. Similarly, the Rac activity biosensor (delCMV-mCitrine-3xp67Phox) was produced through the same cloning strategy, substituting the fluorescent protein in delCMV-mCherry-3xp67Phox (Nanda et al., 2023)[1] with mCitrine using BsrgI and AgeI.

For the construction of the Rnd3 perturbation plasmid (pTriEx-mCherry-Zdk1-Rnd3), the small GTPase insert from pTriEx-mCherry-Zdk1-RhoA Q63L (Addgene #81058) was excised using HindIII-HF and KpnI-HF and replaced via Gibson Assembly with an insert amplified from CMV-mCitrine-Rnd3 using primers 5′-GGTTCTGGTTCTGGTGGTACCGGTTCCGGTTCTGGAAGTG-3′ and 5′-TATACAGCTGTGCGGCCGCAAGCTTTCACATCACAGTGCAGCTC-3′.

To create the siRnd3.7-resistant Rnd3 perturbation construct (pTriEx-mCherry-Zdk1-Rnd3-siRnd3.7r), a portion of the Rnd3 coding sequence in pTriEx-mCherry-Zdk1-Rnd3 was removed by digestion with BspHI and SacI-HF. The resulting fragment was

[1] Nanda S. Investigation of signal networks that control dynamic cell shape changes (Doctoral dissertation), TU Dortmund, 2023

reassembled via Gibson Assembly with an insert amplified from the same plasmid template using mutagenic primers 5′-CAGATGTTAGTACATTAGTAGAACTGTCCAATCACAGGCAGACG-3′ and 5′-GTCAGATGCTCAAGGGGCTTCATGATGTCCCCATAATTTTTGGC-3′.

11.3 siRNA mediated knockdown

Knockdown experiments were conducted using ON-TARGET plus siRNAs (Dharmacon™, Horizon Discovery), specifically targeting *Rnd3* (siRnd3 #6: 5′-CUACAGUGUUUGAGAAUUA-3′; siRnd3 #7: 5′-UAGUAGAGCUCUCCAAUCA-3′) and compared to effects induced by a non-targeting control sequence (siControl #2: 5′-UGGUUUACAUGUUGUGUGA-3′). Gene silencing of Rnd3 was achieved by transfecting the A431 cells plated on 35 mm culture dishes with 30nM siRNA using Lipofectamine™ RNAiMAX (Invitrogen) according to the manufacturer's instructions. Post siRNA transfection, cells were incubated for 24 hours (for fixed-cell experiment) or 48 hours (for live-cell imaging) before being splitted and reseeded onto glass-bottom dishes. For live-cell imaging, siRNA-treated cells underwent a secondary transfection using Lipofectamine™ 3000 to introduce the desired plasmid constructs. Experimental analyses, including imaging of knockdown cells and assessment of knockdown efficiency by Western blotting, were carried out 36–48 hours post-siRNA transfection.

11.4 Western blotting

Cells were rinsed once with ice-cold PBS and lysed on ice for 5 minutes using ice-cold 1× Cell Lysis Buffer (Cell Signalling Technology, #9803). The lysates were centrifuged at 13,000 × g for 10 minutes at 4 °C to pellet insoluble material. The supernatant was collected and quickly freezed in liquid nitrogen and stored at -20°C for further use. The Bradford assay was used to determine the protein concentration of the resulting supernatant.

50µg of protein samples were mixed with 4× Laemmli buffer and boiled for 5 minutes at 95 °C. These samples are then loaded and separated by SDS–PAGE (Bio-Rad, #4561084). The resolved proteins were subsequently transferred onto PVDF membrane (Merck) using a wet transfer system. Prior to transfer, the PVDF membrane was briefly activated in methanol. The transfer was carried out at 70 V for 3 hours at 4 °C.

After transfer, the membrane was blocked for 1 hour at room temperature with Intercept® blocking buffer (LI-COR, #927-60001). Primary antibodies were incubated overnight at 4 °C at a 1:1000 dilution in blocking buffer. The following primary antibodies have been used: Rnd3 (Sigma-Aldrich, 05-723; Lot #3821703) and GAPDH (Cell Signalling Technology, #2118; Lot #14), the latter serving as a loading control.

After washing the membrane 3 times with TBS-T, membranes were incubated at RT for 1 hour with fluorescently labelled secondary antibodies diluted at 1:1000 in blocking buffer: IRDye 680RD anti-Mouse IgG (#926-68070; Lot #D10901-15) and IRDye 800CW anti-Rabbit IgG (#926-32211; Lot #D10831-15). The membrane was again washed 3 times with TBS-T for 5 mins each. Following final washes, the protein bands were imaged using the Odyssey® CLx Imaging System (LI-COR).

11.5 Microscopy

Total internal reflection fluorescence (TIRF) microscopy was performed using an Olympus IX-81 inverted microscope equipped with a motorized TIRF-MITICO illumination combiner, a 60× Apo TIRF 1.45 NA oil immersion objective, and a ZDC autofocus module. For spectral separation of fluorophores emitting in the blue (TagBFP), cyan (mTurquoise2/mCerulean), yellow (mCitrine), and red (mCherry) ranges, the setup incorporated a quadruple bandpass dichroic mirror (ZT405-440/514/561) in combination with the corresponding emission filters (HC 435/40, HC 472/30, HC 542/27, and HC 629/53).

Excitation was provided either by a 514 nm OBIS diode laser (150 mW, Coherent Inc., USA) or by Olympus Cell R diode lasers operating at 405 nm (50 mW), 445 nm (50 mW), and 561 nm (100 mW). Additional wide-field illumination was supplied by a Spectra X light engine (Lumencor). Fluorescence emission was captured using an EMCCD camera (C9100-13, Hamamatsu, Germany) operated at medium gain without pixel binning.

The microscope was enclosed in a temperature-regulated environmental chamber to enable live-cell time-lapse imaging at 37 °C. Imaging was performed using CO_2-independent, HEPES-buffered medium (Pan Biotech) supplemented with 10% fetal bovine serum (FBS). For morphometric imaging and subsequent analysis, automated image acquisition was carried out on the same microscope using wide-field illumination and a UPlanSApo 10×/0.4 NA air objective. Consistent image quality was ensured through software-based autofocus.

11.6 Light-induced Rnd3 perturbation via the LOVTRAP system

The LOVTRAP system was employed to modulate the cytosolic concentration of a target protein in living cells, as originally described by *Wang et al. (2016)*. Here, this method was adapted to dynamically regulate the cytosolic levels of Rnd3. For experiments, cells were transfected with pTriEx-NTOM20-GS-moxBFP-cc-GS-LOV2 (previously characterized in *Kamps et al., 2020*), together with pTriEx-mCherry-Zdk1-Rnd3 and either delCMV-mCitrine-2xRBD (Rho activity sensor) or delCMV-mCitrine-3xp67Phox (Rac activity sensor). In experiments combining this system with Rnd3 knockdown, the siRNA-resistant Rnd3 perturbation construct pTriEx-mCherry-Zdk1-Rnd3-siRnd3.7r was used in place of pTriEx-mCherry-Zdk1-Rnd3.

Optogenetic perturbation of Rnd3 was achieved through illumination with a 445 nm laser in wide-field mode. Owing to the high photosensitivity of the LOV2 domain, a 100× neutral density filter (with the laser set to 100% power) was used to release Zdk1-fused Rnd3 into the cytosol. During the perturbation period, the 445 nm laser remained continuously active, except for brief interruptions during image acquisition. To prevent premature optogenetic activation, fluorescence imaging was

restricted to the 514 nm and 561 nm excitation lines, and BFP fluorescence was recorded only after completion of the time-lapse sequence.

The Rho GTPase activity sensor measurement (A_{Rho}) was quantified by measuring the fluorescence intensity of the Rho GTPase activity sensor (I_{Rho}) across the entire cell adhesion area. Raw intensity values were background-corrected by subtracting the signal from regions outside the cell ($I_{Rho,BG}$) and normalized to the initial background-corrected intensity ($I_{Rho,0} - I_{Rho,0,BG}$) obtained immediately before the optogenetic perturbation.

$$A_{Rho} = \frac{I_{Rho} - I_{Rho,BG}}{I_{Rho,0} - I_{Rho,0,BG}}$$

11.7 Perturbation of Rac/Rho using chemically induced dimerization

Chemically induced dimerization was carried out following the procedures reported previously by *Liu et al. (2014)*. Both the SLF'-TMP dimerizer and the TMP competitor were synthesized and purified according to the procedures outlined in that study. For the experiments, cells were transfected with TagBFP-2xeDHFR-CAAX together with one of the perturbation constructs, either mTurquoise2-NES-2xFKBP'-RhoAQ63LΔCAAX or mTurquoise2-NES-2xFKBP'-RacQ61LΔCAAX. To identify the Rho GTPase signalling crosstalk, cells were co-transfected with delCMV-mCitrine-Rnd3 and the control plasmid delCMV-mCherry.

Dimerization was initiated by adding 10µL of SLF'-TMP dimerizer after 10-minutes of imaging, and the reaction was terminated 20 minutes after addition of dimerizer by introducing 10µL of TMP competitor.

Subsequent image analysis was conducted as outlined by Nanda et al. (2023)[1]. In summary, the fluorescence intensity of Rnd3 (A_{Rnd3}) was quantified using TIRF microscopy, focusing on the central regions of the cell throughout the observation

period. The raw Rnd3 fluorescence intensity measurement (I_{Rnd3}) was corrected by subtracting background intensity measured outside the cell area ($I_{Rnd3,BG}$) and normalized to the initial, background-corrected fluorescence value recorded immediately before perturbation ($I_{Rnd3,0} - I_{Rnd3,0,BG}$). Final corrected Rnd3 sensor readings were calculated by subtracting normalized control measurements from the corresponding normalized Rnd3 measurements.

$$A_{Rnd3} = \frac{I_{Rnd3} - I_{Rnd3,BG}}{I_{Rnd3,0} - I_{Rnd3,0,BG}} - \frac{I_{control} - I_{control,BG}}{I_{control,0} - I_{control,0,BG}}$$

11.8 Rapid perturbation of Rac1 using Photo-activable Rac1

The generation of the photoactivatable Rac1 (PA-Rac1) construct was originally reported by the Klaus Hahn laboratory (Wu et al., 2009). Here, optogenetic perturbations utilising PA-Rac1 were conducted following the procedures described by Nanda et al. (2023)[1,2]. Cells were co-transfected with mCerulean-PA-Rac1 and delCMV-mCitrine-Rnd3, and photoactivation of PA-Rac1 was achieved using TIRF illumination using a 445 nm laser. To prevent excessive activation, a 10,000× neutral density filter was applied, and the laser intensity was adjusted to 30% of its maximum output. During photoactivation, the 445 nm laser remained continuously on except during brief image acquisition intervals.

To eliminate spectral crosstalk between the optogenetic activation and fluorescence imaging channels, imaging was performed exclusively with 514 nm and 561 nm laser excitation lines. The mCerulean fluorescence signal was captured only after completion of the time-lapse sequence to prevent interference with optogenetic control. For these experiments, delCMV-mCherry served as the control sensor and was expressed either together with the Rnd3 sensor or in a different population of cells.

[1] Nanda S. Investigation of signal networks that control dynamic cell shape changes (Doctoral dissertation), TU Dortmund, 2023
[2] Contribution from this thesis

Subsequent data analysis followed the workflow described by Nanda et al. (2023)[1]. Briefly, the Rnd3 activity sensor signal (A_{Rnd3}) was quantified by measuring the fluorescence intensity of the Rnd3 sensor (I_{Rnd3}) across the entire cell adhesion area using TIRF microscopy. Raw fluorescence data were background-corrected by subtracting the intensity outside the cell region ($I_{Rnd3,BG}$) and then normalized to the initial background-corrected intensity measured immediately before Rac1 perturbation ($I_{Rnd3,0} - I_{Rnd3,0,BG}$).

$$A_{Rnd3} = \frac{I_{Rnd3} - I_{Rnd3,BG}}{I_{Rnd3,0} - I_{Rnd3,0,BG}}$$

If the control sensor was expressed together with Rnd3 sensor construct, the corrected Rnd3 activity response was determined by subtracting the normalized fluorescence intensity of the control sensor (delCMV-mCherry) from the corresponding normalized Rnd3 sensor intensity values.

$$A_{Rnd3} = \frac{I_{Rnd3} - I_{Rnd3,BG}}{I_{Rnd3,0} - I_{Rnd3,0,BG}} - \frac{I_{control} - I_{control,BG}}{I_{control,0} - I_{control,0,BG}}$$

11.9 Quantitative analysis of cell morphodynamics and fluorescence signals at the cell periphery during migration

Quantitative analyses of cell edge velocity cross-correlation, signal enrichment during protrusion and retraction events, and cell edge movements were performed following the approach described by Nanda et al. (2023)[1]. In brief, local Rnd3 activity enrichment in A431 cells was assessed by co-transfecting delCMV-mCitrine-Rnd3 with the cell volume marker delCMV-mCherry. Cell boundary movements were

[1] Nanda S. Investigation of signal networks that control dynamic cell shape changes (Doctoral dissertation), TU Dortmund, 2023

tracked using the cell volume marker, independent of fluctuations in Rnd3 activity, with an adapted version of the ADAPT plugin (*Barry et al., 2015*).

The data generated by the ADAPT plugin were subsequently processed using customised ImageJ scripts to obtain parameters including velocity cross-correlation, protrusion and retraction-associated enrichment, and time intervals of protrusion, retraction, and pause phases. To examine the impact of Rnd3 overexpression on cell morphodynamics, CMV-mCitrine-Rnd3 was transfected in place of delCMV-mCitrine-Rnd3.

Cell edge movements > 0.075 µm/min were classified as protrusions, while movements below −0.075 µm/min were classified as retractions. For experiments investigating the impact of siRNA-mediated Rnd3 depletion on cell morphodynamics, delCMV-mCherry was used as the cell volume marker to define cell boundaries.

11.10 Cell morphology analysis

Cell morphology analysis was carried out as described previously by *Lüttig et al. (2025)*. 24 hr following siRNA transfection, cells were replated onto LabTek chambered dishes coated with fibronectin. Following an 8-hour incubation, cells were washed with PBS and fixed with pre-warmed formaldehyde. Subsequently, cells were permeabilized using 0.1% Triton X-100 and stained for F-actin and nuclei with Rhodamine–Phalloidin (1:1000) and Hoechst 33342, respectively, for 30 minutes at room temperature in the dark.

Automated imaging of individual wells was performed, and the resulting images were analysed using Cell Profiler software (*Carpenter et al., 2006*) to quantify cell adhesion area and maximum F-actin fluorescence intensity.

11.11 Investigation of the pulsatile dynamics of Rho activity

To examine the dynamics of Rho activity pulses, cells were first seeded in 35 mm cell culture dishes on day 1 and transfected with the Rho activity sensor (delCMV-mCherry-2xRBD) along with the cell volume marker delCMV-mCitrine on day 2. The following day (day 3), cells were splitted and replated onto glass-bottom dishes for imaging. Cells were imaged for 30 mins with 10s time intervals. Quantification of Rho activity dynamics was performed using a customized ImageJ script previously described by *Graessl et al. (2017)*, with minor modifications of the analysis workflow.

11.12 Image and video analysis software

All image and video analyses were conducted using ImageJ software (*Fiji*; https://imagej.net/software/fiji/). Kymograph analysis was carried out with the built-in Multi Kymograph plugin in ImageJ. Parameters describing cell migration dynamics were quantified using a custom-modified version of the ADAPT plugin, as detailed above (*Barry et al., 2015; Nanda et al., 2023*)[1].

Quantification of maximum F-actin intensity and cell adhesion area was performed using Cell Profiler (*Carpenter et al., 2006*), and the resulting data were further processed in MATLAB. Statistical analysis and data visualization were carried out using GraphPad Prism 10.

11.13 Use of AI

ChatGPT has been used for paraphrasing parts of this thesis and for translating the abstract to German. It has not been used for the generation of any original content for this thesis.

[1] Nanda S. Investigation of signal networks that control dynamic cell shape changes (Doctoral dissertation), TU Dortmund, 2023

12. Plasmid constructs

12.1 Plasmids used in this thesis

No.	Lab no.	Plasmid name	Source
1	162	delCMV-mCherry	(Nanda et al., 2023)
2	163	delCMV-mCitrine	(Nanda et al., 2023)
3	257	delCMV-mCitrine-RBD	(Kamps et al.,2020)
4	262	TagBFP-DA-KRC (D1)	(Liu et al., 2014)
5	278	mTurquoise2-NES-D2-RacQ61L	(Nanda et al., 2023)
6	280	mTurquoise2-NES-D2-RhoAQ63L	(Kamps et al.,2020)
7	318	pTriEx-mCherry-ZdkI	(Wang et al., 2016)
8	358	pTriEX-mCherry-Zdk1-RhoA Q63L	Addgene #81058
9	551	CMV-mCherry-ARHGEF-11	(Müller et al., 2020)
10	552	CMV-mCherry-ARHGEF-12	(Müller et al., 2020)
11	699	delCMV-mCherry-2xRBD (Rhotekin)	(Nanda et al., 2023)
12	778	delCMV-mCherry-3xp67Phox	(Nanda et al., 2023)

13	810	delCMV-mCitrine-3xp67Phox	(Nanda et al.,2023)
14	880	delCMV-mCitrine-2xRBD (Rhotekin)	Suchet Nanda
15	915	CMV-EGFP-RhoE	Addgene #23229
16	917	pTriEx-NTOM20-GS-moxBFP-cc-GS-LOV2	(Kamps et al., 2020)

12.2 Plasmids generated in this thesis

No.	Lab No.	Plasmid name	Cloning method (Insert/Vector plasmid Lab no.)	Oligo pair used	Enzymes used
1	935	CMV-mcherry-Arhgef11-PH-mutant (F1044A_I1046E)	Gibson assembly (551/551)	1&2	PacI/PmlI
2	936	CMV-mcherry-Arhgef12-PH-mutant (F1098A_I1100E)	Gibson assembly (552/552)	3&4	PacI/EcoRI-HF
3	939	CMV-mcherry-Arhgef11-actin-mutant (Arhgef11 ΔFAB(561-585))	Gibson assembly (551/551)	5&6	PmlI/AscI
4	976	CMV-mcitrine-Rnd3	Gibson assembly (257/915)	7	BspEI/AgeI-HF

5	977	delCMV-mcitrine-Rnd3	Restriction digestion and ligation (163,976)		AseI and NheI-HF
6	995	pTriEX-mCherry-Zdk1-Rnd3	Gibson assembly (976/358)	8	HindIII-HF/KpnI-HF
7	998	pTriEX-mCherry-Zdk1-Rnd3-siRnd3.7_resistant	Gibson assembly (995/995)	9	BspHI/SacI-HF

12.3 Oligo pairs for cloning

No.	Forward primer /Reverse primer
1	5′-ATAAGACCTTGGACCTCCACGTGCTGCTGCTGGAGGACCTC-3′ / 5′-ATTCGATAGCGAAGGCCCGTTTATCTGTGG-3′
2	5’-ACGGGCCTTCGCTATCGAATGCACCTCCAAGCTGGGC-3′ / 5′-TAGGAACTTACCTGGTTAATTAATGGTCCTGGTGACGCGGC-3’
3	5′- CAGCGAGTATCCAGAGAAGGAATTCTGTCACCCTCAGAGCTAC-3’ / 5’- ATTCGACGGCTAAAGCTTTGTTATCTGTTGCC-3′
4	5′- CAAAGCTTTAGCCGTCGAATCCATGTCAGACAATGGC-3′ / 5′-TAGGAACTTACCTGGTTAATTAATCAACTTTTATCTGAGTGCTTG-3′
5	5′-CCCTTTTTTTTCCCCAGGGGCGCGCCATGAGTGTAAGGTTACCCC-3′ / 5′-AGAGTCGTTGGACTTCCACAGGGGACAAG-3′

6	5′-TGTGGAAGTCCAACGACTCTCGACCGGAAG-3’ / 5’-AGGTCCTCCAGCAGCAGCACGTGGAGGTCCAAGGTCTTATCCTTG-3′
7	5’-CGTCAGATCCGCTAGCGCTACCGGTCGCCACCATGGTGAGCAAG-3’ / 5’-TTCATGTCGACGGATCTGAGTCCACTTCCAGAACCGGAACCTCCGGACTTGTACAGCTCG-3’
8	5’-GGTTCTGGTTCTGGTGGTACCGGTTCCGGTTCTGGAAGTG -3’ / 5’-TATACAGCTGTGCGGCCGCAAGCTTTCACATCACAGTGCAGCTC -3’
9	5’-CAGATGTTAGTACATTAGTAGAACTGTCCAATCACAGGCAGACG -3’ / 5’- GTCAGATGCTCAAGGGGCTTCATGATGTCCCCATAATTTTTGGC -3’.

13. References

Aoki, K., Maeda, F., Nagasako, T., Mochizuki, Y., Uchida, S., Ikenouchi, J., & Pollard, T. D. (2016). A RhoA and Rnd3 cycle regulates actin reassembly during membrane blebbing. *Proceedings of the National Academy of Sciences of the United States of America*, *113*(13), E1863–E1871. https://doi.org/10.1073/pnas.1600968113

Arthur, W. T., & Burridge, K. (2001). RhoA inactivation by p190RhoGAP regulates cell spreading and migration by promoting membrane protrusion and polarity. *Molecular Biology of the Cell*, *12*(9). https://doi.org/10.1091/mbc.12.9.2711

Arthur, W. T., Quilliam, L. A., & Cooper, J. A. (2004). Rap1 promotes cell spreading by localizing Rac guanine nucleotide exchange factors. *Journal of Cell Biology*, *167*(1). https://doi.org/10.1083/jcb.200404068

Aurandt, J., Vikis, H. G., Gutkind, J. S., Ahn, N., & Guan, K. L. (2002). The semaphorin receptor plexin-B1 signals through a direct interaction with the Rho-specific nucleotide exchange factor, LARG. *Proceedings of the National Academy of Sciences of the United States of America*, *99*(19). https://doi.org/10.1073/pnas.142433199

Banerjee, J., & Wedegaertner, P. B. (2004). Identification of a Novel Sequence in PDZ-RhoGEF That Mediates Interaction with the Actin Cytoskeleton. *Molecular Biology of the Cell*, *15*(4). https://doi.org/10.1091/mbc.E03-07-0527

Barry, D. J., Durkin, C. H., Abella, J. V., & Way, M. (2015). Open source software for quantification of cell migration, protrusions, and fluorescence intensities. *Journal of Cell Biology*, *209*(1), 163–180. https://doi.org/10.1083/jcb.201501081

Be, M. S. B., & Mccormick, F. (1993). *Proteins regulating Ras and its relatives*.

Benink, H. A., & Bement, W. M. (2005). Concentric zones of active RhoA and Cdc42 around single cell wounds. *Journal of Cell Biology*, *168*(3). https://doi.org/10.1083/jcb.200411109

Bidaud-Meynard, A., Binamé, F., Lagrée, V., & Moreau, V. (2019). Regulation of Rho GTPase activity at the leading edge of migrating cells by p190RhoGAP. In *Small GTPases* (Vol. 10, Number 2). https://doi.org/10.1080/21541248.2017.1280584

Blanchoin, L., Boujemaa-Paterski, R., Sykes, C., & Plastino, J. (2014). Actin dynamics, architecture, and mechanics in cell motility. *Physiological Reviews*, *94*(1). https://doi.org/10.1152/physrev.00018.2013

Chikumi, H., Barac, A., Behbahani, B., Gao, Y., Teramoto, H., Zheng, Y., & Gutkind, J. S. (2004). Homo- and hetero-oligomerization of PDZ-RhoGEF, LARG and p115RhoGEF by their C-terminal region regulates their in vivo Rho GEF activity and transforming potential. *Oncogene*, *23*(1). https://doi.org/10.1038/sj.onc.1207012

Cooper, M. S., & Schliwa, M. (1986). Motility of cultured fish epidermal cells in the presence and absence of direct current electric fields. *Journal of Cell Biology*, *102*(4). https://doi.org/10.1083/jcb.102.4.1384

Cotteret, S., & Chernoff, J. (2002). *The evolutionary history of effectors downstream of Cdc42 and Rac*. http://genomebiology.com/2002/3/2/reviews/0002.1http://genomebiology.com/2002/3/2/reviews/0002

Dada, O., Gutowski, S., Brautigam, C. A., Chen, Z., & Sternweis, P. C. (2018a). Direct regulation of p190RhoGEF by activated Rho and Rac GTPases. *Journal of Structural Biology*, *202*(1). https://doi.org/10.1016/j.jsb.2017.11.014

de Seze, J., Gatin, J., & Coppey, M. (2023). RhoA regulation in space and time. In *FEBS Letters* (Vol. 597, Number 6). https://doi.org/10.1002/1873-3468.14578

Dehmelt, L., & Bastiaens, P. I. H. (2010). Spatial organization of intracellular communication: Insights from imaging. In *Nature Reviews Molecular Cell Biology* (Vol. 11, Number 6). https://doi.org/10.1038/nrm2903

Driessens, M. H. E., Hu, H., Nobes, C. D., Self, A., Jordens, I., Goodman, C. S., & Hall, A. (2001). Plexin-B semaphorin receptors interact directly with active Rac and regulate the actin cytoskeleton by activating Rho. *Current Biology*, *11*(5). https://doi.org/10.1016/S0960-9822(01)00092-6

Driessens, M. H. E., Olivo, C., Nagata, K. ichi, Inagaki, M., & Collard, J. G. (2002). B plexins activate Rho through PDZ-RhoGEF. *FEBS Letters*, *529*(2–3). https://doi.org/10.1016/S0014-5793(02)03323-9

Eden, S., Rohatgi, R., Podtelejnikov, A. V., Mann, M., & Kirschner, M. W. (2002). Mechanism of regulation of WAVE1-induced actin nucleation by Rac1 and Nck. *Nature*, *418*(6899). https://doi.org/10.1038/nature00859

Etienne-Manneville, S., & Hall, A. (2002). *Rho GTPases in cell biology*. www.nature.com/nature

Faix, J., & Rottner, K. (2006). The making of filopodia. In *Current Opinion in Cell Biology* (Vol. 18, Number 1). https://doi.org/10.1016/j.ceb.2005.11.002

Foster, R., Nolan, K. M., Thissen, J., & Settleman, J. (1996). Identification of a Novel Human Rho Protein with Unusual Properties: GTPase Deficiency and In Vivo Farnesylation. In *MOLECULAR AND CELLULAR BIOLOGY* (Vol. 16, Number 6).

Friedl, P., & Wolf, K. (2003). Tumour-cell invasion and migration: Diversity and escape mechanisms. In *Nature Reviews Cancer* (Vol. 3, Number 5). https://doi.org/10.1038/nrc1075

Fukuhara, S., Chikumi, H., & Gutkind, J. S. (2000). Leukemia-associated Rho guanine nucleotide exchange factor (LARG) links heterotrimeric G proteins of the G12 family to Rho. *FEBS Letters*, *485*(2–3). https://doi.org/10.1016/S0014-5793(00)02224-9

Fukuhara, S., Murga, C., Zohar, M., Igishi, T., & Gutkind, J. S. (1999). A novel PDZ domain containing guanine nucleotide exchange factor links heterotrimeric G proteins

to Rho. *Journal of Biological Chemistry*, *274*(9). https://doi.org/10.1074/jbc.274.9.5868

Galic, M., Tsai, F. C., Collins, S. R., Matis, M., Bandara, S., & Meyer, T. (2014). Dynamic recruitment of the curvature-sensitive protein ArhGAP44 to nanoscale membrane deformations limits exploratory filopodia initiation in neurons. *ELife*, *3*. https://doi.org/10.7554/eLife.03116

Garcia-Mata, R., Boulter, E., & Burridge, K. (2011). The “invisible hand”: Regulation of RHO GTPases by RHOGDIs. In *Nature Reviews Molecular Cell Biology* (Vol. 12, Number 8). https://doi.org/10.1038/nrm3153

Gardel, M. L., Schneider, I. C., Aratyn-Schaus, Y., & Waterman, C. M. (2010). Mechanical integration of actin and adhesion dynamics in cell migration. In *Annual Review of Cell and Developmental Biology* (Vol. 26). https://doi.org/10.1146/annurev.cellbio.011209.122036

Geoffrey M Cooper. (2000). The Cell, 2nd edition A Molecular Approach. In *Sunderland (MA): Sinauer Associates;* (Vol. 63, Number 6).

Graessl, M., Koch, J., Calderon, A., Kamps, D., Banerjee, S., Mazel, T., Schulze, N., Jungkurth, J. K., Patwardhan, R., Solouk, D., Hampe, N., Hoffmann, B., Dehmelt, L., & Nalbant, P. (2017). An excitable Rho GTPase signaling network generates dynamic subcellular contraction patterns. *Journal of Cell Biology*, *216*(12), 4271–4285. https://doi.org/10.1083/jcb.201706052

Guilluy, C., Garcia-Mata, R., & Burridge, K. (2011). Rho protein crosstalk: Another social network? In *Trends in Cell Biology* (Vol. 21, Number 12, pp. 718–726). https://doi.org/10.1016/j.tcb.2011.08.002

Hirotani, M., Ohoka, Y., Yamamoto, T., Nirasawa, H., Furuyama, T., Kogo, M., Matsuya, T., & Inagaki, S. (2002). Interaction of plexin-B1 with PDZ domain-containing Rho guanine nucleotide exchange factors. *Biochemical and Biophysical Research Communications*, *297*(1). https://doi.org/10.1016/S0006-291X(02)02122-8

Jiang, Y., Jiang, H., Zhou, S., Meng, B., Liu, Z.-J., & Ouyang, S. (2016). Crystal structure of hGEF-H1 PH domain provides insight into incapability in phosphoinositide binding. *Biochemical and Biophysical Research Communications*, *471*(4), 621–627. https://doi.org/10.1016/j.bbrc.2016.01.150

Kamps, D., Koch, J., Juma, V. O., Campillo-Funollet, E., Graessl, M., Banerjee, S., Mazel, T., Chen, X., Wu, Y. W., Portet, S., Madzvamuse, A., Nalbant, P., & Dehmelt, L. (2020). Optogenetic Tuning Reveals Rho Amplification-Dependent Dynamics of a Cell Contraction Signal Network. *Cell Reports*, *33*(9). https://doi.org/10.1016/j.celrep.2020.108467

Knaus, U. G., & Bokoch, G. M. (n.d.). *The p21 Rac/Cdc42-activated kinases (PAKs)*. Komander, D., Garg, R., Wan, P. T. C., Ridley, A. J., & Barford, D. (2008). Mechanism of multi-site phosphorylation from a ROCK-I:RhoE complex structure. *EMBO Journal*, *27*(23), 3175–3185. https://doi.org/10.1038/emboj.2008.226

Kowalczyk, M., Kamps, D., Wu, Y., Dehmelt, L., & Nalbant, P. (2022). Monitoring the Response of Multiple Signal Network Components to Acute Chemo-Optogenetic Perturbations in Living Cells. *ChemBioChem*, *23*(4). https://doi.org/10.1002/cbic.202100582

Kuo, J. C., Han, X., Hsiao, C. Te, Yates, J. R., & Waterman, C. M. (2011). Analysis of the myosin-II-responsive focal adhesion proteome reveals a role for β-Pix in negative regulation of focal adhesion maturation. *Nature Cell Biology*, *13*(4). https://doi.org/10.1038/ncb2216

Ladoux, B., & Nicolas, A. (2012). Physically based principles of cell adhesion mechanosensitivity in tissues. *Reports on Progress in Physics*, *75*(11). https://doi.org/10.1088/0034-4885/75/11/116601

Lambert, J. M., Lambert, Q. T., Reuther, G. W., Malliri, A., Siderovski, D. P., Sondek, J., Collard, J. G., & Der, C. J. (2002). Tiam1 mediates Ras activation of Rac by a

PI(3)K-independent mechanism. *Nature Cell Biology*, *4*(8). https://doi.org/10.1038/ncb833

Lauffenburger, D. A., & Horwitz, A. F. (1996). Cell migration: A physically integrated molecular process. In *Cell* (Vol. 84, Number 3). https://doi.org/10.1016/S0092-8674(00)81280-5

Lee, C. S., Choi, C. K., Shin, E. Y., Schwartz, M. A., & Kim, E. G. (2010). Myosin II directly binds and inhibits Dbl family guanine nucleotide exchange factors: A possible link to Rho family GTPases. *Journal of Cell Biology*, *190*(4). https://doi.org/10.1083/jcb.201003057

Lim, J. I., Sabouri-Ghomi, M., Machacek, M., Waterman, C. M., & Danuser, G. (2010). Protrusion and actin assembly are coupled to the organization of lamellar contractile structures. *Experimental Cell Research*, *316*(13). https://doi.org/10.1016/j.yexcr.2010.04.011

Liu, P., Calderon, A., Konstantinidis, G., Hou, J., Voss, S., Chen, X., Li, F., Banerjee, S., Hoffmann, J. E., Theiss, C., Dehmelt, L., & Wu, Y. W. (2014). A bioorthogonal small-molecule-switch system for controlling protein function in live cells. *Angewandte Chemie - International Edition*, *53*(38). https://doi.org/10.1002/anie.201403463

Lüttig, R., Nanda, S., Chandran, H. T., & Dehmelt, L. (2025). Crosstalk between Rac and Rap GTPases in migrating cells. *Molecular Biology of the Cell, Vol.36, No. 10. https://doi.org/10.1091/mbc.E25-02-0058*

Madigan, J. P., Bodemann, B. O., Brady, D. C., Dewar, B. J., Keller, P. J., Leitges, M., Philips, M. R., Ridley, A. J., Der, C. J., & Cox, A. D. (2009). Regulation of Rnd3 localization and function by protein kinase Cα-mediated phosphorylation. *Biochemical Journal*, *424*(1). https://doi.org/10.1042/BJ20082377

Mattila, P. K., & Lappalainen, P. (2008). Filopodia: Molecular architecture and cellular functions. In *Nature Reviews Molecular Cell Biology* (Vol. 9, Number 6). https://doi.org/10.1038/nrm2406

Medina, F., Carter, A. M., Dada, O., Gutowski, S., Hadas, J., Chen, Z., & Sternweis, P. C. (2013a). Activated RhoA is a positive feedback regulator of the Lbc family of Rho guanine nucleotide exchange factor proteins. *The Journal of Biological Chemistry*, *288*(16), 11325–11333. https://doi.org/10.1074/jbc.M113.450056

Miki, H., Suetsugu, S., & Takenawa, T. (1998). WAVE, a novel WASP-family protein involved in actin reorganization induced by Rac. *EMBO Journal*, *17*(23). https://doi.org/10.1093/emboj/17.23.6932

Müller, P. M., Rademacher, J., Bagshaw, R. D., Wortmann, C., Barth, C., van Unen, J., Alp, K. M., Giudice, G., Eccles, R. L., Heinrich, L. E., Pascual-Vargas, P., Sanchez-Castro, M., Brandenburg, L., Mbamalu, G., Tucholska, M., Spatt, L., Czajkowski, M. T., Welke, R. W., Zhang, S., … Rocks, O. (2020). Systems analysis of RhoGEF and RhoGAP regulatory proteins reveals spatially organized RAC1 signalling from integrin adhesions. *Nature Cell Biology*, *22*(4). https://doi.org/10.1038/s41556-020-0488-x

Nalbant, P., & Dehmelt, L. (2018). Exploratory cell dynamics: A sense of touch for cells? In *Biological Chemistry* (Vol. 399, Number 8, pp. 809–819). Walter de Gruyter GmbH. https://doi.org/10.1515/hsz-2017-0341

Nanda, S., Calderon, A., Sachan, A., Duong, T. T., Koch, J., Xin, X., Solouk-Stahlberg, D., Wu, Y. W., Nalbant, P., & Dehmelt, L. (2023). Rho GTPase activity crosstalk mediated by Arhgef11 and Arhgef12 coordinates cell protrusion-retraction cycles. *Nature Communications*, *14*(1). https://doi.org/10.1038/s41467-023-43875-y

Nobes, C. D., & Hall, A. (1995). Rho, Rac, and Cdc42 GTPases regulate the assembly of multimolecular focal complexes associated with actin stress fibers, lamellipodia, and filopodia. *Cell*, *81*(1). https://doi.org/10.1016/0092-8674(95)90370-4

Ohta, Y., Hartwig, J. H., & Stossel, T. P. (2006). FilGAP, a Rho- and ROCK-regulated GAP for Rac binds filamin A to control actin remodelling. *Nature Cell Biology*, *8*(8). https://doi.org/10.1038/ncb1437

Paluch, E. K., Aspalter, I. M., & Sixt, M. (2016). Focal Adhesion-Independent Cell Migration. *Annual Review of Cell and Developmental Biology*, *32*. https://doi.org/10.1146/annurev-cellbio-111315-125341

Parsons, J. T., Horwitz, A. R., & Schwartz, M. A. (2010). Cell adhesion: Integrating cytoskeletal dynamics and cellular tension. In *Nature Reviews Molecular Cell Biology* (Vol. 11, Number 9). https://doi.org/10.1038/nrm2957

Pollard, T. D., & Borisy, G. G. (2003). Cellular motility driven by assembly and disassembly of actin filaments. In *Cell* (Vol. 112, Number 4). https://doi.org/10.1016/S0092-8674(03)00120-X

Pollard, T. D., & Cooper, J. A. (2009). Actin, a central player in cell shape and movement. In *Science* (Vol. 326, Number 5957). https://doi.org/10.1126/science.1175862

Ridley, A. J. (2011). Life at the leading edge. In *Cell* (Vol. 145, Number 7). https://doi.org/10.1016/j.cell.2011.06.010

Ridley, A. J. (2015a). Rho GTPase signalling in cell migration. In *Current Opinion in Cell Biology* (Vol. 36, pp. 103–112). Elsevier Ltd. https://doi.org/10.1016/j.ceb.2015.08.005

Ridley, A. J. (2015b). Rho GTPase signalling in cell migration. *Current Opinion in Cell Biology*, *36*, 103–112. https://doi.org/10.1016/j.ceb.2015.08.005

Ridley, A. J., Schwartz, M. A., Burridge, K., Firtel, R. A., Ginsberg, M. H., Borisy, G., Parsons, J. T., & Horwitz, A. R. (2003). Cell Migration: Integrating Signals from Front to Back. In *Science* (Vol. 302, Number 5651). https://doi.org/10.1126/science.1092053

Riento, K., & Ridley, A. J. (2006). Inhibition of ROCK by RhoE. In *Methods in Enzymology* (Vol. 406). https://doi.org/10.1016/s0076-6879(06)06041-1

Riou, P., Kjær, S., Garg, R., Purkiss, A., George, R., Cain, R. J., Bineva, G., Reymond, N., McColl, B., Thompson, A. J., O'Reilly, N., McDonald, N. Q., Parker, P. J., & Ridley, A. J. (2013). 14-3-3 proteins interact with a hybrid prenyl-phosphorylation motif to inhibit G proteins. *Cell*, *153*(3), 640–653. https://doi.org/10.1016/j.cell.2013.03.044

Sahai, E. (2005). Mechanisms of cancer cell invasion. In *Current Opinion in Genetics and Development* (Vol. 15, Number 1). https://doi.org/10.1016/j.gde.2004.12.002

Sanz-Moreno, V., Gadea, G., Ahn, J., Paterson, H., Marra, P., Pinner, S., Sahai, E., & Marshall, C. J. (2008). Rac Activation and Inactivation Control Plasticity of Tumor Cell Movement. *Cell*, *135*(3). https://doi.org/10.1016/j.cell.2008.09.043

Scheffzek, K., & Welti, S. (2012). Pleckstrin homology (PH) like domains - versatile modules in protein-protein interaction platforms. *FEBS Letters*, *586*(17), 2662–2673. https://doi.org/10.1016/j.febslet.2012.06.006

Schmidt, A., & Hall, A. (2002). Guanine nucleotide exchange factors for Rho GTPases: turning on the switch. *Genes & Development*, *16*(13), 1587–1609. https://doi.org/10.1101/gad.1003302

Small, J. V., Stradal, T., Vignal, E., & Rottner, K. (2002). The lamellipodium: Where motility begins. In *Trends in Cell Biology* (Vol. 12, Number 3). https://doi.org/10.1016/S0962-8924(01)02237-1

Svitkina, T. (2018). The actin cytoskeleton and actin-based motility. *Cold Spring Harbor Perspectives in Biology*, *10*(1). https://doi.org/10.1101/cshperspect.a018267

Symons, M., & Settleman, J. (2000). Rho family GTPases: More than simple switches. In *Trends in Cell Biology* (Vol. 10, Number 10). https://doi.org/10.1016/S0962-8924(00)01832-8

Vicente-Manzanares, M., Ma, X., Adelstein, R. S., & Horwitz, A. R. (2009). Non-muscle myosin II takes centre stage in cell adhesion and migration. In *Nature Reviews Molecular Cell Biology* (Vol. 10, Number 11). https://doi.org/10.1038/nrm2786

Vicente-Manzanares, M., Newell-Litwa, K., Bachir, A. I., Whitmore, L. A., & Horwitz, A. R. (2011). Myosin IIA/IIB restrict adhesive and protrusive signaling to generate front-back polarity in migrating cells. *Journal of Cell Biology*, *193*(2). https://doi.org/10.1083/jcb.201012159

Vikis, H. G., Li, W., He, Z., & Guan, K. L. (2000). The semaphorin receptor plexin-B1 specifically interacts with active Rac in a ligand-dependent manner. *Proceedings of the National Academy of Sciences of the United States of America*, *97*(23). https://doi.org/10.1073/pnas.220421797

Wang, H., Vilela, M., Winkler, A., Tarnawski, M., Schlichting, I., Yumerefendi, H., Kuhlman, B., Liu, R., Danuser, G., & Hahn, K. M. (2016). LOVTRAP: An optogenetic system for photoinduced protein dissociation. *Nature Methods*, *13*(9), 755–758. https://doi.org/10.1038/nmeth.3926

Watanabe, N., & Mitchison, T. J. (n.d.). *Single-Molecule Speckle Analysis of Actin Filament Turnover in Lamellipodia*. Retrieved https://www.science.org

Webb, D. J., Parsons, J. T., & Horwitz, A. F. (2002). Adhesion assembly, disassembly and turnover in migrating cells - Over and over and over again. In *Nature Cell Biology* (Vol. 4, Number 4). https://doi.org/10.1038/ncb0402-e97

Wennerberg, K., Forget, M. A., Ellerbroek, S. M., Arthur, W. T., Burridge, K., Settleman, J., Der Channing, C., & Hansen, S. H. (2003). Rnd proteins function as RhoA antagonists by activating p190 RhoGAP. *Current Biology*, *13*(13), 1106–1115. https://doi.org/10.1016/S0960-9822(03)00418-4

Wu, Y. I., Frey, D., Lungu, O. I., Jaehrig, A., Schlichting, I., Kuhlman, B., & Hahn, K. M. (2009). A genetically encoded photoactivatable Rac controls the motility of living cells. *Nature*, *461*(7260), 104–108. https://doi.org/10.1038/nature08241

Yamada, K. M., & Sixt, M. (2019). Mechanisms of 3D cell migration Nature reviews | Molecular cell Biology. *Nat Rev Mol Cell Biol*, *20*.

Eidesstattliche Versicherung (Affidavit)

Sachan, Arya
Name, Vorname
(Surname, first name)

243770
Matrikel-Nr.
(Enrolment number)

Belehrung:

Wer vorsätzlich gegen eine die Täuschung über Prüfungsleistungen betreffende Regelung einer Hochschulprüfungsordnung verstößt, handelt ordnungswidrig. Die Ordnungswidrigkeit kann mit einer Geldbuße von bis zu 50.000,00 € geahndet werden. Zuständige Verwaltungsbehörde für die Verfolgung und Ahndung von Ordnungswidrigkeiten ist der Kanzler/die Kanzlerin der Technischen Universität Dortmund. Im Falle eines mehrfachen oder sonstigen schwerwiegenden Täuschungsversuches kann der Prüfling zudem exmatrikuliert werden, § 63 Abs. 5 Hochschulgesetz NRW.

Die Abgabe einer falschen Versicherung an Eides statt ist strafbar.

Wer vorsätzlich eine falsche Versicherung an Eides statt abgibt, kann mit einer Freiheitsstrafe bis zu drei Jahren oder mit Geldstrafe bestraft werden, § 156 StGB. Die fahrlässige Abgabe einer falschen Versicherung an Eides statt kann mit einer Freiheitsstrafe bis zu einem Jahr oder Geldstrafe bestraft werden, § 161 StGB.

Die oben stehende Belehrung habe ich zur Kenntnis genommen:

Official notification:

Any person who intentionally breaches any regulation of university examination regulations relating to deception in examination performance is acting improperly. This offence can be punished with a fine of up to EUR 50,000.00. The competent administrative authority for the pursuit and prosecution of offences of this type is the chancellor of the TU Dortmund University. In the case of multiple or other serious attempts at deception, the candidate can also be unenrolled, Section 63, paragraph 5 of the Universities Act of North Rhine-Westphalia.

The submission of a false affidavit is punishable.

Any person who intentionally submits a false affidavit can be punished with a prison sentence of up to three years or a fine, Section 156 of the Criminal Code. The negligent submission of a false affidavit can be punished with a prison sentence of up to one year or a fine, Section 161 of the Criminal Code.

I have taken note of the above official notification.

Ort, Datum
(Place, date)

Unterschrift
(Signature)

Titel der Dissertation:
(Title of the thesis):

Spatio-temporal coordination of Rho GTPase activity patterns in cell migration.

Ich versichere hiermit an Eides statt, dass ich die vorliegende Dissertation mit dem Titel selbstständig und ohne unzulässige fremde Hilfe angefertigt habe. Ich habe keine anderen als die angegebenen Quellen und Hilfsmittel benutzt sowie wörtliche und sinngemäße Zitate kenntlich gemacht.
Die Arbeit hat in gegenwärtiger oder in einer anderen Fassung weder der TU Dortmund noch einer anderen Hochschule im Zusammenhang mit einer staatlichen oder akademischen Prüfung vorgelegen.

I hereby swear that I have completed the present dissertation independently and without inadmissible external support. I have not used any sources or tools other than those indicated and have identified literal and analogous quotations.

The thesis in its current version or another version has not been presented to the TU Dortmund University or another university in connection with a state or academic examination.*

*Please be aware that solely the German version of the affidavit ("Eidesstattliche Versicherung") for the PhD thesis is the official and legally binding version.

Ort, Datum
(Place, date)

Unterschrift
(Signature)

technische universität
dortmund

Fakultät für Chemie
und Chemische Biologie

Datum: _____

An die/den Vorsitzende/n des Promotionsausschusses
der Fakultät für Chemie und Chemische Biologie der TU Dortmund

Eigenständigkeitserklärung für Dissertationen

nach der Ergänzung zur Promotionsordnung vom 29.10.2010
(Promotionsstudiengang) am 20.11.2023

Ich versichere hiermit an Eides statt, dass ich die vorliegende Dissertation mit dem folgenden Titel

Spatio-temporal coordination of Rho GTPase activity patterns in cell migration

selbstständig und ohne unzulässige fremde Hilfe verfasst habe. Ich habe keine anderen als die angegebenen Quellen und Hilfsmittel benutzt sowie wörtliche und sinngemäße Zitate kenntlich gemacht. Ich erkläre zudem, dass ich beim Einsatz von Schreib- und Bildwerkzeugen, die durch Künstliche Intelligenz (KI) unterstützt werden, diese in der Übersicht verwendeter Hilfsmittel mit ihrem Produktnamen, meiner Bezugsquelle sowie der spezifischen Methodik vollständig aufgeführt habe und, bei Übernahme von durch generative Schreibwerkzeuge erstellten Texten, die betreffenden Textstellen in der Arbeit als mit KI-generierter Unterstützung verfasst gekennzeichnet habe. Die Arbeit hat in gleicher oder ähnlicher Form noch keiner Prüfungsbehörde vorgelegen. Ich habe sichergestellt, dass durch die Verwendung generativer Modelle kein fremdes geistiges Eigentum verletzt wurde und ich kein wissenschaftliches Fehlverhalten etwa in Form von Plagiaten begangen habe.

Name: Sachan, Vorname Arya

Matrikelnummer: 243770

Datum, Unterschrift _____